ABSTRACT

WORSHAM, ELIZABETH KIRKPATRICK. Dynamic Modeling and Analysis of a Pulp and Paper Mill and Small Modular Reactor Coupling for Carbon-Neutral Manufacturing (Under the direction of Dr. Stephen Terry and Dr. Andre Mazzoleni).

Small Modular Reactors (SMRs) are reactor designs of less than 300 MW generally planned for deployment as multi-module nuclear power plants. The possibility for factory manufactured, flexible sized plants opens the applications for nuclear power to different communities and industries, including manufacturing plants which utilize fossil fuels to produce both steam and electricity. This dissertation examines the feasibility of coupling small modular reactors with two mid-size pulp and paper mills in the southeastern United States. A steady-state model of each mill is developed in Aspen HYSYS based on real data from the operation of each mill and modified to include the SMR while maintaining steam quality requirements and making few changes to existing equipment. Dynamic models of each plant are developed in Dymola to demonstrate possible plant conditions with several control schemes and configurations, including steam storage. Preliminary design data for a flexible heat exchanger for the secondary side of the SMR is included to illustrate the transfer of heat from steam generation in the module to steam that can be utilized by the process. Preliminary results suggest that while SMR coupling to both mills is physically feasible, the economic feasibility is limited by the differences in steam and electricity demand of each plant. When the SMR is sized for steam demands, Plant A requires a small amount of steam compared to its electricity needs, resulting in a deficit of electricity, while Plant B results in an overgeneration of electricity. Dynamic analysis concludes that the addition of a thermal storage system can reduce the deficits, but brings its own challenges. Each plant can determine the best configuration and control scheme based on electricity and heat needs, duration of peaking, and other features of the plant operation. Ultimately, implementation of SMRs with

manufacturing processes would benefit from a partnership with a local utility to purchase excess electricity generated by the SMR. This will help manufacturing corporations meet their environmental and cost savings goals while meeting the need for cost-effective base-load power across the United States.

Dynamic Modeling and Analysis of a Pulp and Paper Mill and Small Modular Reactor Coupling for Carbon-Neutral Manufacturing

by
Elizabeth Kirkpatrick Worsham

A dissertation submitted to the Graduate Faculty of
North Carolina State University
in partial fulfillment of the
requirements for the degree of
Doctor of Philosophy

Mechanical Engineering

Raleigh, North Carolina
2020

APPROVED BY:

_____	_____
Dr. Stephen Terry	Dr. Andre Mazzoleni
Committee Chair	Committee Chair
_____	_____
Dr. Richard Gould	Dr. Joseph Doster

BIOGRAPHY

Elizabeth was born and raised in Cincinnati, OH, and was told by her parents that she was destined to be an engineer from a very early age. Through years of FIRST robotics programs, she eventually decided to fulfill the prophecy and pursue a mechanical engineering degree at Embry-Riddle Aeronautical University in Daytona Beach, FL. She became fascinated by thermodynamics early on and dreamed of working on projects that would help the world increase the efficiency of power generation. After graduation, she headed to N.C. State to pursue her Ph.D. in mechanical engineering. Elizabeth will soon start her postdoctoral research at Idaho National Laboratory in Idaho Falls, ID. She hopes to use to her expertise to educate the public on nuclear technologies and inspire young people to pursue careers in engineering.

ACKNOWLEDGMENTS

I would like to acknowledge my family, Mom, Dad, Matthew and Thomas, for always pushing me to go above my own expectations, and Tyler, for being there when I needed him and staying with me while I moved from place to place that was rarely anywhere near him.

Thank you to my Grandfather Dr. A. Douglas Worsham for inspiring me to get my Ph.D. at NC State, and to my Grandmother Carolyn, who I never met, but made his achievement possible by hand-typing every copy of his dissertation.

I would also like to thank my advisor, Dr. Terry, for taking a chance on another Ph.D. student, and being just generally the best advisor.

Thanks to my committee, for putting in their time to help me graduate.

Thank you to my mentors and co-workers at Idaho National Laboratory for giving me moral, material, and intellectual support, specifically Dr. Shannon Bragg-Sitton, Dr. Konor Frick, and Daniel Mikkelson.

Lastly, I would like to acknowledge Nuclear Energy University Programs for funding me through the Integrated University Programs Fellowship.

TABLE OF CONTENTS

LIST OF TABLES

LIST OF FIGURES

Chapter 1: Introduction

Growing concerns regarding the overuse and lasting impacts of our natural resources are shifting the world into a new era. Fortunately, the benefits of fuel conservation and alternative power extend beyond the effects of reduced carbon emissions. Increases in energy efficiency save fuel and operating costs for businesses and product users, and power solutions such as solar, wind, and nuclear fuels help decrease foreign energy dependence.

With conservation of natural resources now a global priority, industries are looking for alternative fuels and processes to generate power and heat. Integrated paper mills use a variety of sustainable and fossil fuels to generate on-site energy, but these fuels could be replaced by a nuclear power source to reduce carbon output.

Small Modular Reactors are compact, factory fabricated nuclear power plants that can be transported by truck or rail to a nuclear power site [1]. Unlike current plants, which generate 1,000 MW or higher, these small reactors can generate up to 300 MW [1]. The US Department of Energy encourages industrial use of Combined Heat and Power (CHP), or cogeneration, to increase the amount of energy extracted from a given amount of fuel and to decrease carbon production. Use of CHP can increase the efficiency of a typical power generation system from 40 percent to 80-93 percent and can reduce the CO_2 release rate of the system by 50 percent [2].

Nuclear energy sources have not been traditionally considered for CHP because of the size of the plants, but SMRs can bridge that gap to provide both power and heat to large industrial applications. Integrated paper mills are a natural fit for this application because most mills already utilize CHP to provide large quantities of electricity and low-pressure steam, and heat and electricity demands remain at a stable ratio throughout the year [3]. High pressure (27-40 bar) steam is used to turn backpressure turbines, which generate electricity while producing a

pressure drop. Medium pressure (10-12 bar) steam is extracted for paper drying and other uses. The remaining low pressure (3-5 bar) steam is used in chip digesters and other applications.

Paper mills currently utilize a mix of fuels to generate steam, including fossil fuels, wood waste, and black liquor, a byproduct of the paper manufacturing process containing a mixture of pulping residues and inorganic chemicals. Currently, black liquor recovery boilers reclaim these chemicals to produce heat for steam generation [4]. Alternatively, the chemical can be gasified for a more efficient means of electricity production or sold as a fuel to other entities. While black liquor and wood waste are renewable and, therefore, carbon neutral, the other fuels contribute to carbon pollution. An SMR could replace traditional fossil fuels for steam generation, while the black liquor is burned to supplement steam production or gasified and sold.

The emergence of gasification technology along with SMRs presents an opportunity to increase the efficiency of the Kraft Cycle by transforming black liquor into a more mobile fuel, replacing fossil fuels elsewhere in the cycle. Gasification technology converts carbon-containing materials into synthetic gas (syngas) using heat in the absence of air. The major benefit of gasification is that the energy produced from the gas is more versatile than that of solid fuels and can be implemented easily into a CHP process. Syngas production also provides a cleaner burn than traditional fuels, and the CO_2 is emitted as a concentrated gas at high pressures, reducing the costs of separating and capturing CO_2.

This work is part of the Idaho National Laboratory's Joint Use Modular Plant Program (JUMP). JUMP is a key component of the Carbon-Free Power Project (CFPP) in which the Utah Associated Municipal Power Systems will build the first NuScale Power Plant at the DOE INL site. Via collaboration among the U.S. DOE, UAMPS and INL, JUMP proposes to use one small modular reactor (SMR) module within a 12-module NuScale plant for research, development,

and demonstration (RD&D) activities. A priority RD&D application is to demonstrate integrated energy system options that utilize nuclear energy to support industrial energy users or chemical processes in addition to grid electricity demand. Key applications include SMR integration with thermal energy storage (TES) for grid load following, and the integration of process heat use for cogenerating electricity and material goods (e.g. hydrogen, paper, chemicals, freshwater).

This project consists of three parts which will further the mission of the JUMP program:

1. Perform preliminary design of the JUMP tertiary heat transfer loop in conjunction with the thermal energy storage system (TES).
2. Determine the feasibility of black liquor gasification to replace natural gas use in the lime kilns.
3. Demonstrate the coupling of an SMR to provide process steam for a moderate sized integrated paper mill in the Carolinas.

The larger purpose of this research is to obtain an understanding of the effects of varying demands of steam and power on the SMR and will determine what controls and control sequences are needed to protect the SMR while maintaining product quality. SMRs are a fairly new technology, and there have been limited studies of their application. By proving the compatibility of SMRs with a large-scale manufacturing application, it can be expanded to other plants and processes that utilize CHP. Additionally, by demonstrating the use of SMRs as a hybrid energy system, manufacturers will consider their use as an addition to their current infrastructure, rather than a replacement requiring a complete overhaul to their systems.

Table 1. Definition of Terms.

SMR	Small Modular Reactor
LR	Large Reactor
MWe	Megawatts Energy (Electric)
MWt	Megawatts (Thermal)
kWe	Kilowatts (Electricity)
kWt	Kilowatts (Thermal)
CHP	Combined Heat and Power
MBTU	One Thousand British Thermal Units
MMBTU	One Million British Thermal Units
SA	Steam Accumulator
DT	Dekatherms (10^6 BTU)

Chapter 2: Previous Work

2.1.1 Nuclear Power and SMRs

2.1.2 Benefits and Applications

When a person thinks of a nuclear power plant, they probably imagine a large facility with huge cooling towers outputting thousands of megawatts of electricity. SMRs, however, benefit greatly from their compact design, with one of the primary benefits being versatility. Vijuc et. al suggest "SMRs could be broadly used by smaller utilities, by smaller countries with financial or infrastructural constraints, in isolated regions for distributed power needs, and for various other non-electrical application" [1]. There exists a "unique market niche" for small grid systems, where "industrial infrastructure is not sufficient and the unit cost of electricity generation is very high with conventional technology" in places such as remote areas in Alaska, developing countries, and Pacific-basin islands [2].

SMRs can also be useful for applications in large cities. Ochiai et. al. wrote a recommendation to install a district heating system using a small reactor underground Tokyo, citing "the land is very expensive in the big city, so the reactor has to be installed very deep underground" [3]. Using the heating system, hot and cold water could be distributed to buildings at a range of 5 km from the reactor. If not for the small-scale modularity of SMRs, utilizing nuclear power would be space and economically prohibitive. SMRs also share the same environmental benefits as large reactors. Sambuu and Obara wrote a recommendation for district heating using a small reactor in Mongolia, on the basis that "using nuclear energy can be one of the ways to satisfy the increasing energy demand and to solve the air pollution issue in Mongolia" [4].

Reliable power generation is critical for any industry. Fortunately, an SMR has increased reliability over a traditional NPP due to its modularity and small scale. A study by Doyle et. al found that when using multiple modules: “in contrast to traditional plant, which cannot assure power at any level, power output can be assured at a NuScale plant at approximately 50% of total plant capacity at 99.9% reliability, and 17% of total plant capacity at 99.99% reliability [5]. In addition to baseload power generation, an attractive feature of a modular design is “staggered refueling of modules” [6]. Independence between modules, including the power conversion systems assures that “other modules can continue to produce electricity (or steam) while one of the modules is offline for refueling” [6].

A major problem associated with large scale plants is pointed out by Lovins, who writes: “The big transmission lines that highly concentrated nuclear plants require are also vulnerable to lightning, ice storms, rifle bullets, and other interruptions. The bigger our power plants and power lines get, the more frequent and widespread regional blackouts will become” [7]. Small modular reactors can mitigate this problem by doing exactly what he suggests in his essay: “Because 98–99 percent of power failures start in the grid, it’s more reliable to bypass the grid by shifting to efficiently used, diverse, dispersed resources sited at or near the customer” [7]. Small modular reactors can be connected directly to the user, bypassing the grid and offering increased reliability versus reliability on the vulnerable and widespread equipment of the power grid.

2.1.3 Economics

When nuclear reactors were first designed, they were built on the idea that the cost to produce each additional kW of power decreased as more capacity was added. However, this “economy of scale” tends to disfavor SMRs as compared to larger reactors [1]. Instead, SMRs

benefit from the "learning economy," where the cost of each unit produced decreases sequentially. According to Vujic:

"The average costs of production decline in real terms as a result of production experience as businesses cut waste and find the most productive means of producing output on a bigger scale. Evidence across a wide range of industries into so-called progress ratios, or experience curves or learning curve effects, indicate that unit manufacturing costs typically fall by between 70% and 90% with each doubling of cumulative output. Businesses that expand their scale can achieve significant learning economies of scale."

SMRs can benefit from this economy because standardized parts are replicated in the factory production of SMRs. An Nth-of-a-Kind (NOAK) plant will always cost less than a First-of-a-Kind (FOAK) plant, because of the lessons learned in the construction and deployment of earlier units. The learning curve generally flattens out after 5-7 units, so NOAK can be reached by SMRs with less MWe installed for SMRs than large reactors [8].

This learning economy extends to using multiple SMRs on one site rather than investing in one large reactor. Carelli argues that installing multiple SMRs on a site allows a firm to benefit from a three-level learning economy, consisting of cost-reducing effects related to the supplier's, utility's and plant organization's cumulative experience [9]. SMRs can also share some fixed costs, which may be decreased through cumulative experience.

The prevailing "One-of-a-Kind approach to accommodate the customized interests of individual customers has contributed to increased licensing, construction, and operational complexities" [10]. From 2003-2008, the estimated cost of constructing a nuclear power plant increased at a rate of 15% per year [11]. In July 2017, two AP1000 reactors were abandoned in South Carolina after 5 years of construction because of regulatory disputes and rising

construction costs. Lowering or eliminating the risk premiums associated with increased costs and construction delays makes a significant contribution to making nuclear more competitive. A 2003 study by MIT found that with a risk premium and without a carbon emission charge, nuclear is more expensive than either coal (without sequestration) or natural gas. Eliminating this risk premium decreases the nuclear life cycle cost for it to become competitive with coal and natural gas, even without a carbon emission charge [11].

In 2008, Lovins, Sheikh, and Marovich wrote a scathing article criticizing the idea that nuclear power was the key to addressing climate change. Their main arguments were: nuclear power plants are costly and slow to build, so relying on it would "reduce and retard climate protections," and that plants are unreliable, with 27% of all 132 U.S. Nuclear plants completely failing for a year or more at least once, and all plants must shut down every 17 months for maintenance and refueling [7]. They argued that while a kWh of nuclear power displaced all the CO_2 emitted by a kWh of coal, so does a kWh from wind, recovered heat, or end-use efficiency, which are all more cost-effective solutions, saving more carbon per dollar [7]. These criticisms are baseless if applied to SMR technology. The learning economy eliminates the costliness and time of a one-of-a-kind project and using multiple reactor modules provides redundancy for improved reliability. In addition, SMRs do not suffer from the intermittencies of wind or solar power.

Several studies have addressed the economic advantages of SMRs as compared to LRs. Carelli found that when SMRs and LRs are competing in the same market, the two are practically equivalent in terms of capital cost [9]. The O&M cost, however, is slightly higher for SMRs, although it consists of only a small portion of the total cost. When considering a model for economy of scale, a site with four SMRs (335 MW) has an O&M cost 24% greater than a site

with one 1,350 MW LR [12]. Ingersoll conducted a sensitivity study for both O&M costs and capital cost payback with a $4-14/MMBtu range for natural gas price and a range of $0-60/MT for carbon emissions tax to compare the costs of an SMR and natural gas when coupled with an oil refinery. The results showed that O&M costs become favorable for a NuScale-coupled refinery with a NG price of about $5/MMBtu and no carbon tax. The savings become significantly larger with an increase in NG price or carbon tax. A NG price of $9.50/MMBtu allows a 25-year payback of the total capital investment even without a carbon tax added. In this analysis, NuScale economics show viability for supporting large refinery applications, even in the absence of emissions penalties [6].

SMRs are also comparatively cost effective when used for district heating. Sambuu notes that for a system with an outlet temperature around 500K (440°F), the number of tubes would be reduced compared to a conventional reactor, which reduces the overall cost of the system [4]. Jaskloski et. al found that the total cost of combined electricity, heat generation, and transmission in a nuclear cogeneration plant can be lower than fossil-fuel cogeneration depending on the type of reactor used, although the annual costs of heat production and transport were only 2.3-3.3% of the total annual costs of nuclear cogeneration [13]. If given an emission allowance price of 27 Euros (about 31 US dollars) per ton of CO_2, a nuclear plant operating in partial cogeneration has the lowest annual costs of all considered nuclear and fossil-fuel configurations [13].

Islam considered the cost of a microgrid consisting of 100 MW with varying percentages of electricity supplied by an SMR. With no SMR, 80% wind, and 20% solar, the total cost was $29,586. With 50% SMR, 40% wind and 10% solar, the cost was $20,428. If an SMR supplied 100% of the electricity, the cost would drop to $11,270, less than half the cost without an SMR. SMR technology is proving to be cost competitive with popular renewable resources [14].

2.1.4 Loading Methods

Although it is most economical to operate nuclear power plants at full load all the time, there has been recent interest in equipping reactors with load following capabilities, operating in load-following mode or following a variable load program with one or two large power changes per day. There are several reasons why this may be necessary:

"In France, load-following is needed to balance daily and weekly power variations of the electricity supply and demand, since nuclear power plants have such a large share in the national mix. In Germany, load-following became important in recent years when a large share of intermittent sources of electricity generation (i.e. wind) was introduced into the national mix. [15]*"*

Load following capabilities can help to improve the availability of wind power. In China, wind power is advancing rapidly, however "the power grid often refuses to link up to wind power generation sites typically in remote locations to its network, leading to a large amount of idle capacity [16]." Combining nuclear combined-cycle with wind power generation using the capabilities of variable power production by adding natural gas to meet grid demand can lead to further economic and environmental benefits [16]. According to Cany: "overall, having a flexible nuclear fleet provides the economic advantage of adjusting adequately supply and demand, without being obliged to shut-down nuclear reactors and compensating this by starting up flexible power plants with higher marginal costs [17]."

Coupling a nuclear power plant with a conventional fossil fuel superheater can also improve the thermal efficiency and load following capability of a plant. In this coupling scheme, the steam generated by the nuclear plant is further heated to superheated condition before entering the HP turbine. This increases the quality of steam and eliminates the need for a

moisture separator and reheater while reducing the stage of the feedwater heater. The efficiency and thermodynamic performance of the plant is improved because the steam portion and steam quality entering the turbine is better. Using exhaust gas from the gas turbines, the thermal efficiency of the AP1000 can be improved from 30.23% to 45.78%, and the thermal efficiency of an SMR can be improved from 22.41% to 44.99%. This increase has the additional benefit of increasing competitiveness of nuclear energy compared to traditional fossil fuel power plants, which have a thermal efficiency of 36.48% [18]. Coupling an SMR with a superheater and reheater can be designed for flexible operation down to 65% of full power load while maintaining 100% of the core reactor power [18].

In a study by Ingersoll, NuScale SMRs were shown to be compatible with load-following applications. In the case study, the only generation options were wind and nuclear with "sufficient nuclear power to supply all expected demand but allowing preferential use of the non-dispatchable wind power [19]." The analysis showed that "the NuScale module could adequately compensate for wind output variations using a combination of power maneuvering and turbine bypass, or turbine bypass alone [19]."

According to Ingersoll, load following with nuclear plants requires "complicated maneuvering procedures and plant components that can tolerate thermal cycling [19]." Power management options of the NuScale plant include: taking one or more modules offline for extended periods of low grid demand, maneuvering reactor power for one or more modules during intermediate periods to compensate for hourly changes, or bypassing the modules steam turbine directly to the condenser for rapid responses to load or wind generation [19].

Even if the capability is there, load following is not always a reasonable option. To match supply and demand, some nuclear power plants may stop completely. In 2014, more than half of

the shutdowns occurred during the summer (in periods of low demand), and 90% shut down during weekends. Forty-one reactors shut down at least once for load following purposes. On average, nuclear reactors have to stop once a year for load following motives [17].

There are also many questions surrounding the impact of load-following operations on the equipment within a nuclear power plant. Rakereng notes that "daily power level maneuvering requires frequent insertion or withdrawal of control rods, which leads to a different nuclear core burnout and power distributions compared to operating at baseload power [20]." According to the NEA, most of the currently used nuclear power plants have strong maneuverability capabilities in their design, so there is at most only a small impact of load-following on the acceleration of aging of large equipment components, but some influence on the aging of some operational components. Load-following can cause some increase in maintenance costs [21].

Fischer completed a study of the impacts of load-following on the fuel rods. At the end of the study, "the two test fuel rods did not release any activity during the two cycling experiments [22]". The power cycling tests performed at various power levels and burnups showed that fuel rod performance during cycling compares well to the performance of fuel rods under essentially constant load at similar power levels [22]. Ping studied the dynamic characteristics of the entire load following system, and found that the limiting factor in response time was not the reactor, but the air pump in his system [23], showing that the reactor performs reasonably well in load-following operations compared to the rest of the system.

Load following does pose some significant risks to the economics of a nuclear power plant. NPPs have high fixed costs and low variable costs (fuel) when compared to fossil fuel units, which have lower fixed costs but higher variable costs due to their fuel consumption. Therefore, any system which contains both nuclear and fossil fuel units, with the goal to

minimize fuel costs, would run the nuclear unit at steady full output as much as possible, with fossil fuel units providing automatic response operation to changes in load. The same is true even if the nuclear unit has the capability to be flexible [24]. Power scheduling in fossil fuel units works well because instantaneous operating costs are determined with reasonable accuracy by fuel consumption rates. Nuclear plants are a batch process, so fuel cost can only be evaluated accurately by considering at least one fuel cycle, making it difficult to determine the economically optimal way of operating a system where some NPPs are operating in load-following mode [25]. Operating an NPP at constant load is also beneficial to make up for the initial investment. According to Locatelli, almost all the related costs of an NPP are fixed or sunk, so to be affordable, the NPP needs to maintain a high capacity factor. Reducing power production increases the incidence of fixed costs on the unit output cost [26].

Several studies have estimated the potential losses associated with operating an NPP at less than base load. A study by Jaskolsi et al. varied the electrical output in an NPP by extracting steam at different points in the turbine. They found that the loss of electric power at maximum thermal load was 3.1-5.9% of gross electric power output in the traditional condensing mode [13]. Using data from various studies, Cany estimated the unit capability factor to be reduced by 0.5-2% with load following operation [17]. According to Lokhov, “in France, the impact of load-following on the average unit capacity factor is sometimes estimated at about 1.2% [15].” Economic losses are an important factor to consider when using an NPP for load following operations. However, there are ways to implement load following without sacrificing thermal or power output from the reactor.

2.1.5 Cogeneration

Because load following can reduce the load factor of the plant and jeopardize the economics, nuclear flexibility can instead be achieved by baseload operation coupled with new outlets that represent a flexible demand for electric power [17]. This idea of "LF by Cogeneration [27]," is to meet electricity market demand fluctuation while avoiding economic penalties. In many areas, the thermal power available from an SMR for non-electricity products aligns with the thermal load or water needs of an urban area. By deploying SMRs as cogeneration plants, it increases the possibility for SMRs to reap profits that would be lost by a LR [9]. There are many more benefits to nuclear cogeneration, including increased efficiency, reduced energy consumption and emissions, reduced environmental and health consequences, and increase the utilization of nuclear energy by substituting it for other fuels [28].

Jaskolski et al. studied the relative performance of nuclear CHP to various fossil fuels, finding that "a nuclear power plant can be a competitive combined heat and power technology even at relatively low price of CO_2 allowances… This parameter proved critical for nuclear cogeneration competitiveness" [13]. They also noted "turbine modifications required to convert a nuclear power plant to partial cogeneration mode are a low risk investment, since they constitute only a small fraction of total capital expenditures" [13]. Current NPPs can be converted to operate in partial cogeneration mode by extracting steam from both the LP turbine bleeders and the HP/LP or IP/LP crossover pipe. Modifications of the primary cycle or nuclear reactor thermal capacity or both are not required [13]. Similarly, steam could be extracted from a power turbine from a NuScale plant, and in some cogeneration designs, like adding a reverse osmosis process, normal power conversion systems can be left virtually unaltered [29].

Cogeneration is an important technology to reduce fuel consumption and CO_2 emissions. In a study of utility scale cogeneration by Rosen, "Annual uranium use by the electrical utility and related emissions decrease in all scenarios, by between 3% for low penetration of utility-based cogeneration and 35% for high penetration" and, "annual emissions of carbon dioxide decrease for all scenarios, by between 13% and 47% for the electrical utility sector [28]." Annual electricity consumption in the studied province decreased by between 3% and 30%, which also reduced electrical generation by corresponding percentages [28]. Cogeneration has the potential to significantly contribute to mitigating the contribution of the utilities sector to climate change.

Most importantly, nuclear cogeneration increases the utilization of the entire plant by diverting idle power and steam to produce a separate product. One well studied application for nuclear cogeneration is district heating. A study by Tulkki et al. assessed the performance of a nuclear reactor in CHP mode to produce district heating. Operating the reactor in CHP as compared to producing heat only increased the utilization rate, because the heat only plant would need to operate at a low power during the summer when demand is low. Alternatively, the CHP plant can adjust for seasonal and daily changes in demand [30].

The flexibility of the SMR to adjust steam and electricity output depends largely on where steam is extracted in the turbine. The power output of a steam turbine is largely dependent on the exhaust pressure, therefore if only exhaust steam is extracted, electrical and steam outputs are largely fixed at full operating power [29]. Using a controlled extraction turbine introduces limitations to the amount of steam that can be supplied due to minimum and maximum allowable exhaust flow. Maximum flexibility is achieved by splitting the main steam flow. In a desalination application, Ingersoll showed that extracting main steam yielded the maximum possible water output of a single NuScale module for all thermal distillation cycles considered in his study. In a

desalination plant, further flexibility can be achieved by a combination thermal distillation and reverse osmosis, which uses only electricity [29].

Another potential application for NPP and SMR cogeneration is hydrogen production. A medium scale hydrogen plant of about 200 tons per day of hydrogen would require six NuScale modules and provide enough hydrogen for a mid-size commercial ammonia plant of approximately 1,150 tons/d, a typical distributed scale petroleum refinery of 40,000 to 50,000 barrels/day, or a cluster of steel refining mills [6]. Locatelli et al. studied the viability of hydrogen production by alkaline water electrolysis (AWE) for SMR cogeneration. They concluded that AWE, as an electrical application, "is a flexible technology that can be easily coupled with SMRs." The economic viability of producing hydrogen is reasonable when the demand and price for electricity is low, and otherwise it becomes more profitable to produce electricity [27]. This makes it a great candidate for flexible cogeneration involving electricity demand.

Nuclear cogeneration is already in use around the world, but SMRs can extend its application to remote areas, as well as to industrial application. Of the nominally 400 commercial nuclear plants around the world, 59 are being used for district heating, and 12 are being used for water desalination. To date, no commercial reactor plant has been used to provide process heat directly to an industrial application [6].

2.2 Gasification

The pulp and paper industry is "one of the largest sources of indigenous, renewable and sustainable raw material in the United States," with 278 million dry tons processed each year, and likely an additional 100 million dry tons or more of residuals in the vicinity of these mills [31]. The main byproduct of the paper-making process is black liquor, a slurry of wood fibers

and process chemicals, and the kraft process uses this as a major fuel source for the plant while recycling the liquor. According to Vakkilainnen, "for every ton of pulp produced, the kraft pulping process produces about 10 tons of weak black liquor or about 1.5 tons of black liquor dry solids that need to be processed through the chemical recovery process" [31]. In total, 200 million tons of black liquor dry solids are burned in recovery boilers globally every year, amounting to 700 million tons of high pressure steam [31]. This makes black liquor "the fifth most important fuel in the world, next to coal, oil, natural gas, and gasoline" [32]. Unfortunately, the efficiency of converting black liquor to steam is typically lower than fossil fuel combustion because the heat is used to evaporate the water entering with the black liquor, heat of reaction is consumed in the production of Na_2S, and heat is carried out with the molten smelt [32].

This discrepancy has been the driving force of developments in gasification technology, with the potential for much greater electricity production if the liquor can be burned as gas in a gas turbine for combined cycle power generation [32]. Black liquor is an excellent candidate for gasification, given that its generation and processing are already integral to the manufacturing, and it contains about six times more energy than other biomass byproducts (bark and wood wastes) generated at a typical mill [31]. However, since the availability of the liquor is determined by parameters related to production, it is unlikely for a mill to have a perfect match between the available black liquor and fuel requirements [33]. Therefore, another fuel source is required to balance the requirements of the plant.

The benefits of pursuing Black Liquor Gasification Combined Cycle (BLGCC) and biomass gasification extend beyond the benefits to pulp and paper mills. According to Larson, "the full benefits of the hydrogen economy can be realized when the source of the hydrogen is domestically produced renewable energy, and biomass has the potential to be one of the lowest

cost options for producing hydrogen from renewable resources." In addition to being a springboard for a new biomass based energy industry, "BLGCC could ultimately be important in the development of a hydrogen energy infrastructure" [31]. By pursuing the commercialization of BLGCC technology, the pulp and paper industry would stand to share [in] energy, environment and economic benefits … while catalyzing the creation of a larger biorefinery industry that might produce still greater private and public benefits" [31].

2.2.1 Scale

As stated previously, black liquor is not only an important fuel, but an abundant resource throughout the world. A study by Larson found that "under a future scenario, in which 5% of all new electricity supply in the Southeast region is mandated to be renewable, aggressive deployment of BLGCC systems could meet nearly half of the required renewable electricity supply in 2020" [31]. The higher thermodynamic efficiency of gas turbine based cogeneration compared to steam turbine cogeneration is reflected in a higher electricity to steam production capability [31]. Comparing BLGCC technologies to the current recovery boilers, "BLGCC systems are able to produce more electricity than needed by the mill, while meeting the same steam demand as a Tomlinson System. The consequence of this is that for the same process steam demand, a BLGCC requires additional fuel to be consumed to maximize electricity production" [31]. In contrast, mills using Tomlinson boilers will need to purchase some electricity to meet their demands [31]. However, a study by Farahani found that with the combination of both gas and steam combined cycle turbines, "the BLGCC system can produce, approximately, twice as much electricity per ton of black liquor compared to a conventional recovery boiler" [31].

2.2.2 Environmental benefits

On a national scale, BLGCC technology in "utility-scale" configurations provide economic, environmental and energy security benefits, including the potential to displace more than 360 trillion Btu of fossil fuels per year within the first 25 years, corresponding to a reduction of more than 35 million tons of CO_2 emissions per year [31]. Additionally, BLGCC systems provide a variety of environmental benefits, with "considerable improvements in air emissions, some improvements in water pollution, and a similar solid waste profile as Tomlinson technology" [31] per unit of black liquor processed.

One of the most attractive features of gasification technology is low emissions. Gas turbine combustion is efficient because of high overall air-fuel ratios, and contaminants are removed from the syngas upstream to protect the turbine from damage and recover the pulping chemicals [31]. In addition to CO_2 emissions, it could significantly reduce SO_2 and NOx emissions, and other emissions to a lesser extent. In an aggressive market scenario, "the cumulative CO_2 offsets would amount to roughly 4% of the expected increase in total CO_2 emissions from the grid in the 2008-2035 timeline (absent the introduction of BLGCC systems)" [31].

This proposed study is interested in a carbon-neutral fuel scenario for pulp and paper mills. Net-zero carbon emissions are achieved if the CO_2 emitted in using biomass for energy is photosynthetically removed from the atmosphere by replacement biomass growth. A study by Farahani explored the possibilities of producing CO_2-free paper at a pulp and paper mill, concluding that it is possible under some conditions. Most notably: "the amount of biomass used as a supplemental fuel to replace fossil fuel inputs is important to reduce emissions at the mill. This replacement would most effectively be achieved by increasing the capacity of the BLGCC

which will seriously alter the energy balance of a pulp and paper mill [33].” Producing carbon-neutral paper will require more thoughtful implementation than simply replacing the current fuel with syngas.

2.2.3 Economics

In addition to being environmentally favorable, BLGCC technologies are economically advantageous to Tomlinson boilers. Assuming a commercially mature cost for both systems, an IRR of 20% is possible for an installed BLGCC system without considering the value of environmental or renewable benefits, and 35% when considering these benefits (Larson p.ii). When a similar renewable energy premium and renewable production tax credit is applied similarly to the levels for wind power in some states, the financial performance of high-temperature BLGCC cases are overwhelmingly attractive for both mill-scale and utility-scale systems [31].

An important aspect of the economics of BLGCC systems is the ability to convert its environmental benefits into monetary value, by selling excess NOx allowances or selling renewable electricity to meet a renewable portfolio standard. In the long term, carbon trading or another scheme to reduce greenhouse gas emissions may come into play, as well as existing and potential Federal and state incentives to promote renewable energy resources [31].

BLGCC technology already has a high monetary value for emissions reductions. Using the price for SO_2 allowance as of 2003 of \$160/ton, the SO_2 reductions have a market value of nearly \$400 million for a 25-year forecast period. NOx, conservatively valued at \$2,000/ton over the same period, would have a market value of \$2.2 billion. If CO_2 trading was implemented at a value of \$25/metric ton of carbon, the CO_2 value would be \$2.1 billion [31].

The contribution of BLGCC systems would be significantly beneficial to areas with a regional RPS (Renewable Portfolio Standards). In 2003, Larson predicted the contributions of Tomlinson and BLGCC systems to these standards. With natural growth of the industry, Tomlinson BASE technology could contribute 4.4 billion kWh to RPS in the southeastern United States by 2020. BLGCC technology in the same time period would contribute over 36 billion kWh by 2020 (p.S24). BLGCC is also superior to wind power in terms of capital investment. The total incremental investment (above the replacement of the Tomlinson systems) required to produce 36 billion kWh of generation from BLGCC would be approximately $6.3 billion in 2003 dollars. If the same amount of energy was produced by new wind power, 12,000 MW of wind turbines would need to be installed at a capital investment of $8.3-9.4 billion in 2003 dollars [31]. RPS, voluntary green power programs offered through utilities, and emissions trading markets all give the industry an opportunity for a second revenue stream through renewable power generation [31].

2.2.4 Implications for the Lime Kiln

BLGCC technology has a significant impact on the operation and loading of the lime kiln. Both high-temperature and low-temperature gasification options exist for BLGCC. The black liquor gasification process can also be categorized based on the form of sodium, smelt or solid form. The process where sodium is held in a solid form is operated at a lower temperature than the smelt process [33]. The process for recovering pulping chemicals for BLGCC is modified from the Tomlinson boiler process, where during gasification there is a natural partitioning of sulfur to the gas phase and sodium to the condensed phase. The lower the gasification temperature, the more complete the partitioning of sulfur and sodium. In the low temperature process, over 90% of sulfur in the black liquor will leave the gasifier as H_2S gas. In

the higher temperature process, slightly more than half the sulfur leaves in gas phase [31]. This sulfur-sodium split offers the opportunity to use new pulping chemistries which can help improve pulp yield, enabling a mill to decrease wood input costs compared to conventional pulping, amounting to $4 million per year at the mill in Larson's case study [31]. However, a consequence of this natural sulfur-sodium split is a higher causticizer and lime kiln load compared to the Tomlinson boiler [31].

In the case study by Larson, the gasification system required an estimated 44% more causticizing/lime kiln capacity for low temperature, 16% for a high-temperature gasification than the conventional Tomlinson system. The high incremental load for the low temperature system could require installation of an additional causticizer and lime kiln, while the smaller increment for the high temperature system could be accommodated by firing the lime kiln with oxygen-enriched air, resulting in a small increase in the size of the air separation unit [31].

Larson estimates that the incremental IRRs for mill-scale high-temperature BLGCC case relative to investments in a new Tomlinson system are reasonably attractive at 18.5% to 21.1% with baseline assumptions. The low-temperature system has much lower financial performance because of the increase in lime kiln capacity. With the increase in capacity, the incremental IRR for this case compared to Tomlinson systems is only 9%, but if costs associated with the lime kiln requirement were eliminated, the IRR would increase to 13% [31]. Larson suggests that low-temperature BLGCC systems present an opportunity to completely eliminate the lime kiln using direct causticization or another method. Without accounting for the added costs of direct causticizing, but eliminating all costs associated with the lime kiln, the IRR increases to 17% [31].

2.3 Thermal Storage Systems

There have been many studies done to investigate the uses of steam accumulators to assist power plants during times of peak loads. Providing steam from an accumulator during peak steam demand for a manufacturing plant is similar to providing steam to produce electricity during peak demand. In both cases, it is vital to have a backup system that reacts quickly to changing loads. If the necessary steam is not provided, production will cease, which will result in lost revenue, equipment damage, and unhappy customers. Specifically, for the paper mill, the boilers continue to produce steam during scheduled and unscheduled outages, and the mill is forced to exhaust the steam. If that steam was collected for later use, it would increase overall efficiency for the plant and decrease fuel costs.

Although there were no studies found where steam accumulated was used for a process, studies on peak power generation from steam accumulators offer valuable insight into their benefits and limitations when incorporated into a plant.

2.3.1 Buffer Storage Systems for Nuclear Power

In a perfect system, a boiler would be designed to provide a constant steam supply that matched the needs of the system exactly. In reality, steam demand in a system fluctuates and the boiler must be capable of supplying the maximum amount of steam the system might need at all times. If steam demand increases above the limits of the boiler, rapid depressurization can occur, reducing the steam quality and causing low-water shutdowns. Because of this, “engineers must oversize the boiler, design in back pressure regulators to control depressurization, or use a steam accumulator” [34].

Sun et. al. categorizes steam systems into controllable steam sources (CSS), where flow rate, pressure, and temperature are steady, periodic, or can be controlled, and uncontrollable

steam sources (UCSS), in which steam generation is influenced by other factors, and flow rate, temperature and pressure fluctuate and vary over a large range [35]. In a CSS, systems such as a nuclear power plant, the steam accumulator buffers and balances the steam generation and consumption.

Steam accumulators are used in industry and power plants to "adjust for differences between steam production and consumption rates" [36]. "Buffer storage" is the use of steam accumulators "to allow fast load changes of the turbine without a load change of the boiler and its furnace" (Beckmann p.91). Buffer storage systems are characterized by short reaction times and high discharge rates, though the thermal capacity is in the range of 5-10 minutes [37]. Beckmann notes: "Steam storage systems are theoretically unlimited in peak power and are really separate plants connected to the main plant by only a charging line and a condensate return" (Beckmann p.190).

2.3.2 Advantages

Although nuclear reactors can be designed for load following, "the most economical and reliable operation is base load, or producing maximum power all the time" [38]. In this case, steam accumulators are beneficial by capturing excess steam during times of low demand, rather than exhausting it from the system. For industrial applications, energy storage minimizes system costs by "moving energy use from one period of time to another" and "keeping the power demand for the whole system equal or less than the maximum value… of the power demand according to the electricity contract" [39].

Beckmann notes that "there is even more incentive to use energy storage for nuclear power plants than with coal-fired plants" (p.188). A buffer system allows a nuclear power plant to move "away not only from oil, but fossil fuels altogether" (p.189). Considering the high

capital cost of a reactor island, a storage system permits maximum use of the investment, potentially decreasing payback time. Additionally, “cyclical operation of a nuclear reactor is detrimental to its fuel elements”, and base load operation minimizes temperature cycling of the fuel (p.189).

A study by Steinmann et. al. employed a buffer system in a study of solar-thermal power plants to protect the components from the effects of high thermal transients resulting from sudden variations in solar insolation. The fast reaction time of the buffer system simplified the control of the power plant by allowing an extended reaction time for backup systems, which are intended to compensate for longer periods of reduced insolation [37].

According to Stevanovic: “the application of a steam accumulator substantially increases the energy efficiency of the steam supply” [36], and “its widespread use can be attributed rapid steam discharge rate, and elimination of steam load fluctuation [35]. Sun notes that the thermal efficiency of a boiler decreases with increasing load fluctuation and increases in load disturbance amplitude [35]. The advantages of a steam accumulator are illustrated through various studies. Merritt concluded that “sized right, steam accumulators will greatly shorten cycle times of autoclaves and similar equipment while maintaining good steam quality” [34]. Tari et. al. calculated a small savings by installing a steam accumulator for power generation in an existing pulp and paper mill [39]. Daniels studied steam accumulators as buffer storage for a small modular reactor, and found that the capacity factor for one week increased from 76.0% to 91.2% with the addition of a steam storage system [38].

2.3.3 Limitations

The major limitation of a buffer system is that it is intended to be used only for short periods of time, “with more prolonged load changes being met by boiler control” (Beckmann

p.91). The studies by both Daniels and Tari confirmed that for the specified setup, energy storage was only achievable from one hour to a few hours at a time, respectively [38] [39].

It may be possible to extend the time response of the steam accumulator. According to Yang “The regenerative rate of the steam accumulator is related to the steam flow and steam pressure, the greater the steam flow and the higher the pressure, the greater the regenerative rate of the accumulator, and the less time needed to achieve the same hot filling pressure.” [40]. Steinmann suggests “the response time of storage systems intended for operation over several hours can be extended if steam accumulators are used in the initial phase of storage operation” [37]. Extending the response time of long-term storage also helps to improve the cost efficiency [37].

Chapter 3: Theory and Assumptions

3.1 Small Modular Reactors

Small Modular Reactors are compact, factory fabricated nuclear power plants that can be transported by truck or rail to a nuclear power site [1], generating up to 300 MW. This design is coupled with a NuScale SMR, consisting of as many as twelve 150 MWe reactor cores with other primary system components housed in steel containment vessels and immersed in a large pool of water. The fuel assemblies used are shorter than in tradition pressurized water reactors (PWR), but consist of the same geometry, materials, and fuel type. Up to two twelve-core modules can be connected to produce power [3].

A typical large fossil fuel boiler has a thermal efficiency of 80-90%. The majority of the losses are through heat leaving the boiler stack, about half from the temperature of the gas and the rest from the water vapor created during combustion. Losses for natural gas fired boilers are higher because of the large amount of water vapor created during combustion (about 90 lb water per MMBTU fired). When connected to a Rankine power cycle, boiler heat is supplied to generate steam that flows through a turbine to a low-pressure condenser. Most of this heat is lost through the condenser in order to reject the entropy generated in the boiling process. A typical fossil fuel Rankine cycle plant has a thermal efficiency of around 30-40% [41]. In nuclear power plants, there is no stack, which improves overall fuel to power efficiency, but a lower boiler steam temperature and pressure results in lower turbine power and efficiency. Modern PWR nuclear power plants have an efficiency of about 33-35%. A typical fossil fuel industrial power cycle has an efficiency closer to 20-25%, because they use backpressure turbines rather than condensing turbines to provide heat to the process - essentially eliminating the heat lost in a condenser.

Despite the similar overall efficiency of a PWR compared to a fossil fuel plant, nuclear fuel burns carbon free, and produces a greater amount of energy per unit fuel. One uranium fuel pellet contains the energy equivalent of one ton of coal or 3 barrels of oil [42]. Additionally, nuclear power plants worked at full capacity 92% of the time in 2017, compared to 54% for coal plants and 55% for natural gas plants [43].

3.1.1 Economic Assumptions

NuScale estimates the capital costs of a plant in 2014 dollars to be $5,078 per kWe net [7], and SMR Start estimates Fixed O&M costs at $135/kW-yr and variable O&M at $3/MWh [8]. The current cost of uranium fuel can be estimated at $0.0052/kWh. Assuming both natural gas and uranium prices escalate at 3% per year, investment in an SMR returns a payback around year 5. This estimate uses a natural gas price of $3/MMBtu, which is about the average natural gas price in the US, and much lower than the average for the Carolinas, which is where the plant is located. The volatility of NG prices makes it difficult to predict an accurate payback period, however the natural gas price would have to decrease to $1.80/MMBtu at the time of installation for a payback around year 10, and $0.80/MMBtu for a payback of 30 years, the average for a traditional reactor [9]. Prices have not historically dropped this low, and with a lifetime of 60 years, a facility would see a quick payback from their investment as well as accumulating savings over a long time, especially because uranium fuel prices have been historically stable. If the U.S. and Europe were to implement carbon taxes, the attractiveness of SMRs would increase with the increased savings, although those savings don’t need to be included for the SMR to be a valuable investment.

3.1.2 Anatomy of an SMR

The main goal of any commercial power plant is to produce heat, electricity, or both heat and electricity. In the case of coal or natural gas power plants, this heat is produced through chemical combustion. In the case of a nuclear reactor, heat is produced due to the energy released by splitting atoms within the fuel. The NuScale SMR is a pressurized water reactor (PWR), which distinguishes itself from a boiling water reactor (BWR) in that the feedwater does not come into direct contact with the reactor core. Figure 1 shows the application of a PWR to generate electricity. The reactor core and control rod structure are contained within the primary coolant loop, which transfer heat to the secondary loop (typically water) through a heat exchanger. In this case, the primary loop boils off steam which flows through a turbine to produce electricity.

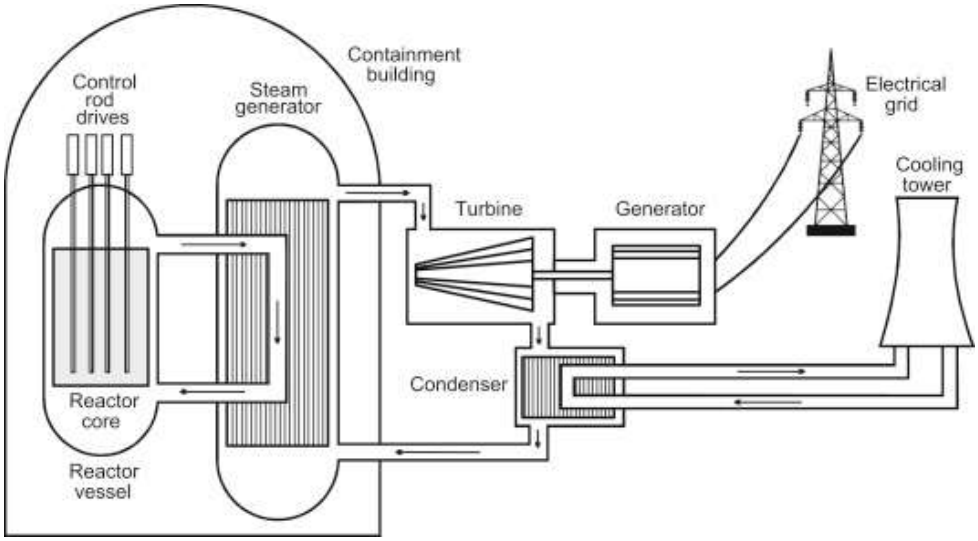

Figure 1. Typical Design of a Pressurized Water Reactor.

The NuScale small modular reactor is essentially a scaled down version of the reactor containment building. The fuel assemblies are shorter than traditional PWR fuel assemblies, but use the same geometry, materials, and fuel type [29]. The SMR reactor cores differ primarily in

footprint size than in function (Figure 2). Superheated steam exits the steam generator into a main header, where it can be extracted or sent to a dedicated turbine-generator system. Low pressure steam exits the turbine to the condenser, where it is recirculated to the feedwater system.

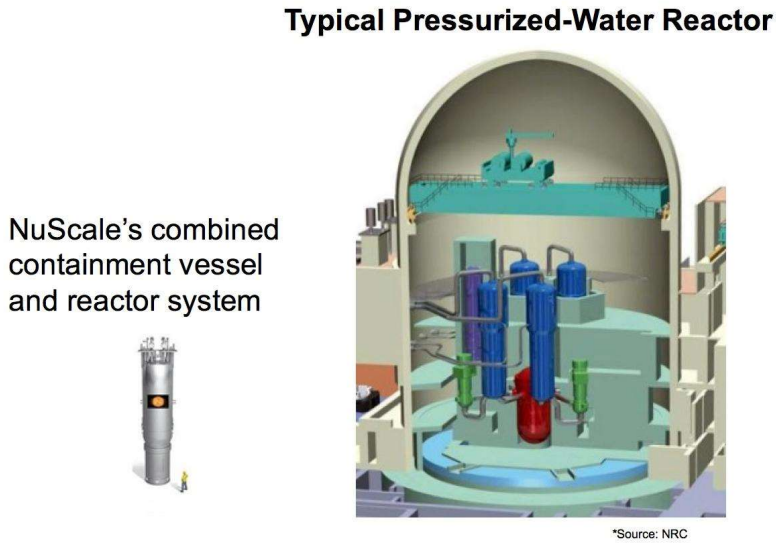

Figure 2. Size Comparison of a NuScale Module Versus a Typical PWR Containment Vessel.

3.1.3 Full Load Characteristics

The system characteristics of the NuScale SMR are based on publicly available information on the system. Each NuScale module core consists of a 60 MWe generator coupled to the 160 MWth fission powered steam generator. Up to 12 module cores can be connected to produce 720 MWe. On the steam side, a 45 MW condensing turbine receives nominal full load steam at 500 psia (34.5 bar), 575°F (302°C), at a rate of 536,200 lb/hr (67.6 kg/s). The condenser operates at 0.75 psia (0.05 bar).

The total heat transfer from the steam generator can be verified using the inlet and outlet enthalpy. The inlet enthalpy, h_i was found to be 271 Btu/lb (630 kJ/kg) for 300°F (149°C) water at 500 psia (34.5 bar) [38]. Interpolating from the NIST JANAF tables, the enthalpy of the

superheated steam, h_o, is 1,282.5 Btu/lb (2,983 kJ/kg). The saturation temperature at 500 psia is 467.1°F (241.7°C), verifying that the steam will be superheated. The heat input, Q_{in}, is described in the equation below.

$$Q_{in} = \dot{m}(h_o - h_i)$$

$$Q_{in} = \left(536{,}200\,\frac{lb}{hr}\right)\left(1{,}283\,\frac{Btu}{lb} - 271\,\frac{Btu}{lb}\right)\left(\frac{1\ MW}{3.413x10^6\,\frac{Btu}{hr}}\right)$$

$$Q_{in} = 159.0\ MW$$

The steam generator is rated at 160 MW thermal output, so with less than 1% error, these inlet and outlet conditions are reasonable.

3.2 Heat Exchanger Theory

3.2.1 Parallel vs. Counterflow Heat Exchangers

A parallel heat exchanger is one in which the two working fluids flow in the same direction, while in counterflow heat exchangers, working fluids flow in the opposite direction (Figure 3). Counterflow heat exchangers are the most common flow pattern for heat exchangers and present many advantages over parallel flow configurations.

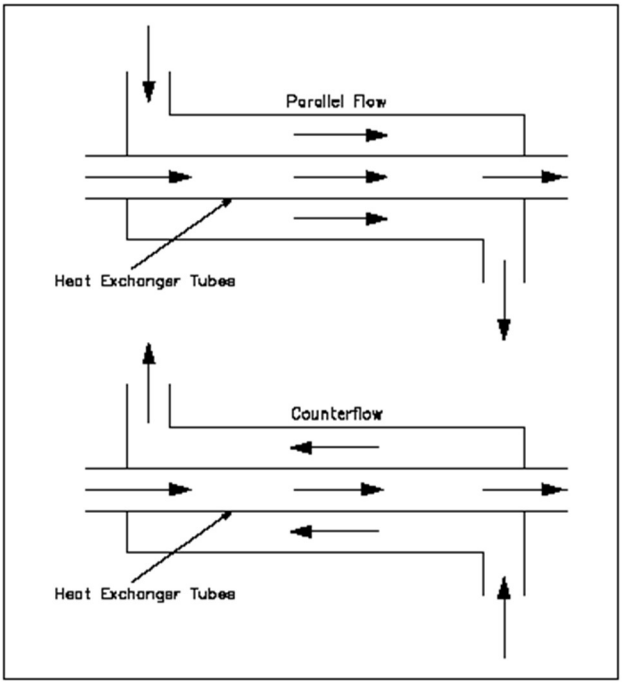

Figure 3. Fluid Flow of a Parallel Flow Heat Exchanger (Top) and a Counterflow Heat Exchanger (Bottom) [44]

Figure 4 shows the difference in temperature profiles between the two flow arrangements. The parallel flow heat exchanger is advantageous when two fluids are required to be brought to the same temperature [44]. Because the temperature difference between the two fluids gradually decreases along the path, the heat transfer rate decreases, resulting in a smaller overall heat transfer. For heat exchangers in which a phase change occurs, T_h or T_c stays constant throughout the entire phase change.

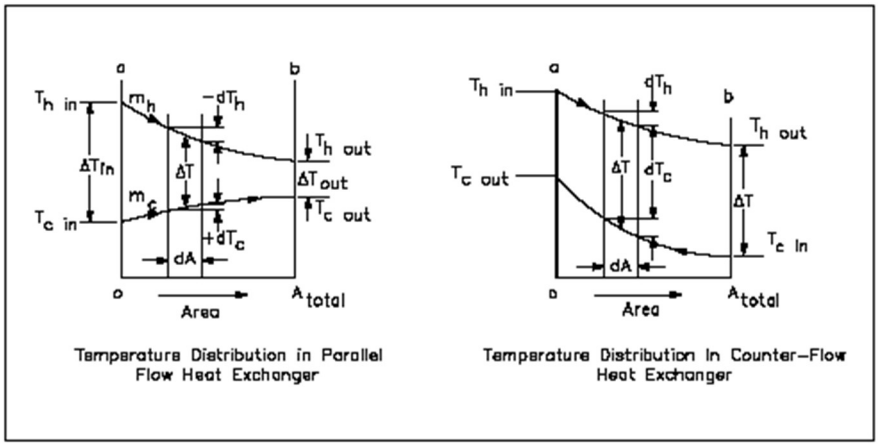

Figure 4. Heat Exchanger Temperature Profiles [44] **.**

The parallel flow heat exchanger maintains a more uniform temperature difference between the two fluids over the area, which allows for a more uniform heat transfer, and minimizes thermal stresses within the heat exchanger [44]. Additionally, the outlet temperature of the cold fluid can approach the inlet temperature of the hot fluid.

3.2.2 Types of Heat Exchangers

The most common type of heat exchanger is a shell and tube heat exchanger, which consists of a system of tubes housed within an outer cylindrical cell. The “tube-side” fluid is put in thermal contact with the “shell-side” fluid as it flows from inlet to outlet. This design is advantageous because the tube bundle creates a large surface area for heat transfer.

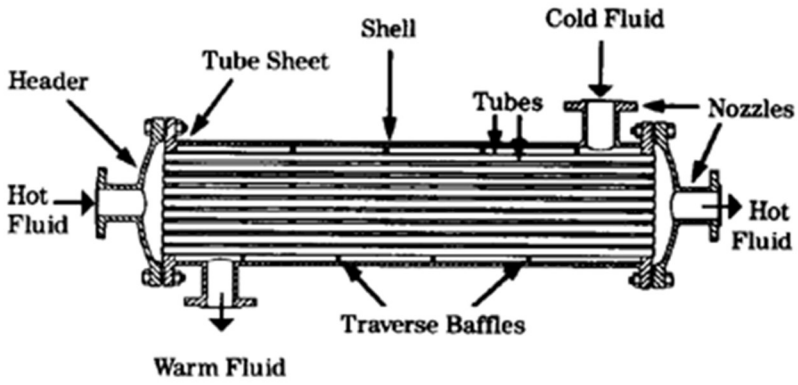

Figure 5. Diagram of a Typical Shell and Tube Heat Exchanger [45].

Plate and frame heat exchangers are advantageous over shell and tube for many applications, due to an increased contact surface area and a more compact design. Additionally, plate heat exchangers are easier to clean and maintain. As opposed to welded plates, gasketed plate heat exchangers can be disassembled easily, and increased capacity can be added at any time. The disadvantage to plate heat exchangers is that due to the movement of fluids there is a chance of greater pressure loss. Newer technologies have been working to mitigate this problem while maintaining the high heat transfer that make these heat exchangers so advantageous.

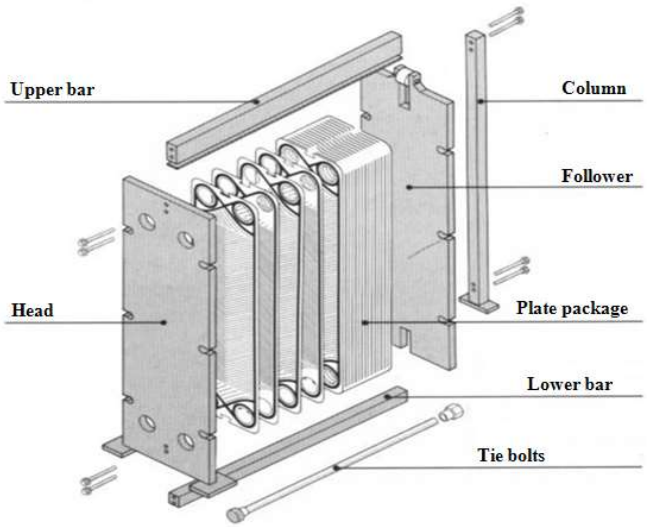

Figure 6. Diagram of a Typical Plate and Frame Heat Exchanger [46].

3.3 Multi-Effect Evaporation

Multiple effect evaporators (MEEs) are heat exchanger trains used to increase the concentration of a solution by boiling off excess water using the vapor created in the previous effect. The benefit is that more than 1 lbm (0.45 kg) of water can be boiled off with 1 lbm of steam input. One common type of MEE is the backward feed arrangement, in which the feed is introduced in the last effect, and steam is introduced in the first. In this arrangement, the first effect is at the highest pressure and each subsequent effect operates at a lower pressure than the previous. Throughout the evaporators, steam will flow naturally from high to low pressure, but a pump is required to move the feed through the evaporator train. In a single effect (Figure 7), the feed is sprayed over tubes filled with steam. The steam within the tubes transfers heat to the feed and condenses, while steam evaporates from the feed to be sent to the next effect (Figure 8).

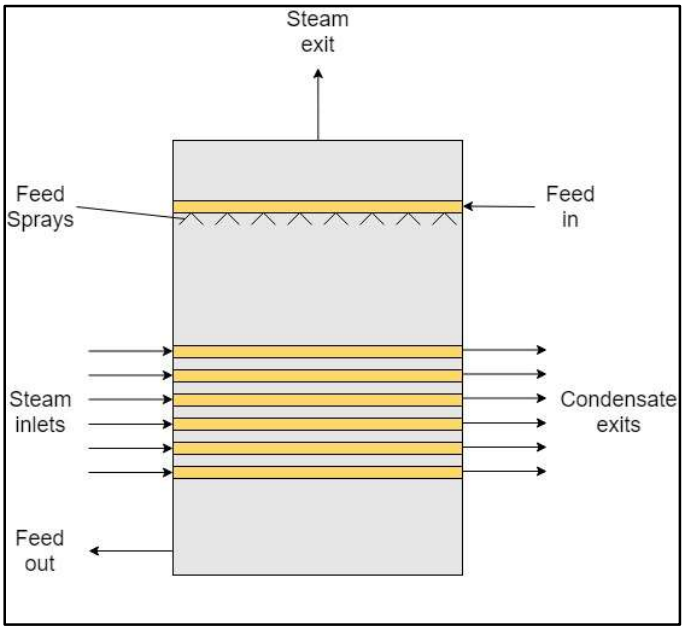

Figure 7. Diagram of a Single Evaporator Effect [47].

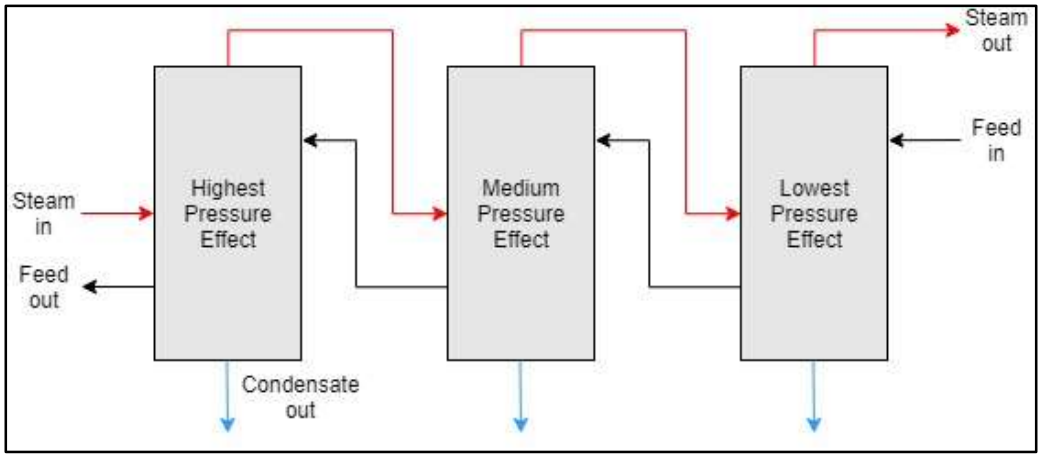

Figure 8. Diagram of a 3-Effect Counter-Flow Evaporator [47].

3.4 Biomass Gasification

Combustion occurs with sufficient oxygen to oxidize the fuel completely. Alternatively, gasification occurs with insufficient oxidizer so that complete oxidation does not occur. Because gasification occurs at lower temperatures than combustion, gasifiers can have longer lifetimes and lower maintenance costs, and produce fewer emissions. The synthetic gas (syngas) produced by gasifiers can be converted to electricity with reciprocating engines, gas turbines, or fuel cells, which have greater efficiencies than a steam turbine [48].

The gasification process begins the same as combustion, but energy is obtained from the oxidation of the solid particles after pyrolysis, rather than the volatile gases. While combustion requires a significant amount of air to produce reactions, gasification requires a limited amount of air with a controlled pressure and temperature to avoid combustion reactions and yield high rates of CO, CO_2 and H_2.

The carbon rich solid particles leftover after pyrolysis are oxidized with a combination of oxygen, carbon dioxide and water vapor to form CO and H_2 [49].

$C + ½ O_2 \leftrightarrow 2CO$

$C + CO_2 \leftrightarrow 2CO$ (Bouduard reaction)

$C + H_2O \leftrightarrow CO + H_2$ (heterogeneous water–gas reaction)

The resulting gas is called syngas, which has a variety of uses in different industries. A major benefit to syngas is that it produces a very clean burn. Carbon monoxide and hydrogen have a similar energy density by volume, and only need to take one oxygen atom to arrive at the products of complete combustion, CO_2 and H_2O [50].

Typical gasification does not treat the process of volatile combustion and char gasification separately; rather, it "recycles" the products of the hydrocarbon combustion to oxidize the char and produce gases that can be burned again. In a process called reduction, oxygen atoms are stripped from the combustion products at a high temperature to produce combustible gases.

3.5 The Kraft Recovery Process and Black Liquor

The Kraft process uses sodium hydroxide (NaOH) and sodium sulfide (Na_2S) to pulp wood. About 30 million tons/year of kraft pulp are produced globally, making it the dominant pulping process in the pulp and paper industry. The kraft process is advantageous over other pulping process due to the high strength of the pulp, the ability to process and handle almost all species of softwood and hardwood, and its high chemical recovery efficiency (about 97%). The high chemical recovery is what makes the kraft cycle an interesting candidate for gasification technology. Figure 9 shows a simplified flowsheet version of the Kraft Recovery Process.

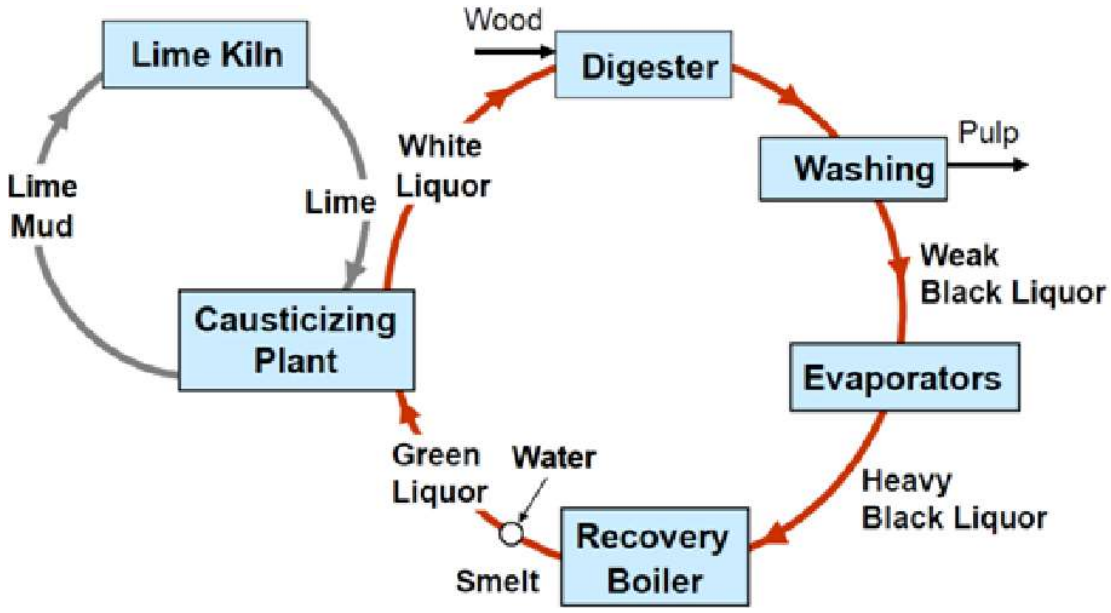

Figure 9. Flowsheet Diagram of the Kraft Recovery Process [32].

According to Tran and Vakkilainnen, "the kraft process has three main functions: i) minimizing the environmental impact of waste material (black liquor); ii) recycling pulping chemicals, NaOH and Na_2S; and iii) co-generating steam and power." The process begins with the digestion of wood into "white liquor," a water solution of sodium sulfide and sodium hydroxide. The white liquor chemically dissolves the lignin which binds the cellulose fibers in the wood together. When this cooking is complete, the contents of the digester are transferred to an atmospheric tank, or "blow tank", and then to the pulp washers, where the spent cooking liquor is separated from the pulp. The pulp then proceeds through stages of washing, drying, and bleaching, before being pressed and dried into a finished product [32].

The pulp wash water is combined with the spent cooking liquor to form a "weak black liquor" of about 55 percent solids, which is concentrated in a multiple effect evaporator to form a "strong black liquor," usually 65% solids or higher. The concentrated black liquor is then sprayed into the recovery boiler to form Na_2S [32].

The inorganic sodium and sulfur are recovered as molten smelt, consisting mostly of Na_2S and Na_2CO_3. The molten smelt is dissolved with water in the dissolving tank to form green liquor, which is sent to the causticizing plant. The causticizing plant reacts Na_2CO_3 with lime (CaO) to create NaOH, while the Na_2S passes through unchanged. This "white liquor," consisting mostly of NaOH and Na_2S, is returned to the digester for reuse in pulping, which the precipitated lime mud ($CaCO_3$) from the causticizer is washed and reheated in the lime kiln to a high temperature to regenerate CaO for reuse in the causticizer [32].

Chapter 4: Flexible Design for Steam Generation in an SMR Module

4.1 Background

With the introduction of renewable energy, the way we generate and receive our electricity is fundamentally changing. Renewables like wind and make up an ever-increasing percentage of the grid, driving down the price of electricity when they are online. However, when the sun isn't shining and the wind isn't blowing, electrical demands on traditional base load generators increases sharply over a short period of time that they may or may not be able to meet. The "Duck Curve" in Figure 10 represents the differences in electricity demand and generation in a single day in March in California.

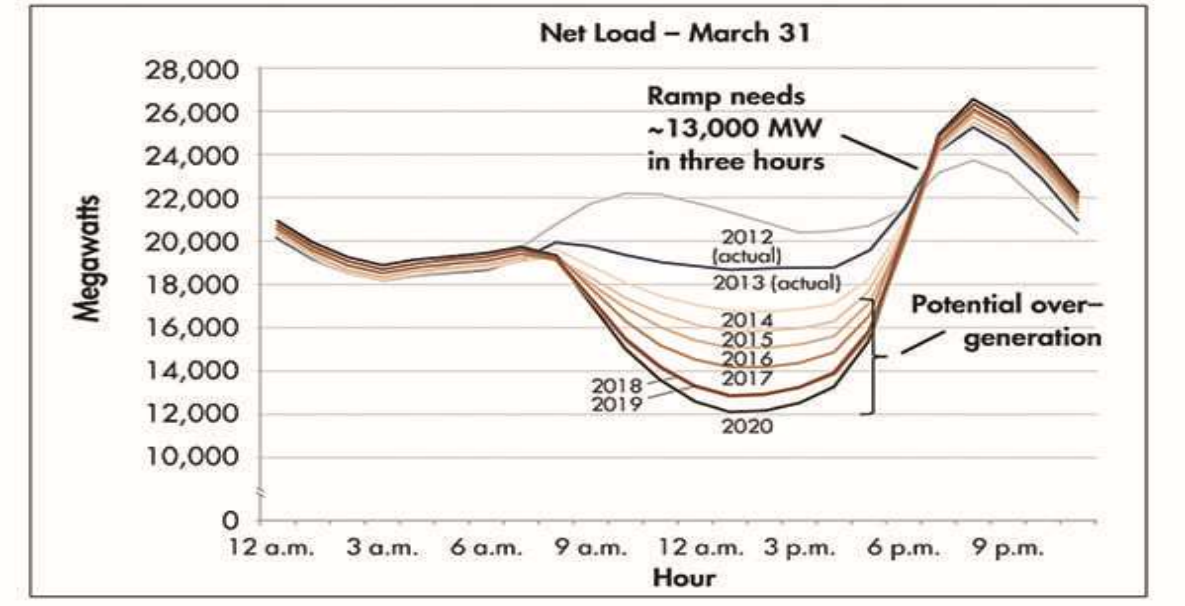

Figure 10. The "Duck Curve" for a Single Day in March [51].

This oscillatory pricing structure is economically challenging for base-load power plants, as predictions of profits and losses are no longer straightforward, and instead depends on weather patterns. One solution to this is to use the steam generated by base-load plants during times of low load or price to produce other valuable products such as hydrogen or potable water, or

simply store energy in a thermal reservoir. The Joint Use Modular Plant (JUMP) program at INL proposes to use a NuScale power module to support the research and demonstration of such systems.

4.1.1 Manufacturing

Manufacturing plants are a natural application for Small Modular Reactors because many utilize both steam and electricity to deliver products. The US Department of Energy encourages industrial use of Combined Heat and Power (CHP), or cogeneration, to increase the amount of energy extracted from a given amount of fuel and to decrease carbon production. Use of CHP can increase the efficiency of a typical power generation system from 40 percent to 80-93 percent and can reduce the CO_2 release rate of the system by 50 percent [52].

Figure 11 shows the highest process temperature required within the plant vs the average size of the plant in energy consumption per day. The size of the dot represents the relative yearly energy consumption of the industry within the United States

Some of the most energy intensive manufacturing sectors are depicted in this chart. Paper products, metals, chemicals and petroleum products dominate the energy market. All these industries would benefit from cogeneration and SMRs and are targets for the JUMP program. The average plant size in each of these industries can be accommodated by a multiple of NuScale cores.

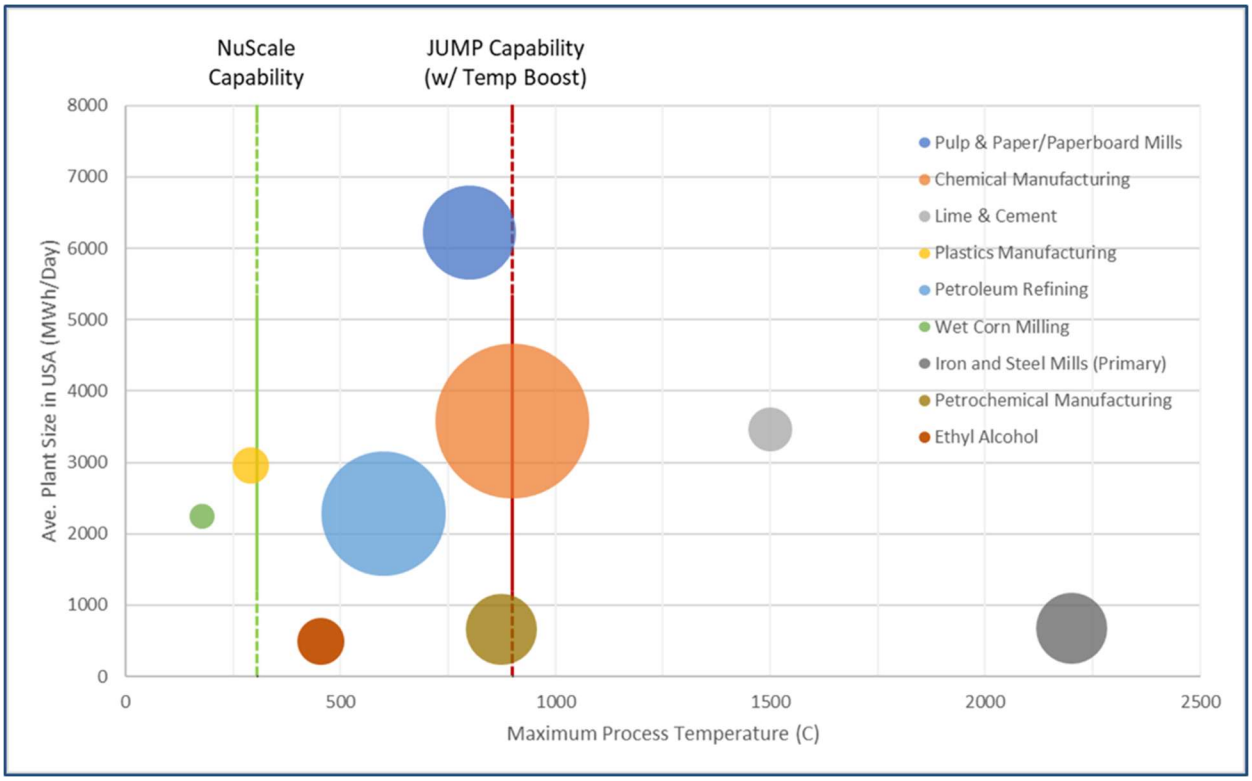

Figure 11. Comparison of Thermal Energy Use in the Industrial Sector [53].

4.1.2 Coal Conversion

Coal can be converted to organic gases and liquids to be used in conventional oil- and gas-fired processes. Presently, commercial coal conversion is uncommon in the United States because of competition from natural gas and oil, and the utility of coal in its solid state. Coal liquification and gasification both utilize process steam in the conversion process. If natural gas prices were to increase, or carbon taxes were implemented, the cleaner burn from coal in the liquid or gaseous state would become a more attractive option.

4.1.3 High Temperature Steam Electrolysis

There is increasing interest in hydrogen as a fuel, because its combustion with oxygen results in water. Currently, hydrogen production in North America is performed almost exclusively by steam reforming of methane (which still produces CO_2), however, the use of

natural gas makes this project non-renewable and therefore not ideal for large scale production [54]. In 2009, the Department of Energy, through its Nuclear Hydrogen Initiative (NHI) chose High Temperature Electrolysis as the most appropriate advanced nuclear hydrogen production technology for near-deployment [54]. INL's High Temperature Steam Electrolysis research program housed on-site makes it an ideal candidate for integration with the JUMP program.

4.1.4 Desalination

With population on the rise, so is the demand for water and energy. However, the carbon emissions from energy production contributes to climate change, leaving parts of the earth in a drought. Desalination can be an answer for areas who don't have access to reserves of fresh groundwater. Typically, one would think of desalination as a solution only on the coast, but more than half of all groundwater is saline [55], giving it widespread effectiveness, especially in desert areas that are far from a large water source. However, desalination is a very energy intensive process, consuming 10-13 kWh per thousand gallons [56], or 2 kWh per person per day [57].

The most widely used process for thermal desalination is multi-effect distillation (MED) or multi-effect evaporation. In this process, water is boiled in a sequence of vessels, with lower pressures in each consecutive effect. The vapor boiled off one effect is used to heat the next, then flows out as condensate. The products are a highly concentrated salt solution, and a reserve of fresh water. The high energy use comes primarily from the steam used to heat the initial effect. MED requires a thermal heat source, and Small Modular Reactors (SMRs) are attractive for these applications because they produce both steam and electricity without the production of greenhouse gases. A steam line from the secondary side of the plant can act as the heat source for the MED system, and typically a tertiary heat transport loop is required to ensure that no nuclear contaminants are carried over to the distillation plant from the secondary loop. This steam is

typically extracted from a low-pressure turbine stage, which decreases the electrical output of the power plant [57].

Reverse osmosis removes contaminants from water by pushing the water through a semi-permeable membrane using a pressure greater than the natural osmotic pressure. The amount of pressure applied depends on the salt concentration of the feedwater, with higher concentrations requiring more pressure. RO is not a thermal desalination process but does require electricity for pumping power. Electricity needed for pumping depends on many factors such as salinity, type of membrane, and flow rate, however, it can be estimated conservatively as 11 kWh per 1,000 gal of clean water produced [57].

4.2 Design Considerations

The SMR secondary side is to be designed such that it is easily retrofitted for many applications. The primary side of the SMR is designed to make electricity by passing high temperature and pressure steam through a turbine. Alternatively, main steam can be diverted before the turbine to satisfy a multitude of other purposes. To optimize the economic value of this system, theoretically, there should be an ability to divert 0% to 100% of the main steam to alternative use at any time, however, studies have shown that the maximum amount of steam that can be diverted from the reactor is 50% [58] of the total mass flow. Some steam will always be diverted to keep the heat transfer loop operational.

Another requirement for the secondary side is a thermal energy storage system. This will help to increase system efficiency by capturing otherwise dissipated heat during times of low demand, and accounting for fluctuations in demand to either the electric turbines or the process. It is imperative that the steam provided meets the required quality for the process, however, the

implications and steam outputs of the thermal storage system are currently unknown. The following steps are proposed to determine final design:

1. Design IHX on the SMR side in conjunction with TES
2. Design discharge heat exchanger
3. Determine max steam quality out of TES discharge
    - If quality does not meet process specs, design separate process heat exchanger (PHX)
    - If quality does meet specs, determine if losses in efficiency to process are acceptable
4. Test design with changing electricity and changing process demands

Because JUMP is an experimental system, it must be flexible in its design to accommodate many processes as well as accommodate design changes for testing processes. The IHX will be designed for both mineral oil (Therminol 66) and molten salt (HITEC) as the heat transfer fluid. Figure 12 shows the proposed preliminary design of the JUMP thermal energy distribution system, including the thermal storage system.

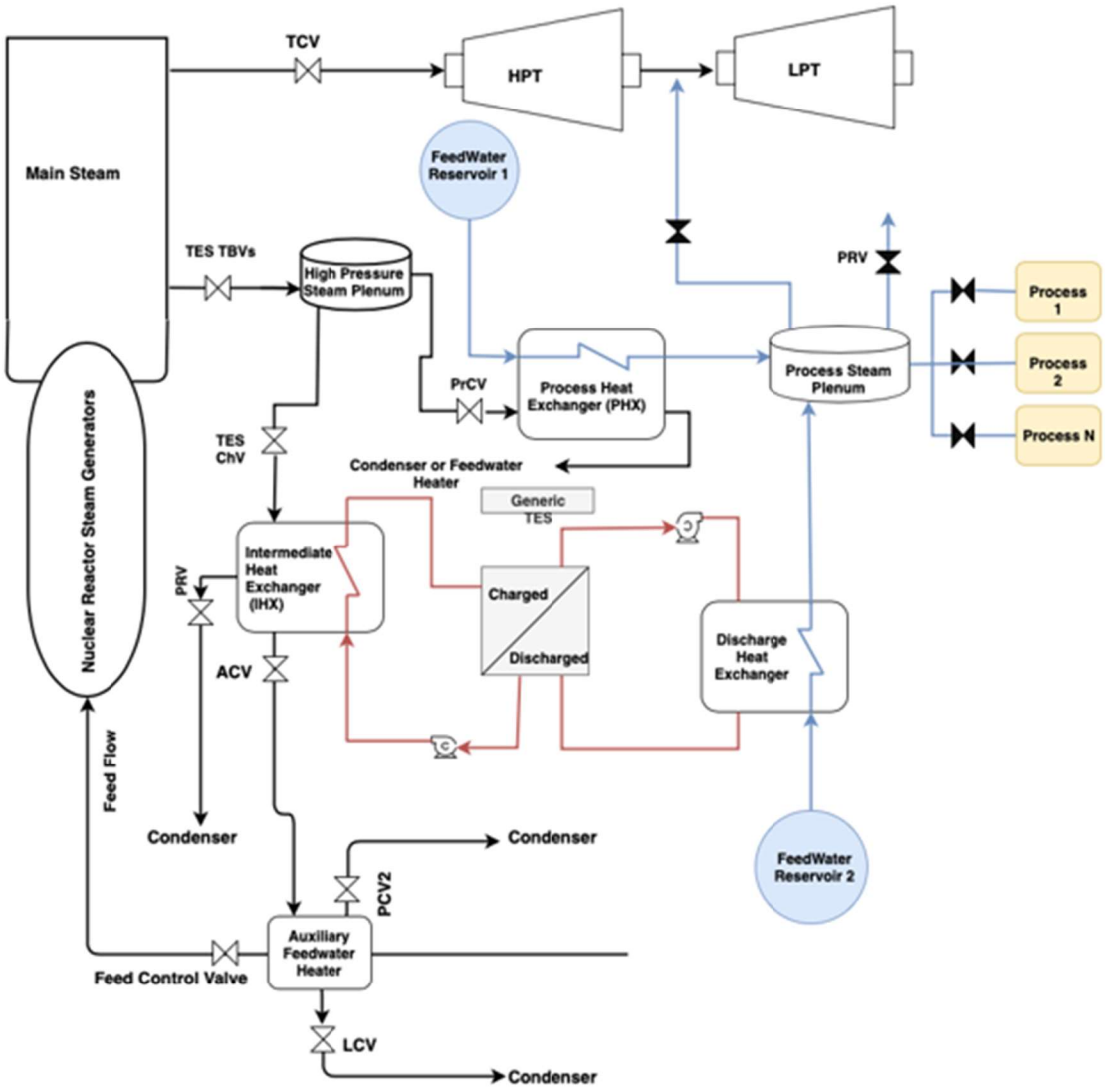

Figure 12. Proposed Design of JUMP Thermal Energy Distribution System.

4.3 Multi-Region Heat Exchanger Design

4.3.1 Desuperheating Theory

Because the thermal energy storage fluid will remain in a single phase when heat is transferred from the secondary side steam, the intermediate heat exchanger on the SMR side is effectively a condenser with thermal oil or molten salt as the coolant. The purpose is to extract as much sensible heat as possible from the secondary steam to run the storage system at a maximum

temperature difference. To do this, it is imperative that sensible heat is efficiently transferred from the superheated steam as it enters the condenser. Typical applications for desuperheaters are to absorb superheat before the steam enters the condenser, thus increasing the heat transfer coefficient of the vapor and reducing the size requirements for the heat exchanger. Figure 13 is an example of a direct contact desuperheater, in which cooling water is sprayed into the steam to absorb superheat.

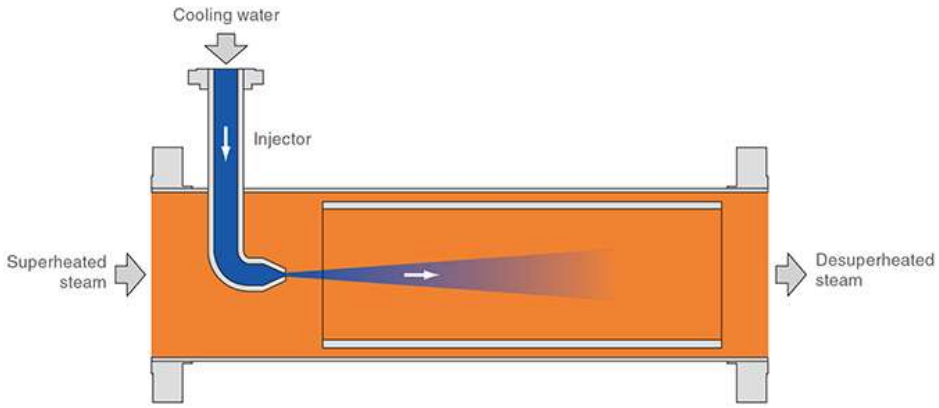

Figure 13. Example of an Axial Injection Spray Desuperheater [59].

The purpose of a condenser within a typical Rankine cycle is to remove heat from the working fluid and return it to a condensed state before being pumped back to the evaporator. In a counterflow condenser, the fluid that is to be heated enters on the subcooling side and increases in temperature while absorbing latent heat from the other fluid. Towards the end of the condensation phase, the fluids are at the risk of reaching a "pinch point" in which there is a very small temperature difference between the two. Figure 14 shows a heat release curve for a typical condenser with the pinch point occurring at point D. Pinch points lead to high thermal losses due to external irreversibilites [60]. The pinch point can be mitigated by adding a desuperheater, which will cool the fluid to a saturated phase before it enters the condenser. Desuperheaters are

useful for waste heat recovery applications and are frequently used in feedwater heaters and refrigeration applications.

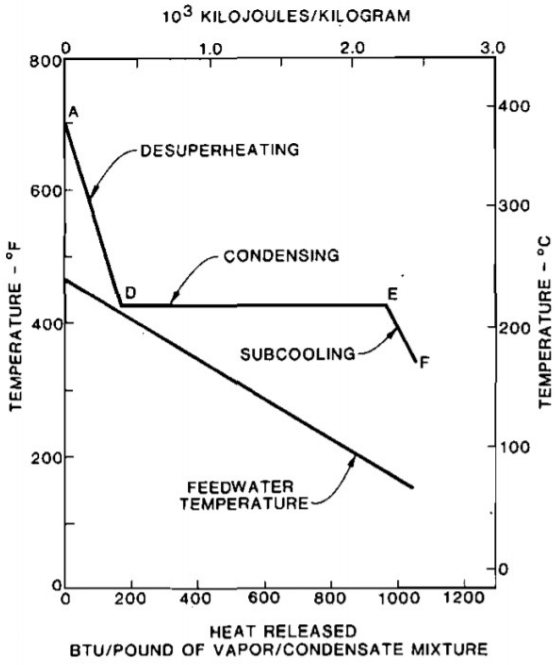

Figure 14. Typical Condensing Curve for a Counterflow Heat Exchanger [61].

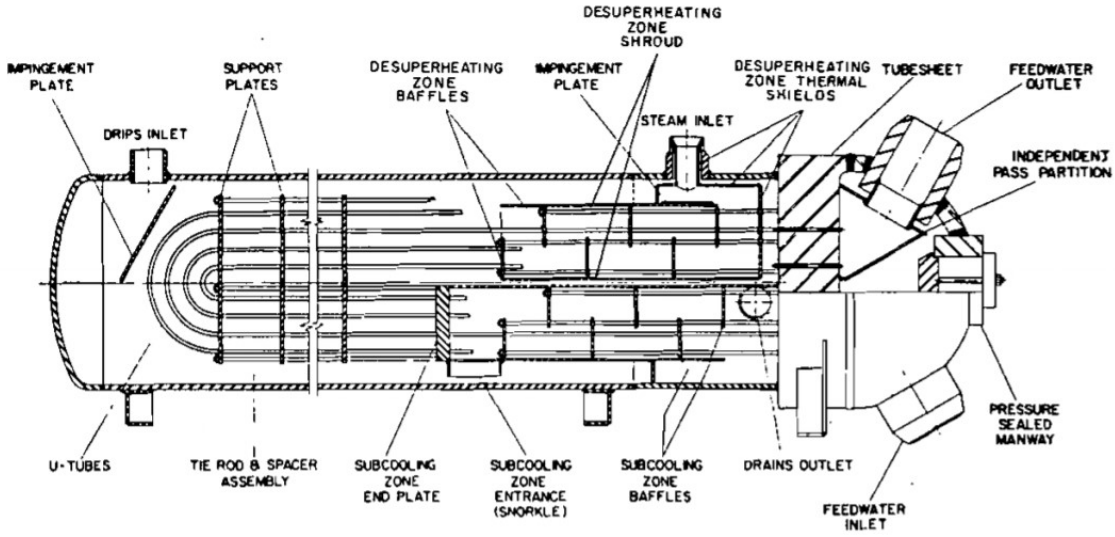

Figure 15. Heat Exchanger Diagram with Three Zones [61].

Figure 15 shows a diagram of a shell and tube heat exchanger with desuperheating and subcooling zones. This differs from a traditional condenser because the zones are shrouded and separated from the "condensing zone." Figure 16 shows an example of a heat release curve from this type of countercurrent heat exchanger.

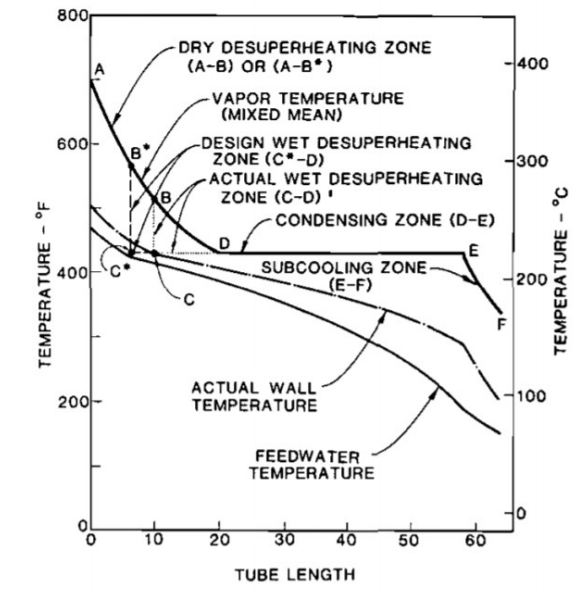

Figure 16. Typical Heat Release Curve for a Three Zone Counterflow Heat Exchanger [61].

The first portion of the condenser is the "dry superheating zone" where some of the superheat is removed by convective heat transfer across the heat transfer surface, which is at a greater temperature than the saturation temperature of the vapor. The "wet desuperheating zone" is the portion of the condenser where "the superheated vapor is in direct contact with condensate upon a portion of the tube surface" [61]. The desuperheating of the vapor is the result of heat transfer from the vapor to the condensate. "Depending upon the relative rates between condensate and wall, the average temperature of the condensate may increase or decrease." Every condenser with superheated vapor includes a wet desuperheating zone.

In the “condensing zone”, vapor at the saturation temperature makes contact with condensate on the heat transfer surface and is changed to liquid. This region is also the “film-type subcooling zone,” where “condensate on the tube surface is exposed to saturated vapor and is cooled below the saturation temperature.”

The last area of the condenser is the “submerged subcooling zone”, where “the tube surface is immersed in condensate and the liquid is cooled to a temperature below the saturation temperature.” The area typically has a loop seal or dam-type baffle to submerge the tubes.

4.4 Preliminary Design

Before developing a detailed model of the heat exchanger, it is necessary to understand the relationships between the design variables and establish a reasonable design range for each variable. The preliminary model will not consider pressure drops, fouling factors, material type, or fluid flow characteristics.

4.4.1 Initial Sizing

“Area allocation in multi-zone feedwater heaters” by Hussaini, Zubair and Antar details a method for determining the size of each zone in a 3-zone heat exchanger. The method involves discretizing the heat exchanger into small segments of an elemental area, ΔA. Discretized heat equations are applied to each segment to progressively determine the temperature profiles. The model considers the following assumptions: Uniform heat transfer coefficient in each zone, uniform fluid properties, no heat loss to the surroundings, and negligible pressure loss on the shell side. Hussaini et al. determined that the numerical approach gave less than 1% difference in each zone compared to the LMTD approach [62].

Zone 1 is the desuperheating zone, where heat transfer occurs by sensible heat exchange only. The first segment envelopes the shell inlet and tube outlet. The shell inlet temperature is

known, and the tube outlet can be set to any designed temperature within the operating range of the fluid. The overall heat transfer coefficient, U, cannot be determined accurately without the type and thickness of the heat exchanger material, and the characteristics of fluid flow, however, it can be assumed at any reasonable value for initial design purposes. In this case, the overall heat transfer coefficients were assumed to be 400 W/m^2°C in the desuperheater section, 700 W/m^2°C in the condenser, and 350 W/m^2°C in the subcooler, based on typical coefficients for water-oil heat exchangers, although not Therminol 66 specifically [63]. The following energy balance equations are used to find heat transfer rates and temperature distributions for both the shell and tube side [62].

$$\Delta q(i) = U_1 \Delta A(T_s(i) - T_t(i))$$

$$T_t(i+1) = T_t(i) - \frac{\Delta q(i)}{C_t}$$

$$T_s(i+1) = T_s(i) - \frac{\Delta q(i)}{C_s}$$

In Zone 2, the condensing zone, latent heat is transferred from the steam to the heat transfer fluid until the saturated steam is converted completely to a saturated liquid. The shell side is at the saturation temperature for the entirety of the zone. Because this section contains a mixture of liquid and vapor, the enthalpy in each segment cannot be calculated without knowing the quality. Instead, the area needed for this section can be determined using the total heat transfer of the section: the latent heat of vaporization times the mass flow rate [62].

$$\Delta q(i) = U_2 \Delta A(T_{sat}(i) - T_t(i))$$

$$T_t(i+1) = T_t(i) - \frac{\Delta q(i)}{C_t}$$

Zone 3 is the subcooling zone, where both the shell and tube side fluids are in liquid phase. In zone 3, heat exchange occurs by sensible heat transfer only, so the same equations

apply as in zone 1. The end of the heat exchanger will be determined by setting a tube inlet design temperature within the operating ranges of the heat transfer fluid [62].

$$\Delta q(i) = U_3 \Delta A(T_s(i) - T_t(i))$$

$$T_t(i+1) = T_t(i) - \frac{\Delta q(i)}{C_t}$$

$$T_s(i+1) = T_s(i) - \frac{\Delta q(i)}{C_s}$$

Establishing design regions is a difficult task because all the variables are dependent on each other.

The shell inlet temperature is fixed to the main steam condition, 307°C (584°F), however the design temperatures for the tube inlet and outlet are chosen based on the desired temperature delta across the thermal storage system. Theoretically, the shell side (steam) mass flow rate should vary from 0% to 50% of the main steam flow rate, but some steam may still need to flow through the heat exchanger to keep it operating and prevent serious thermal cycling. For design purposes, the heat exchanger must be able to operate from 10% to 50% main steam flow rate. It's unlikely that the system will operate between those two conditions for more than the ramp-up or ramp-down periods.

The hot and cold tank temperatures are bound by the saturation temperature of the main steam, and the freezing point of water. The upper bound is the saturation temperature to ensure heat transfer in the desuperheater by maintaining the temperature difference even with variable flow rates. Future design phases will include raising the upper limit for a smaller range of designs. To raise performance of the discharge heat exchanger, the hot tank temperature was set to the upper bound temperature.

4.4.2 Experimental Method

This study will determine the appropriate size and operating parameters of the flexible heat exchanger by testing its performance over a series of flow rates.

After the initial sizing, the previous method is implemented in reverse to simulate the performance of the heat exchanger with a varied steam flow rate. A temperature control valve will be placed at the outlet of both the charging and discharging heat exchangers to control the temperature going in and out of the storage tanks. By holding the inlet and outlet temperatures constant, the mass flow rate of thermal fluid required to maintain the temperature difference can be determined through iterative methods.

The initial sizing determines the size of each zone only for the design point. As the flow rate changes, the boundary of each zone can shift. The redesign study is set up such that the area of each section stays constant, but the steam can desuperheat, condense, or subcool in any section depending on the conditions within each zone. The iterative method determines the "inlet" temperature of the thermal fluid and tests it against the desired temperature. The mass flow rate of thermal fluid is changed until the inlet temperature matches the desired temperature.

The model was run at 12 design points, combinations of a design steam flow rate and the cold tank temperature of the fluid. Steam flow rate design points were 130,000 kg/hr (~50% of main steam), 100,000 kg/hr, 50,000 kg/hr and 5,000 kg/hr (~5%). Cold tank temperature design points were 40 C, 26 C, and 5 C.

4.5 Results for Therminol 66

The design temperature and maximum steam flow rate for each design point is set, and the remaining variable to determine the heat exchanger design is the mass flow rate of the heat transfer fluid. The approximate mass flow rate was determined by finding the highest flow rate

that would allow the model to converge. The maximum used is precise only to 2-3 significant digits and is shown in Figure 17. The same designs were tested for lesser flow rates, and performance was determined not to improve. Figure 18 through Figure 21 show the results of this study. The flow rates used for the following design studies are listed in Figure 17.

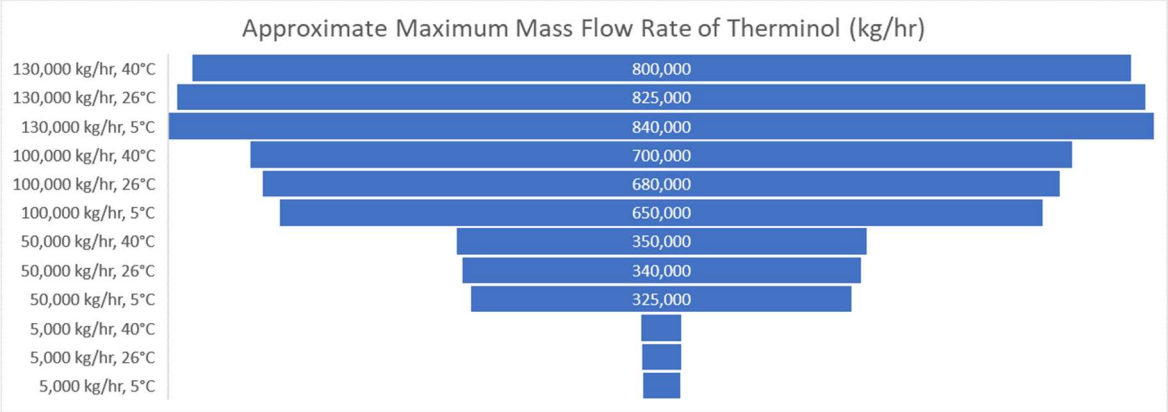

Figure 17. Approximate Maximum Mass Flow Rate.

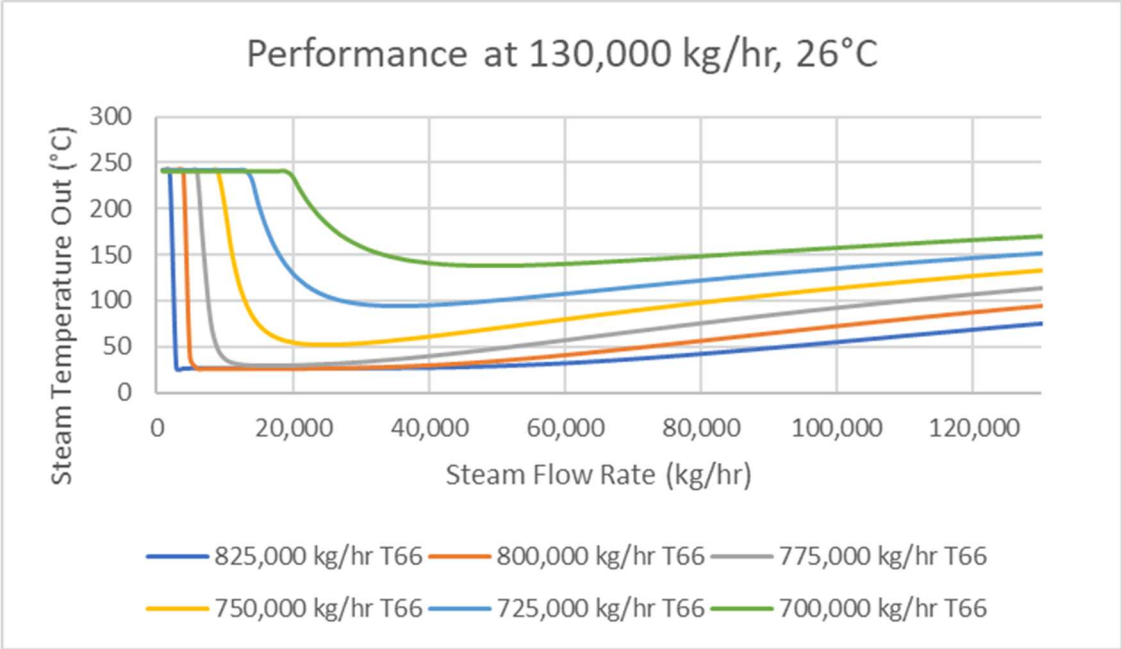

Figure 18. Performance of IHX at 130,000 kg/hr Steam, 26°C Inlet Temperature.

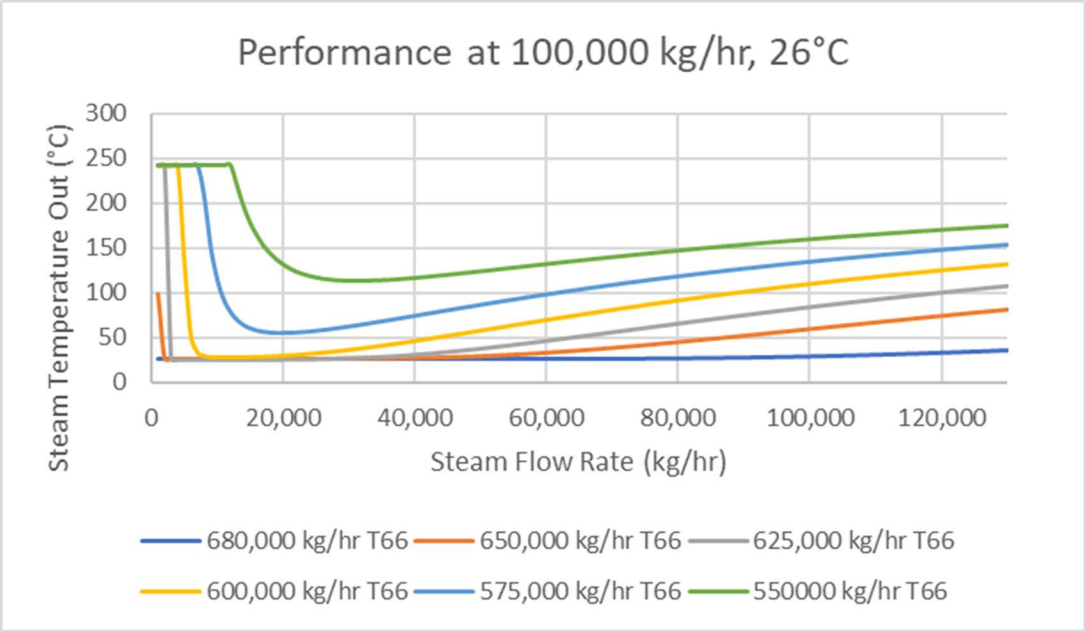

Figure 19. Performance of IHX at 100,000 kg/hr Steam, 26°C Inlet Temperature.

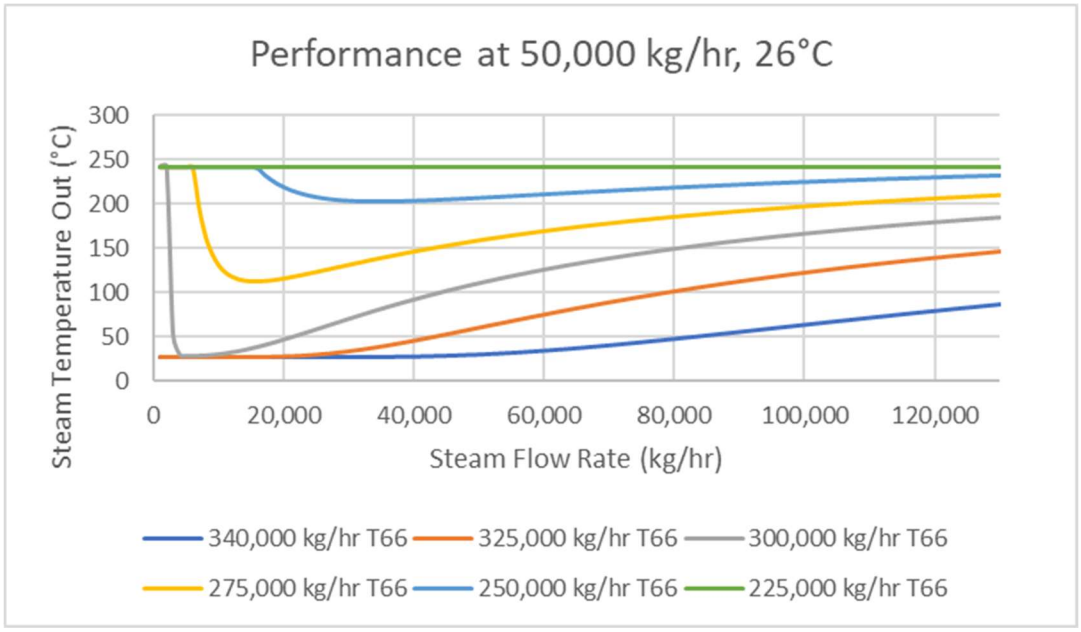

Figure 20. Performance of IHX at 50,000 kg/hr Steam, 26°C Inlet Temperature.

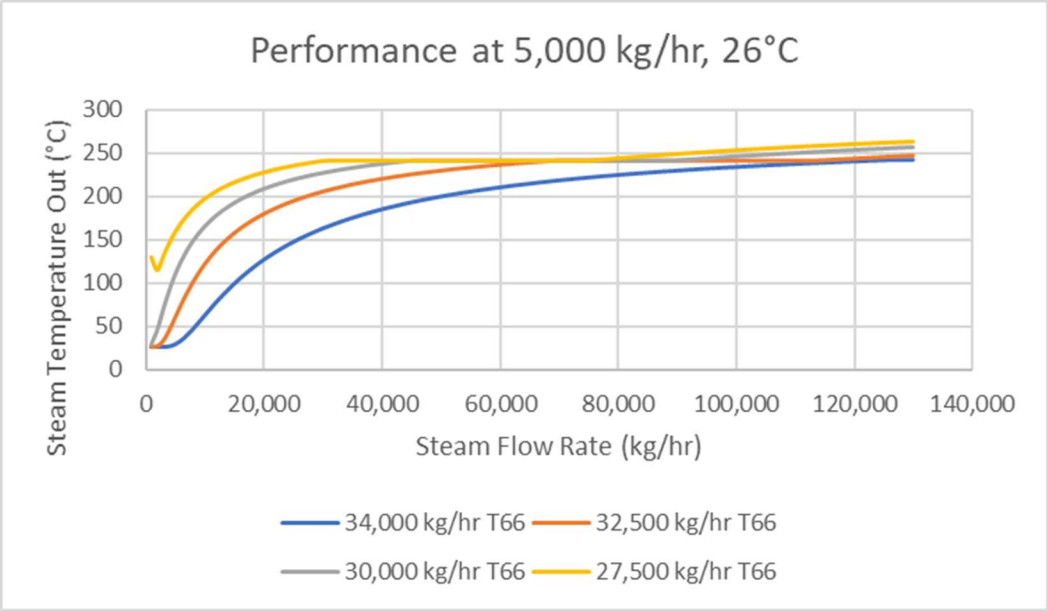

Figure 21. Performance of IHX at 5,000 kg/hr Steam, 26°C Inlet Temperature.

Another variable in the design process are determining the design steam mass flow rate. In this case, it is important to look at the variability of the steam temperature exiting the heat exchanger. A lower temperature generally means better heat transfer performance. The heat transfer rate itself across each case is not comparable, because it is a factor of area and mass flow rate which are variable across each design. Comparing the outlet temperature gives a better comparison because it is comparing processes by their product and not the process itself. At a cold tank (Therminol inlet) temperature of 40°C (Figure 22), design flow rates of 5,000 kg/hr and 100,000 kg/hr offered relatively consistent performance across the entire range of steam flow rates, although at 100,000 kg/hr the performance was significantly more consistent. The performance of the 130,000 kg/hr design did not exceed the previously mentioned flow rates and has especially poor performance at low flow rates because of a significant decrease in mass flow rate of Therminol to maintain the temperature difference across the TES system. The 5,000 kg/hr design has the worst overall performance, only matching the performance of the other flow rates

at very low flow rates. For a design temperature of, 40°C this narrows the design range to be centralized around 100,000 kg/hr.

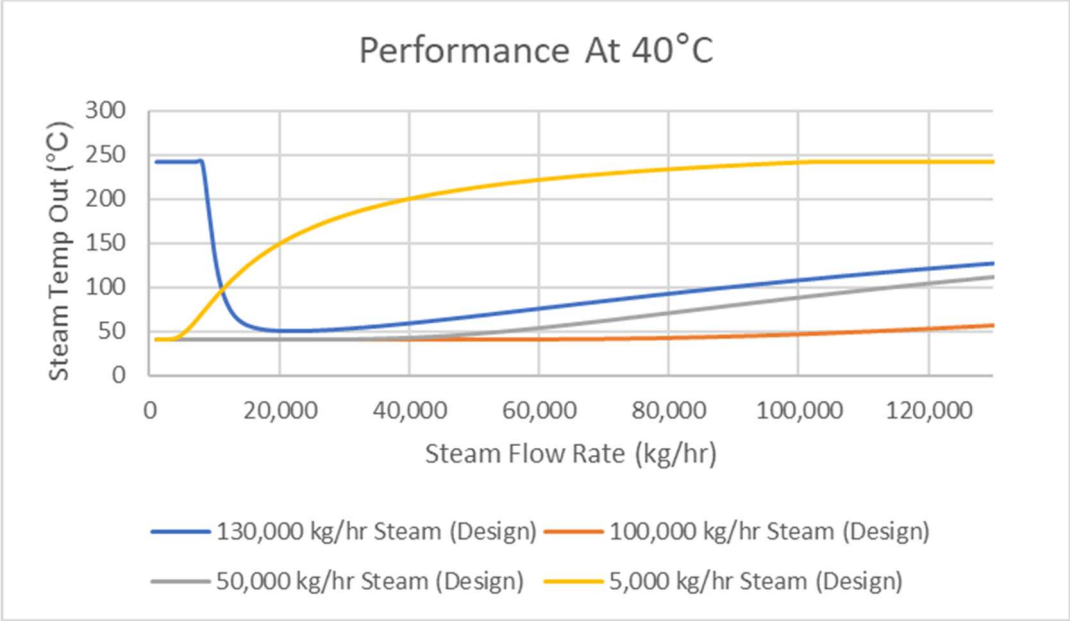

Figure 22. Performance of IHX at 40°C Inlet Temperature for All Steam Designs.

The designs showed similar performance at a design temperature of 26°C (Figure 23), although the performance at 130,000 kg/hr and 50,000 kg/hr were much closer at the upper range of flow rates. This gives further reasoning that design ranges above and below 100,000 kg/hr should be explored to find the optimum design flow rate.

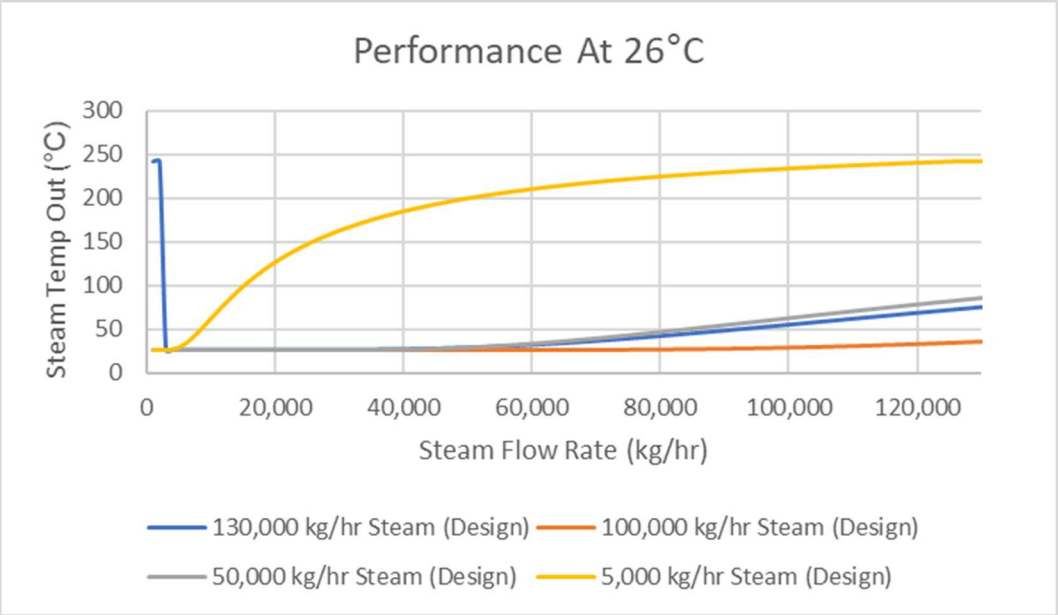

Figure 23. Performance of IHX at 26°C Inlet Temperature for All Steam Designs.

At 5°C, performance of the 100,000 kg/hr and 130,000 kg/hr designs are nearly identical across the entire design range. A smaller heat exchanger with similar performance would be best to decrease costs.

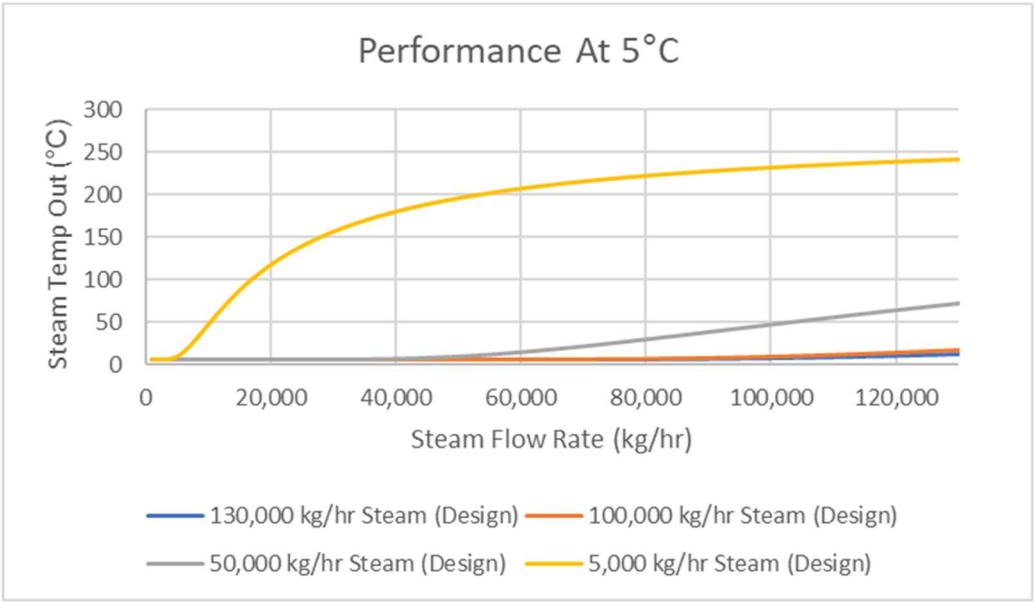

Figure 24. Performance of IHX at 5°C Inlet Temperature for All Steam Designs.

The two main variables that affect the cost of the heat exchanger are the area and the mass of the heat transfer fluid within the system. The area is static, but the total mass of fluid needed can vary based on installed pumping power. A smaller area and lower mass flow rates are preferred to decrease costs. Figure 25 shows the area of the three zones for each design case. The subcooling section contains the most area in most cases, especially those with a lower Therminol inlet temperature. A larger subcooling section could indicate that the two fluids are reaching a "pinch point," meaning the temperatures are so close that the heat transfer rate is low. Figure 26 overlays the total area with the maximum flow rate that would be needed for each design (at the maximum steam flow rate, 130,000 kg/hr).

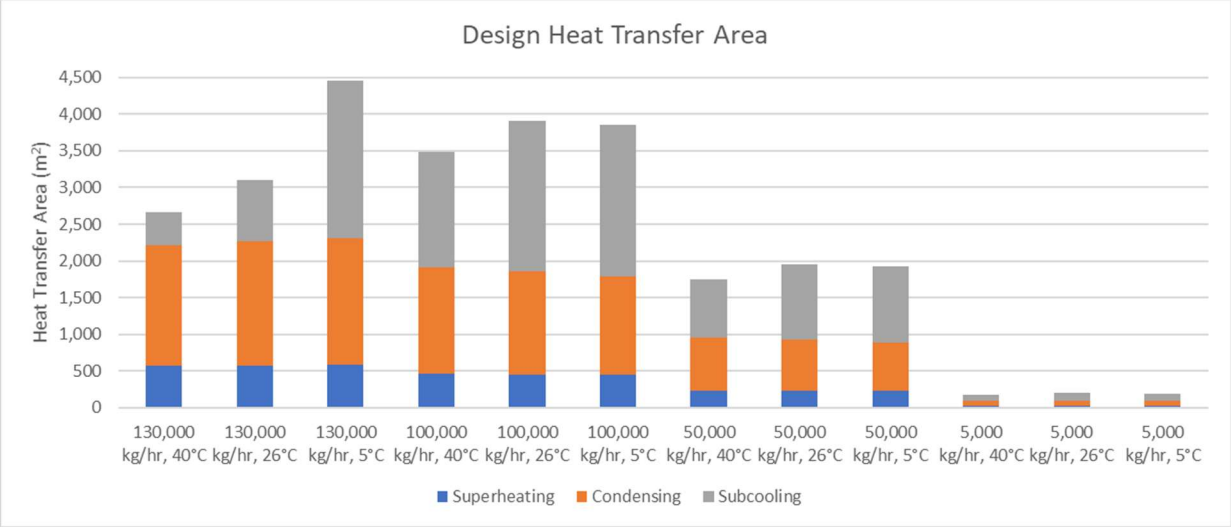

Figure 25. Design Heat Transfer Area.

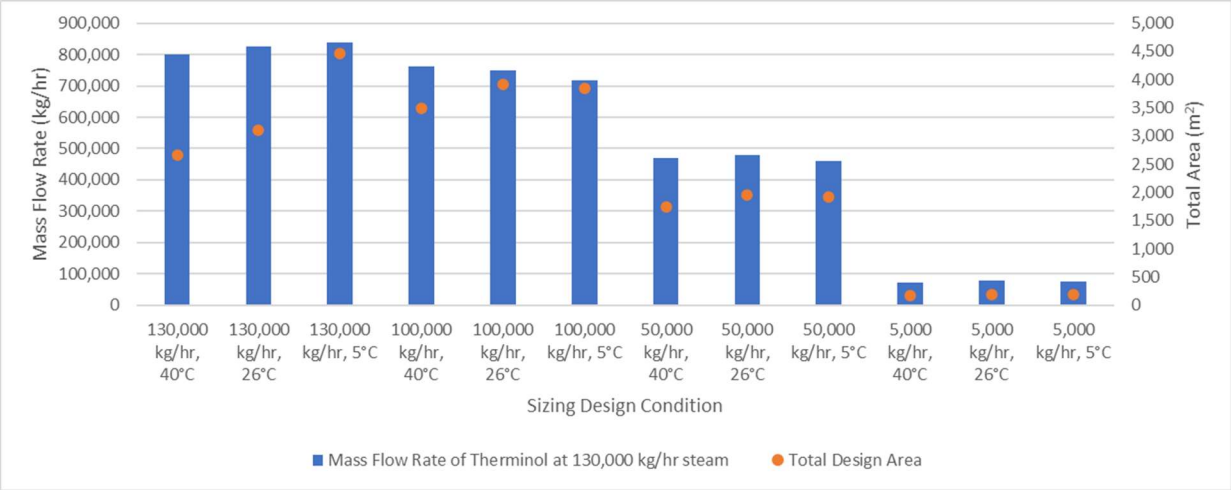

Figure 26. Therminol Mass Flow Rate Versus Design Area.

Although the area varies significantly between designs, the total heat transfer for each design at a single steam mass flow rate is less varied. At the maximum steam flow rate, Figure 27 shows an overlay of the heat transfer at this point a higher heat transfer rate does not necessarily mean a lower steam outlet temperature.

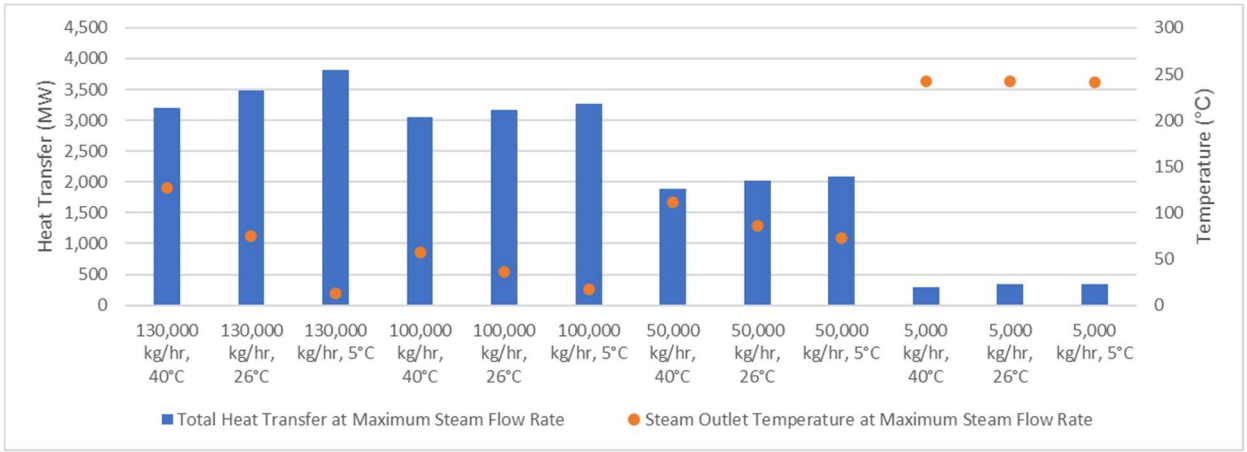

Figure 27. Total Heat Transfer Versus Steam Outlet Temperature.

Chapter 5: Carbon-Neutral Steady State Integration of the SMR and Pulp and Paper Mill

This chapter uses English units because these units are standard in Aspen HYSYS. Chapters 3 and 6 use Metric units because that is the INL standard.

5.1 Background

The major consumer of fossil fuels in the kraft cycle is the combustion of natural gas for heat, which causes the reactions for calcination of lime in the lime kiln. The calcination process releases about 0.786 lb (.357 kg) of CO_2 for every 1 lb (.45 kg) of quicklime produced [64]. When added to the carbon dioxide production by combustion, the amount is not trivial; emissions from the lime industry are near 1% of the total produced by humans [65]. Eliminating the use of fossil fuels to produce heat would have a significant impact on making the kraft process carbon neutral.

This paper presents alternative sources of thermal energy to replace fossil fuel combustion in the lime kiln. The ideal energy source would have minimal capital cost and alterations to the current process or equipment while eliminating CO_2 emissions of combustion. The three sources considered are concentrated solar power, biomass combustion, and electric heating. The ideal solution is one that reaches an operating temperature of 1,652°F (900°C), requires no alterations to the chemical recovery cycle and minimal alterations to the existing equipment, is commercially available and is available for continuous 24-hour operation.

5.2 Steady-State Plant Analysis

Two integrated paper mills are studied for integration with an SMR Two integrated paper mills are studied for integration with an SMR. In each case, the system was integrated to incorporate minimal structural changes to the mill. However, the real data provided from the mill supports the changing of steam flow through the turbines, as the system can change steam flow

through the turbines from about 40% to 110% of the steady-state steam flow rates in order to meet the demands of the plant.

5.2.1 Plant A

Plant A is a medium-sized integrated pulp and paper mill in the Southeastern United States. Total steam demand is approximately 1.6 million lb/hr (202 kg/s) with 85% of steam produced by carbon-neutral wood waste. The plant generates up to 100 MW electricity from two turbines that can meet the electricity demands of the plant. The plant buys and sells additional electricity based on the demands of the plant and production factors that affect the generation of the turbines.

Plant A produces 1500 psia (103.4 bar) steam from 4 boilers: 2 recovery boilers, 1 natural gas power boiler, and 1 bark power boiler. The steam is fed in parallel to two turbines. Some steam exits turbine 2 at 400 psia (27.6 bar) and is used for small secondary operations. Both turbines output medium pressure steam at 160 psia (11.1 bar) and low pressure at 65 psia (4.5 bar). Steam that is not utilized by the process is sent to the condenser, about 6% of the total produced.

The plant produces much more low-pressure steam than medium pressure. The majority of low-pressure steam is used in the evaporator, deaerator, pulp and paper drying and digesting. Some is used to produce chlorine dioxide, an important chemical in the paper making process. Medium pressure steam is also used in the digesting and drying processes, with a portion used for smelt recovery.

A steady-state model of the plant was created based on a combination of process standard operation as well as single point snapshots during plant operation. Figure 28 shows the steady-state model created in ASPEN HYSYS.

To integrate the SMR, the availability of steam at specific pressures and temperatures must be taken into consideration. Each module can produce up to 531,846 lbm steam per hour, with up to 50% [3] available to be taken off the main steam line. Steam is taken from the main steam header at 500 psia (34.5 bar) and 584°F (307°C). This steam must go through an in intermediate heat exchanger to ensure that the steam used in the process is not activated, or radioactive in some way, due to the SMR. Although the conditions of the steam exiting the intermediate heat exchanger (IHX) have not been determined, it is estimated conservatively to be 400 psia (27.6 bar) and 500°F (260°C).

Figure 29 describes the proposed integration of the SMR, with a goal of requiring as few design changes and equipment addition to the process as possible.

First, the high-pressure steam exiting the IHX does not meet the 1500 psia (103.4 bar)criteria of the boiler steam, but it could be substituted for the 400 psia (27.6 bar) steam exiting Turbine 1. Some steam will be diverted from the IHX to meet the mass flow criteria of the 400 psia steam. The rest is diverted into the second turbine stage with the rest of the 400 psia steam from stage 1.

Some electricity will still be generated by the on-site turbines. By developing a steady-state model, the makeup steam needed for replacing carbon fuel sources and the power produced by the turbines can be estimated.

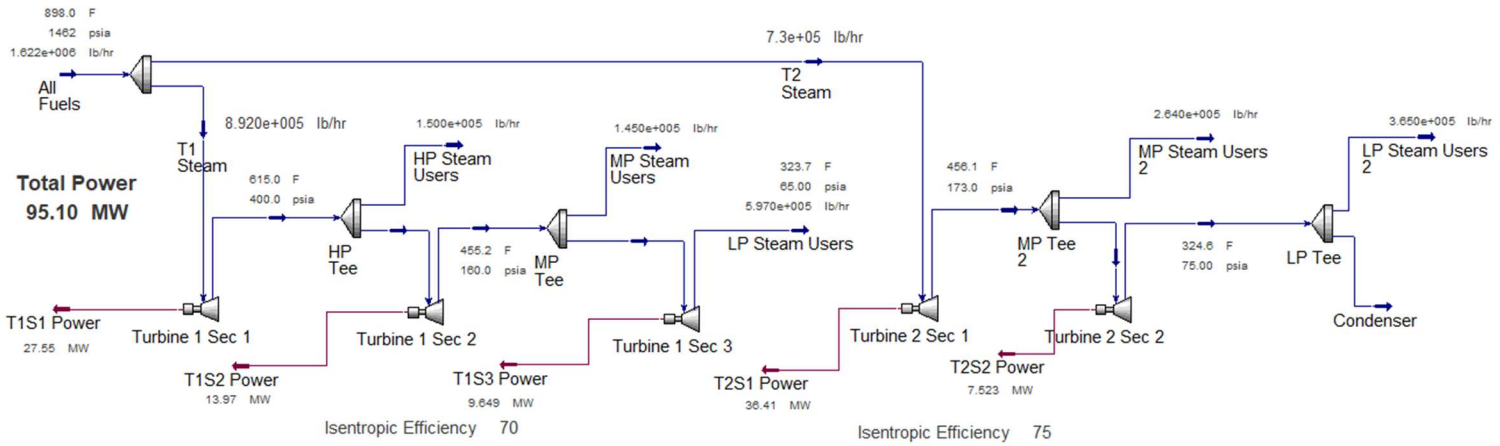

Figure 28. Steady-State Model of Plant A without SMR Integration.

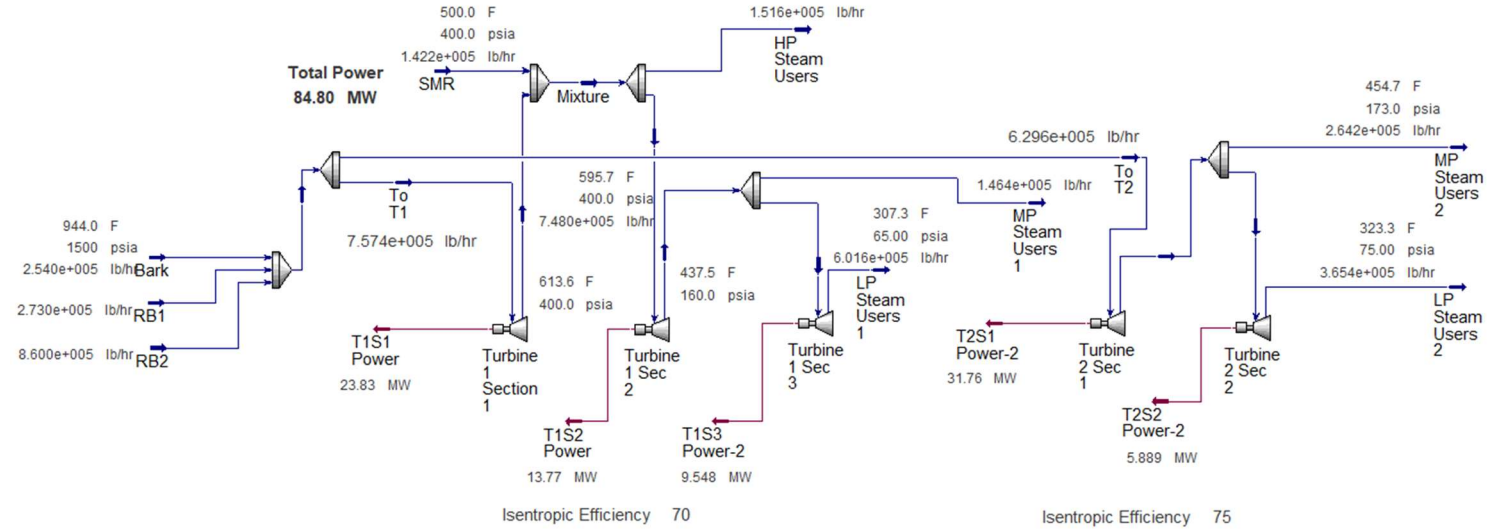

Figure 29. Steady-State Model of Plant A with SMR Integration.

5.2.2 Plant B

Plant B is a medium-sized integrated pulp and paper mill in the Southeastern United States. Total steam demand is approximately 1.7 million lb/hr (214 kg/s) with 36% of steam produced by carbon-neutral wood waste. The plant generates up to 53 MW electricity from two turbines that provide about half of the 86 MW demand for the plant. The plant buys additional electricity from the local utility.

Plant B produces 415 psia (28.6 bar) steam from 5 boilers that burn natural gas and some bark, and 2 black liquor recovery boilers. Steam is extracted after Turbine 1 at 140 psia (9.7 bar) for medium pressure steam and continues to Turbine 2 where it is extracted at 50 psia (3.4 bar) for low pressure steam. Major steam users of the medium pressure steam are paper drying and the multi-effect evaporator. Low pressure steam is used in the digester.

A steady-state model of the plant was created based on standard operations of the plant. The data is outdated, so it was adjusted to project typical improvements in operation and efficiency.

Steam coming from the SMR is estimated to be at or above 400 psia (27.6 psia), so it can be incorporated into the rest of the steam sources and flow directly into the first turbine. However, the steam temperature is significantly below the 700°F (371°C) of the other sources, so more steam will be required from the SMR than the original natural gas source. The low pressure (LP) and medium pressure (MP) steam flow rates will increase as well to meet the heat flow requirements of those streams.

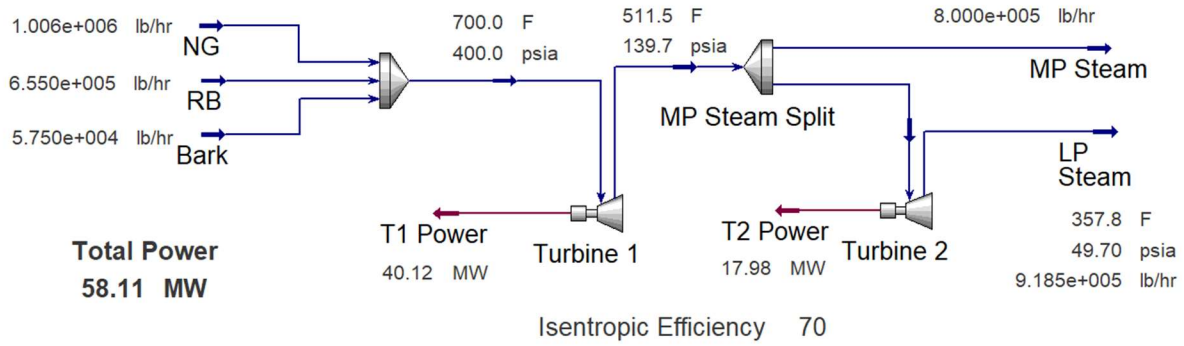

Figure 30. Steady-State Model of Plant B without SMR Integration.

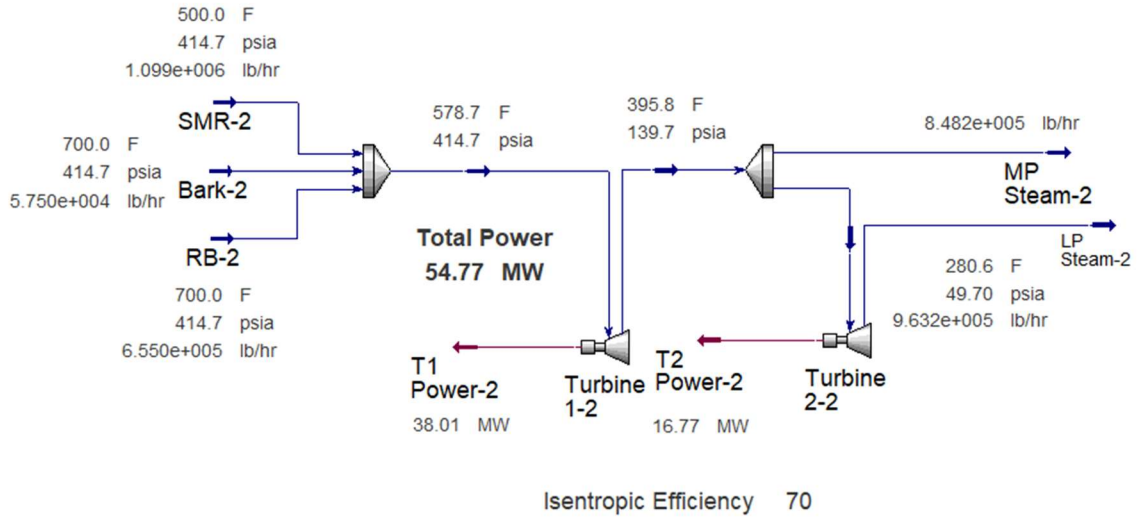

Figure 31. Steady-State Model of Plant B with SMR Integration.

5.3 Summary of Thermal Sources

5.3.1 Black Liquor Gasification

Black liquor gasification technology has been presented as an attractive option for pulp and paper mills over the last several decades, however its impact on the Kraft process leaves many questions about its viability in practice. The combustion of black liquor is vital to the chemical recovery process, removing unwanted solids and providing steam for the mill. An SMR

can make up for the lost steam generation while syngas provides heat for the lime kiln, replacing natural gas and reducing the carbon impact of the mill. The remaining question involves the impact of gasification on the chemistry of the recover process occurring in the lime kiln.

A detailed description of BLGCC technology and its challenges is given in Chapter 2. The considerations for coupling a black liquor gasification process to the kraft cycle reduce the feasibility for using gasification as a replacement for fossil fuels in other areas of the manufacturing process. There is developing research to modify the chemical recovery process to decrease the impact of gasification, however it is unlikely that an existing mill would be willing to make these changes.

5.3.2 Concentrated Solar Power

Concentrated solar power (CSP) has been extensively studied as a carbon-free alternative for lime and cement production because of its ability to produce high temperature fluids. Commercially available technology for CSP includes parabolic trough solar collectors (Figure 32) and tower collectors (Figure 33). Parabolic trough collectors are curved mirrors which focus energy into a central receiver which contains a heated fluid with normal operating temperatures from 662-1,022°F (350-550°C). Solar towers use a series of mirrors focused on a central receiver in the tower to collect radiation. Typical operating temperatures are between 482-1,049°F (250-565°C) [66].

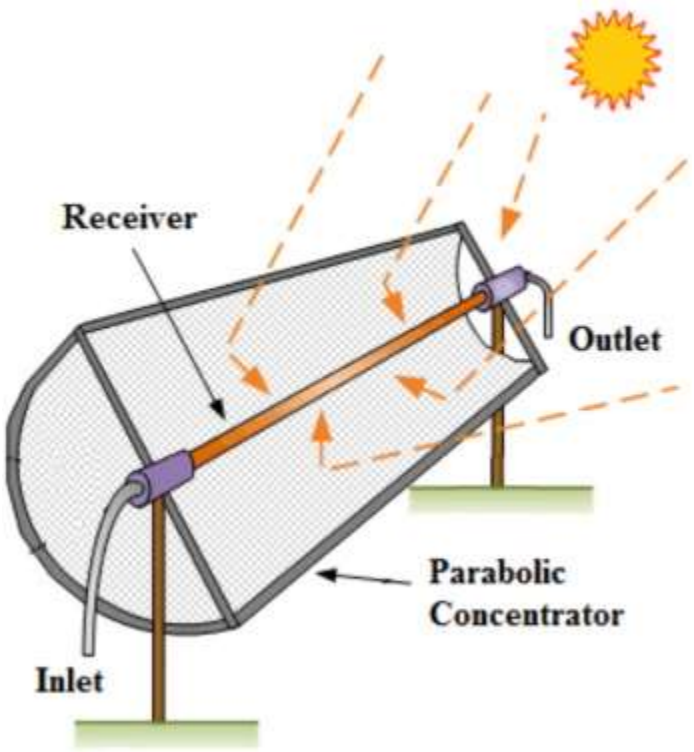

Figure 32. Parabolic Trough Solar Concentrator System [67].

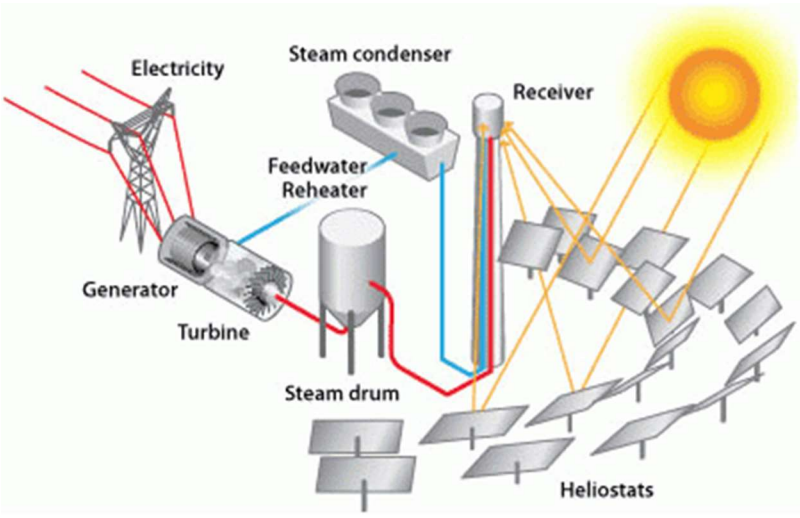

Figure 33. Concentrated Solar Power Tower [68].

To effectively implement CSP, the location of the system must be considered. We will focus on paper mills in the Carolinas, which, based on Figure 34 and Figure 35, receive between

4.5 and 5.2 kWh/m^2/day of solar radiation. Due to the high heat consumption of the kiln and its continuous operation, it would require a large system to provide heat and storage for production. A large system will also require a large parcel of land located as closely as possible to the plant to reduce losses. To produce just 1 MW demand for the entire day in the highest radiation region, the plant would require a PV area of:

$$5.2\frac{kWh}{m^2} * \frac{1\,MWh}{1000\,kWh} = \frac{1}{0.0052}\frac{m^2}{MWh} = 192.3\frac{m^2}{MWh} * 24\frac{MWh}{day} = 4{,}615\,m^2$$

In some areas of Southern New Mexico, the country receives the highest solar irradiation at 8.5 kWh/m^2 [69]. To produce 1 MW demand for the entire day, the plant would require a PV area of:

$$8.5\frac{kWh}{m^2} * \frac{1\,MWh}{1000\,kWh} = \frac{1}{0.0052}\frac{m^2}{MWh} = 117.3\frac{m^2}{MWh} * 24\frac{MWh}{day} = 2{,}823\,m^2$$

Even in the highest radiation regions of the United States, a large amount of land is required to achieve a system of the necessary size.

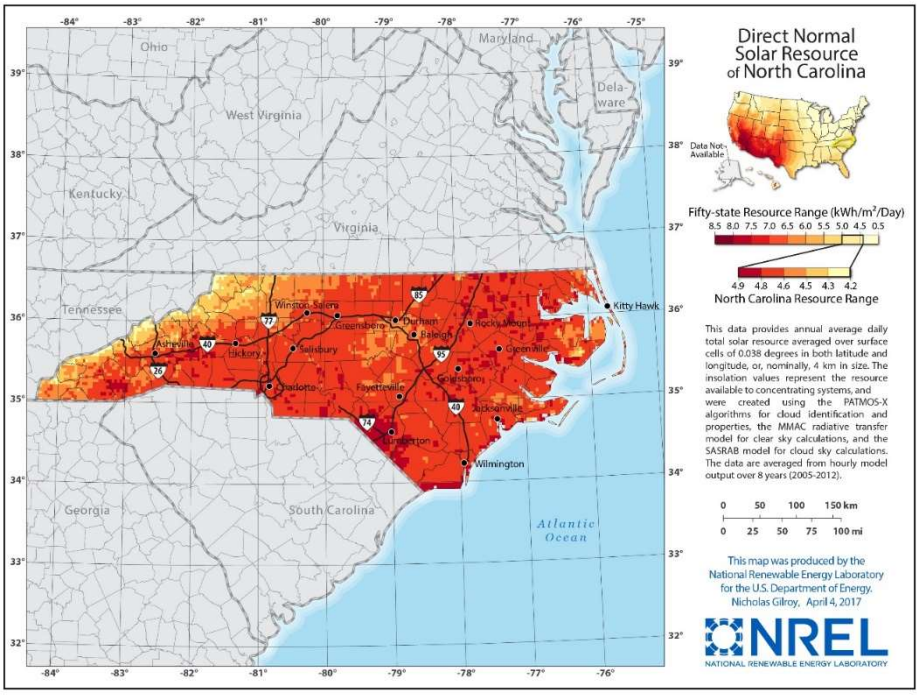

Figure 34. Direct Normal Solar Resource Map of North Carolina [69].

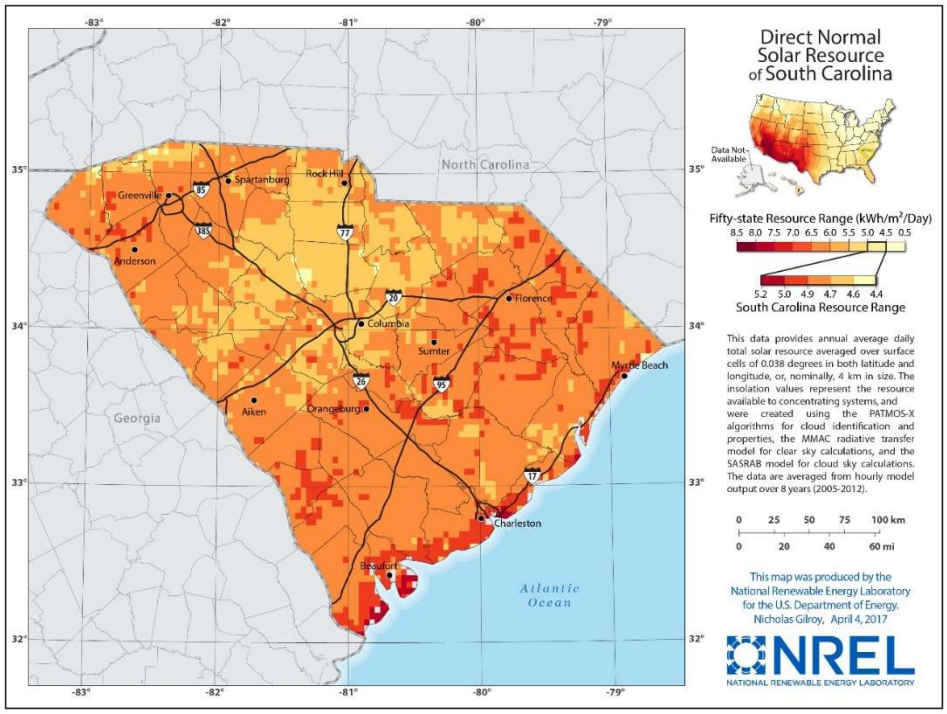

Figure 35. Direct Normal Solar Resource Map of South Carolina [69].

Commercially available CSP is not currently feasible to replace heat from fossil fuels in a currently operating kraft paper mill. The Carolinas do not receive enough solar radiation to make it an economic option at the scale which would be required, and additional heating may be required to reach operating temperature of the kiln. Additionally, the intermittency of solar radiation causes complications for the mill's 24-hour operation, as storage and a backup power source would be required.

5.3.3 Biomass Fuel

A common suggestion for the replacement of any fossil fuel is biomass feedstock. Replacement of the fuel only would require minimal modifications to the current process and equipment while providing an environmentally friendly alternative. Unlike black liquor gasification, biofuels in the form of syngas or bio-oil can be purchased so production would not be needed on-site.

Typically, biomass is a good alternative for processes that produce waste that would otherwise by discarded. The kraft process already utilizes most of its waste products, including firing wood waste to generate steam. An SMR could make up for the lost steam if the wood waste was used elsewhere, but unless a process is built on-site, the waste would have to be transported elsewhere and the fuel brought back for use. This could end of being a costly alternative, especially when a process already exists to utilize this waste.

5.3.4 Hydrogen

Kuparinen and Vakkilainen studied hydrogen as an alternative to fuel oil in the lime kiln. Hydrogen is an attractive fuel because its combustion results in water, does not create carbon dioxide. Hydrogen can also be produced by electricity, which could be provided by the SMR. Integrating the production of hydrogen into the mill would require significant modifications to

the mill. Additionally, an analysis of the mill showed that hydrogen is only an economic replacement for a current fuel at extremely high prices [70], as shown in Figure 36.

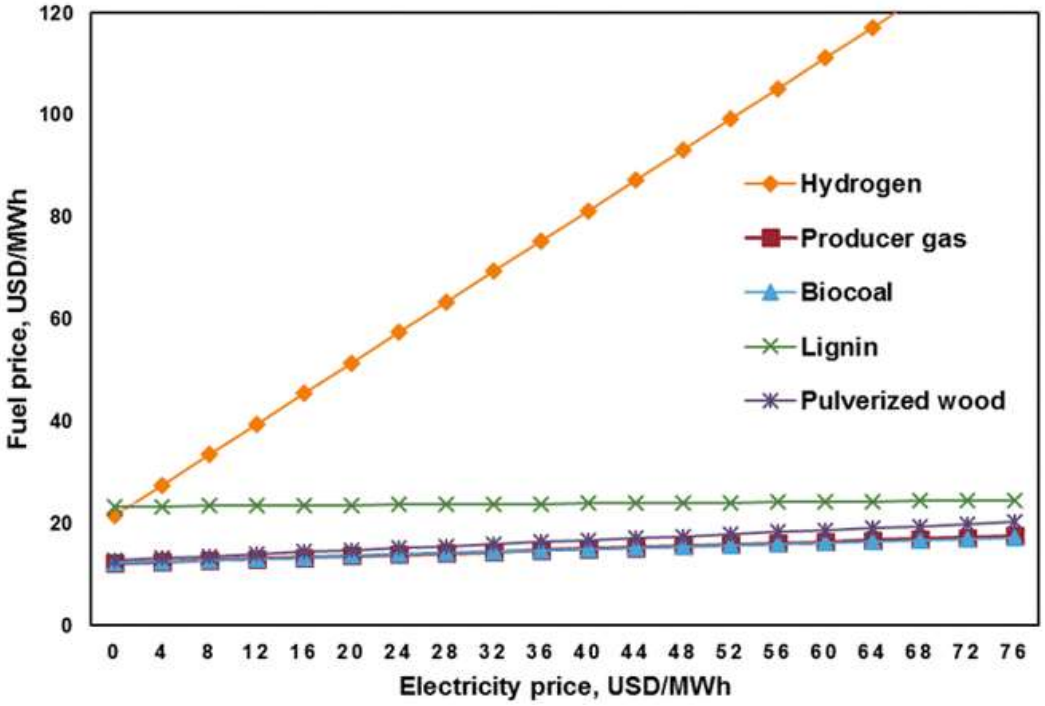

Figure 36. The Breakeven Lime Kiln Fuel Price for the Studied Concepts as a Function of Electricity Price [70].

Hydrogen may be a viable option as a lime kiln fuel if a hydrogen plant co-located with a paper mill to share steam and electricity production from an SMR. Costs associated with the SMR could be shared in exchange for the mill buying hydrogen at a lower price. Because the SMR is based on an economy of multiples rather than an economy of scale, utilizing additional modules in a single plant would bring down costs for both users.

5.3.5 Electric Heating

Electrically heated rotary kilns are not a new concept, but they are generally not used in industry because the price of electricity compared to other fuels. There is not any data available on these kilns, although they are patented and produced in China. Current gas fired kilns could

be retrofitted with electric heating elements, and with electricity produced by the SMR, the price of electricity could become trivial while cutting emissions from the lime kiln.

Despite the material and research costs required to make this option viable for a currently operating kraft process, electric heating still stands out as the optimal replacement for natural gas. Current research shows that only 50% [58] of steam from a module can be extracted from the main steam line and used for thermal power. This means that the SMR will constantly be producing some amount of electricity. This electricity could be used to power the mill, other facilities on site, and the lime kiln. Any excess electricity produced can be sold back to the grid. The only cost associated with producing electricity for the lime kiln is the revenue lost if the electricity was otherwise sold.

One major operating difference between the electric lime kiln and the natural gas kiln is the elimination of additional heat used to evaporate water from the combustion process. When natural gas is combusted in the lime kiln, the combustion products consist of carbon dioxide and water.

$$CH_4 + 2\ O_2 \rightarrow CO_2 + 2\ H_2O$$

The H_2O leaves the stack as steam, and the CO_2 reacts to create lime. Using the electric lime kiln rather than a combustion kiln will save additional heat input on top of the carbon savings

5.4 Electric Kiln Demand Analysis

5.4.1 Plant A

The plant analyzed in this study has two natural gas-fired lime kilns which produce a total of 525 tpd of quicklime and utilize a total of 104 MCFH of fuel. Assuming the plant runs at full capacity 24 hours a day, 350 days a year (to account for delays and outages), the breakeven

cost of converting kilns from natural gas to electric, the lost revenue from electricity sales, and the number of modules needed to meet demand can be calculated. The information given by the plant is shown in Table 2.

Table 2. Lime Production and Natural Gas Consumption at Plant A.

	Load (tons/day)	Demand (MMBTU/ton)	Ave. Natural Gas Use (MCFH)
Lime Kiln 1	200	7	60
Lime Kiln 2	325	6	84

In 2018, the average industrial price of natural gas in North Carolina throughout the year was $6.08/MCF [71]. Based on this price, the cost of natural gas from the lime kilns over the course of a year is:

$$(60\ MCFH + 84\ MCFH) * 350\ days * 24\frac{hours}{day} * \frac{\$6.08}{MCF} = \mathbf{\$7.4\ million}$$

First, it is important to note the current demands of the plant. The plant generates about 100 MW of electricity on site to meet its demand. The total demand for both medium and low-pressure steam is approximately 1.4 million lb/hr (176 kg/s). Each module can produce up to 531,846 lb of steam per hour, with up to 50% [58] available to be taken off the main steam line. The steady-state model estimates that the on-site turbines will generate 84.8 MW when the system is connected to an SMR.

The total electricity demand in MW for the kilns can be calculated from the MMBTU/hr demand of natural gas.

$$200\frac{tons}{day} * 7\frac{MMBTU}{ton} + 325\frac{tons}{day} * 6\frac{MMBTU}{ton} = 3{,}350\frac{MMBTU}{day}$$

$$3{,}350\frac{MMBTU}{day} * \frac{1\ day}{24\ hours} = 139.6\frac{MMBTU}{hr}$$

$$1{,}637.5\frac{MMBTU}{hr} * 0.29307\frac{MW}{\frac{MMBTU}{hr}} = \mathbf{41\ MW}$$

The 41 MW calculated is very conservative when switching from a combustion kiln to an electric kiln. The electric kiln eliminates the hot exhaust losses from the stack as well as losses from the water vapor created during the combustion process.

The stack losses can be calculated based on the losses due to water vapor at 90 lb water vapor created for 1 MMBTU natural gas (3.8 kg for 100 MJ), and the difference in enthalpy from the stack conditions and liquid water at atmospheric conditions.

Table 3. Conditions to Determine Stack Losses.

	Temperature (°F)	Pressure (psia)	Specific Enthalpy (Btu/lb)
Stack Conditions (superheated steam)	500	20	1287
Atmospheric Conditions (liquid water)	77	14	45

The heat loss is about 1,242 Btu/lb (2,889 kJ/kg). Plant A uses 139.6 MMBTU (147,286 MJ) Natural gas per hour.

$$\left(1287\frac{Btu}{lb} - 45\frac{Btu}{lb}\right) * 139.6\frac{MMBTU\ NG}{hr} * 90\frac{lb\ water}{MMBTU\ NG} = 15.6\frac{MMBtu}{hr}$$

$$\frac{15.6}{139.6}\frac{MMBTU}{hr} = 11\%\ Stack\ Loss$$

A more reasonable but still conservative estimate for the heat needed in the electric kiln is about 90% of the original estimate.

$$41\ MW * 90\% = \mathbf{37\ MW}$$

The total MWh generated by this system in a year is calculated below.

$$37\ MW * 24\frac{hours}{day} * 350\frac{days}{year} = \mathbf{310,800}\frac{\boldsymbol{MWh}}{\boldsymbol{year}}$$

With the addition of electric lime kilns, the total electricity demand of the plant is:

$$100\ MW + 37\ MW = \mathbf{137}\ \boldsymbol{MW}$$

In the steady-state model, the SMR must provide 142,200 lbm steam to make up the loss of NG generated steam. In an ideal situation, the SMR would use 50% of its capacity to generate steam, or 265,923 lbm, and 50% to generate electricity, or 30 MW. The number of modules needed to meet the steam demand of the plant can be found by dividing the total steam demand by the maximum steam available from each module.

$$\frac{142{,}200\ lb\ steam}{265{,}923\frac{lb\ steam}{module}} = \mathbf{0.54}\ \boldsymbol{split\ modules}$$

The electricity that these modules will produce is calculated below. Since only a portion of the split module is needed to produce steam, the rest of the capacity can be used to produce more than 30 MW for the SMR.

$$\frac{531{,}846\ lbm - 142{,}200\ lbm}{531{,}846\ lbm} * 60\ MW = 73\% * 60\ MW = \mathbf{43.8}\ \boldsymbol{MW}$$

The total electricity generated by the site is calculated by adding the SMR electricity generation to the generation from the existing turbines.

$$43.8\ MW + 84.8\ MW = \mathbf{129}\ \boldsymbol{MW}$$

Based on the assumptions, the difference between the demand and generation is:

$$129\ MW\ generated - 137\ MW\ demand = -\mathbf{8}\ \boldsymbol{MW}$$

Using only one module to produce exactly the amount of steam needed for the process results in an 8 MW deficit for the plant. There are multiple options available to the plant to make up for this deficit.

Option 1: Continue supplementing electricity with natural gas generator

This option would not require any capital cost investments, but it would difficult to implement a control system to maintain steam quality throughout the plant and generate the proper amount of electricity. Using natural gas to produce electricity requires more steam to be put through the turbines. This would decrease the steam demand from the SMR, increasing electricity generation on the SMR side. The variation in steam between the NG side and SMR side also creates a difficult control scheme to vary flow. Even if this is an economical option, it ultimately nullifies many of the benefits of the SMR: eliminating natural gas purchases and converting the plant to carbon neutral.

Option 2: Purchase electricity from a local utility at industrial rates

This option would require no implementation or capital cost expenditures because the plant is already connected to the grid. However, purchasing electricity from a utility could become costly, and it would be unlikely that this option would allow the plant to be carbon-neutral, which is the major benefit of using the SMR.

The average industrial electricity price in North Carolina is 6.42 ¢/kWh [72]. The yearly cost of this option would be approximately:

$$8\,MW * 1000\,\frac{kW}{MW} * 350\,days * 24\,\frac{hours}{day} * 0.0642\,\frac{\$}{kWh} = \mathbf{\$4.3\ Million}$$

This price would vary based on the rate schedule and changes in demand of the plant. The price of purchasing electricity is less than the $7.4 million the plant spends on natural gas for the lime kilns each year.

Option 3: Install renewable electricity such as solar or wind

Installing a renewable source of electricity would allow the plant to claim it is carbon neutral. These renewables have a high capital cost but low yearly maintenance.

The estimated LCOE (levelized cost of electricity) for new solar generation resources entering service in 2022 is $59.10/MWh, not including tax credits [73]. For an 8 MW solar project, the cost is approximately:

$$8\,MW * 350\,days * 24\frac{hours}{day} * \frac{\$59.10}{MWh} = \mathbf{\$4.0\ million}$$

The southeast United States is not ideal for wind power, except for the immediate coastline and a few mountain ranges. In some locations, it may be an option. The estimated LCOE for new onshore generation resources entering service in 2022 is $48/MWh, not including tax credits [73]. For an 8 MW wind project, the cost is approximately:

$$8\,MW * 350\,days * 24\frac{hours}{day} * \frac{\$48}{MWh} = \mathbf{\$3.2\ million}$$

While these costs are lower per year than purchasing electricity from a utility, it was previously discussed that intermittent renewables are not ideal for processes that run at all times of the day. Additional storage capacity would be needed to make this a feasible option. In addition to the high construction costs, these projects will require lots of open land which may or may not be available near the plant.

Option 4: Install a second module

Installing a second module would increase the total generation capacity of the SMR for 60 to 120 MW. NuScale targets a LCOE of $65/MWh for its first plant [73]. If one module is already installed, another 60 MW module installation would cost:

$$60\,MW * 350\,days * 24\frac{hours}{day} * \frac{\$65}{MWh} = \mathbf{\$32.7\ million}$$

Although the plant only needs 8 MW, it is most efficient to run a nuclear generator at maximum capacity all the time. 60 MW additional is far too much electricity to be utilized by the plant itself, and too much to sell back to the grid. The amount and retail price of electricity

depends entirely on the laws of the state and the policy of the utility. In net metering states, utilities are required to purchase electricity back from the customer at the retail price, however, there are typically caps on the amount you can sell back. At the time of this writing, North Carolina allows projects up to 1 MW to be connected to the grid via net metering, and South Carolina has a limit of 20 kW. In order to sell this electricity to a utility, the plant would likely need to enter into a Power Purchase Agreement (PPA). With a PPA, the plant will most likely be expected to provide a consistent amount of electricity to the grid, so there will still be some over generation to allow for variations in demand of the plant.

It is difficult to calculate the cost that may be offset by a PPA because there is no data for existing nuclear PPAs, however, PPAs are typically slightly above the price of generation. If the facility were to break even on 30 MW sold to a utility, the price would halve from $32.7 million to $16.35 million.

Although there isn't any history of nuclear power plants with PPAs, it's not unlikely that this would be a smart investment by utilities in the future as renewable installation increases and baseload powerplants lose profitability.

5.4.2 Plant B

The plant analyzed in this study has two natural gas-fired lime kilns which produce a total of 350 tpd of quicklime and utilize a total of 104 MCFH of fuel. Assuming the plant runs at full capacity 24 hours a day, 350 days a year (to account for delays and outages), the breakeven cost of converting kilns from natural gas to electric, the lost revenue from electricity sales, and the number of modules needed to meet demand can be calculated. The information given by the plant is shown in Table 4.

Table 4. Lime production and natural gas consumption at Plant B.

	Load (tons/day)	Demand (MMBTU/ton)	Ave. Natural Gas Use (MCFH)
Lime Kiln 1	222	9.3	100
Lime Kiln 2	128	9.3	60

In 2018, the average industrial price of natural gas in North Carolina throughout the year was $6.08/MCF. Based on this price, the cost of natural gas from the lime kilns over the course of a year is:

$$(100\ MCFH + 60\ MCFH) * 350\ days * 24 \frac{hours}{day} * \frac{\$6.08}{MCF} = \$\mathbf{8.2\ million}$$

First, it is important to note the current demands of the plant. The plant generates about 53 MW of electricity on site and purchases 30 MW to meet its demand. The total demand for both medium and low-pressure steam is approximately 1.10 million lb/hr (139 kg/s). Each module can produce up to 531,846 lb of steam per hour, with up to 50% available to be taken off the main steam line. The steady-state model estimates that the on-site turbines will generate 54.77 MW when the system is connected to an SMR.

The total electricity demand in MW for the kilns can be calculated from the MMBTU/hr demand of natural gas.

$$222 \frac{tons}{day} * 9.3 \frac{MMBTU}{ton} + 128 \frac{tons}{day} * 9.3 \frac{MMBTU}{ton} = 3255 \frac{MMBTU}{day}$$

$$3255 \frac{MMBTU}{day} * \frac{1\ day}{24\ hours} = 135.6 \frac{MMBTU}{hr}$$

$$135.6 \frac{MMBTU}{hr} * 0.29307 \frac{MW}{\frac{MMBTU}{hr}} = \mathbf{31\ MW}$$

According to Table 3, the heat loss from water vapor is about 1,242 Btu/lb (2,889 kJ/kg). Plant B uses 139.6 MMBTU (147,286 MJ) natural gas per hour.

$$\left(1287\frac{Btu}{lb} - 45\frac{Btu}{lb}\right) * 135.6\frac{MMBTU\ NG}{hr} * 90\frac{lb\ water}{MMBTU\ NG} = 15.2\frac{MMBtu}{hr}$$

$$\frac{15.2}{135.6}\frac{MMBTU}{hr} = 11\%\ Stack\ Loss$$

The gain in efficiency by switching to the electric kilns is estimated at 90%, as explained in section 4.1.

$$31\ MW * 90\% = \mathbf{28\ MW}$$

The total MWh generated by this system in a year is calculated below.

$$28\ MW * 24\frac{hours}{day} * 350\frac{days}{year} = \mathbf{235,200}\frac{\mathbf{MWh}}{\mathbf{year}}$$

With the addition of electric lime kilns, the total electricity demand of the plant is:

$$83\ MW + 28\ MW = \mathbf{111\ MW}$$

In the steady-state model, the SMR must provide 1.10 million lbm steam to make up the loss of NG generated steam. In an ideal situation, the SMR would use 50% of its capacity to generate steam, or 265,923 lbm, and 50% to generate electricity, or 30 MW. The number of modules needed to meet the steam demand of the plant can be found by dividing the total steam demand by the maximum steam available from each module.

$$\frac{1{,}099{,}000\ lb\ steam}{265{,}923\ \frac{lb\ steam}{module}} = \mathbf{4.13\ split\ modules}$$

The plant will require 5 modules to accommodate the 4.13 split modules needed to produce steam. The electricity that these modules will produce is calculated below. 4 modules will be fully utilized module to produce 30 MW electricity (half of the 60 MW capability). The

fifth module can generate more than 30 MW of steam because it is only partially utilized with steam.

$$4\ modules * 30\ MW + \frac{(1 - .13) * 531{,}846\ lbm}{531,846\ lbm} * 60\ MW = 120\ MW + 87\% * 60\ MW$$

$$= \mathbf{176\ MW}$$

The total electricity generated by the site is calculated by adding the SMR electricity generation to the generation from the existing turbines.

$$54.77\ MW + 176\ MW = \mathbf{231\ MW}$$

Based on the assumptions, the difference between the demand and generation is:

$$231\ MW\ generated - 111\ MW\ demand = \mathbf{+120\ MW}$$

Using 5 modules to produce exactly the amount of steam needed for the process results in a 120 MW overgeneration for the plant. This is because the plant has a very high steam demand and low electricity demand. As discussed for Plant A, Plant B could enter a PPA with a local utility to make up for this. In this case, there is no economic alternative to using the electric lime kilns, because continuing to use gas kilns will result in an even greater overgeneration.

5.5 Cost Analysis

The following cost analysis determines the break-even price for replacing the gas heated lime kilns with electric kilns. This cost only includes the kilns themselves, because the SMR cannot replace the natural gas needed to fuel the lime kilns. Because the chemical recovery process is unchanged, it is not expected that the lime loads will change significantly when using a different kiln. The breakeven price compares the price of natural gas to the price of a new kiln based on its capacity for lime produced.

5.5.1 Plant A

In Plant A, the addition of the electric lime kilns causes an electricity deficit of 8 MW. The breakeven cost of lime kiln includes the cost of installation plus 8 MW from an additional SMR module at $65/MWh LCOE. Assuming that any additional electricity is sold at the LCOE, the total cost of electricity from this module during the year is:

$$8\,MW * 350\,days * 24\frac{hours}{day} * \frac{\$65}{MWh} = \mathbf{\$4.37\ million}$$

The total tons of lime produced during the year is:

$$525\frac{tons}{day} * 350\,days * 24\frac{hours}{day} = \mathbf{4.41\ million\ tons}$$

The cost of electricity per ton of lime produced becomes:

$$\frac{\$4.37\ million}{4.41\ million\ tons} = \frac{\mathbf{\$0.99}}{\mathbf{ton}}$$

Note that the cost of generating electricity from the SMR is similar to purchasing the electricity from a local utility. The installation cost is calculated in tons capacity of the lime kilns, 525 tons. This cost is difficult to obtain from vendors and could include additional expenses such as removal of the old kilns. Figure 10 shows the breakeven cost for just the capital cost of the kiln, and the cost including the price of generating electricity with the SMR. The breakeven cost is the maximum $/ton capacity cost to install a new lime kiln for the plant to achieve a $0 net savings at the end of the year. If the actual cost is less than the breakeven cost, savings will be realized in the first year. At the national average NG price, the kiln breakeven price is $10,000/ton, which is a very conservative estimate for the cost. It is very likely that the plant would save money at that price. When the cost of the SMR is included, there is no breakeven price until the NG Price hits close to $3.50/MCFH. This is less than the state average, but the plant would not likely breakeven until the NG price was closer to the national average.

The breakeven price per ton when electricity generation is included does not hit $10,000 until about $8/MCFH. It is not likely that the price would reach that high unless there is a nationwide energy crisis, fracking is discontinued in the United States, or high carbon taxes are implemented.

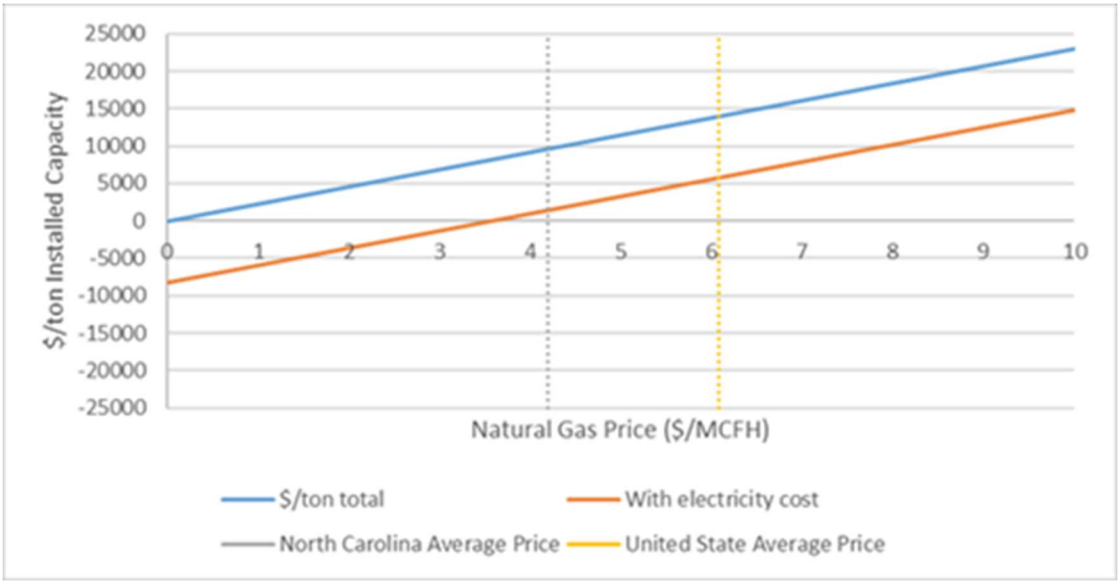

Figure 37. Breakeven Price for an Electric Lime Kiln at Plant A.

Overall, implementing electric lime kilns may not be economical for Plant A. At this time, the only benefits are the intangible benefits of carbon-free production. It is possible that if the plant profits from a PPA with a local utility, the price of electricity used by the plant would decrease and increase the savings overall. Because the price of natural gas is variable, savings may be more likely in the future operation of the plant.

Carbon Taxes

The savings from eliminating natural gas in the lime kiln are variable based on the price of natural gas. The breakeven price is the cost of installing new lime kilns which would be made

up from natural gas savings in a year. This is equivalent to the total price of natural gas from the lime kilns for one year.

Figure 38 shows how the breakeven price varies based on the price of NG and the carbon tax. The average price of natural gas per thousand cubic feet for industrial customers in the United States was $4.10 in 2017 and $4.20 in 2018 [74]. However, the price is volatile based on energy policy and could increase significantly by the time the system is installed. Price forecasts expect the price of natural gas to remain steady, only slightly increasing through 2050 [75]. Meanwhile, the environmental controversy over fracking in the United States threatens the future price based on the lawmakers. Another factor that could affect the breakeven price is carbon taxes. Although they have not been adopted nationally, carbon taxes exist in some northeastern states in California. In the northeast, the carbon tax is $5 per metric ton CO_2 [76].

Taxes incurred from the lime kiln are calculated:

$$(60 + 84\ MCFH) * 24\frac{hours}{day} * 350\frac{days}{year} * 0.059\ \frac{ton\ CO2}{MCF} * \frac{\$5}{ton\ CO2} = \frac{\mathbf{\$357,000}}{\boldsymbol{year}}$$

The total increases quickly as the tax increases. In California, the carbon tax is $15 per metric ton CO_2 [76].

$$(60 + 84\ MCFH) * 24\frac{hours}{day} * 350\frac{days}{year} * 0.059\ \frac{ton\ CO2}{MCF} * \frac{\$15}{ton\ CO2} = \frac{\mathbf{\$1,070,500}}{\boldsymbol{year}}$$

Canada plans to increase its carbon tax from $15 in 2019 to $38 in 2022 [76]. The savings from electric lime kilns in the case of carbon taxes isn't likely to be immediately realized. However, over the long lifetime of the plant, savings may increase significantly in the future.

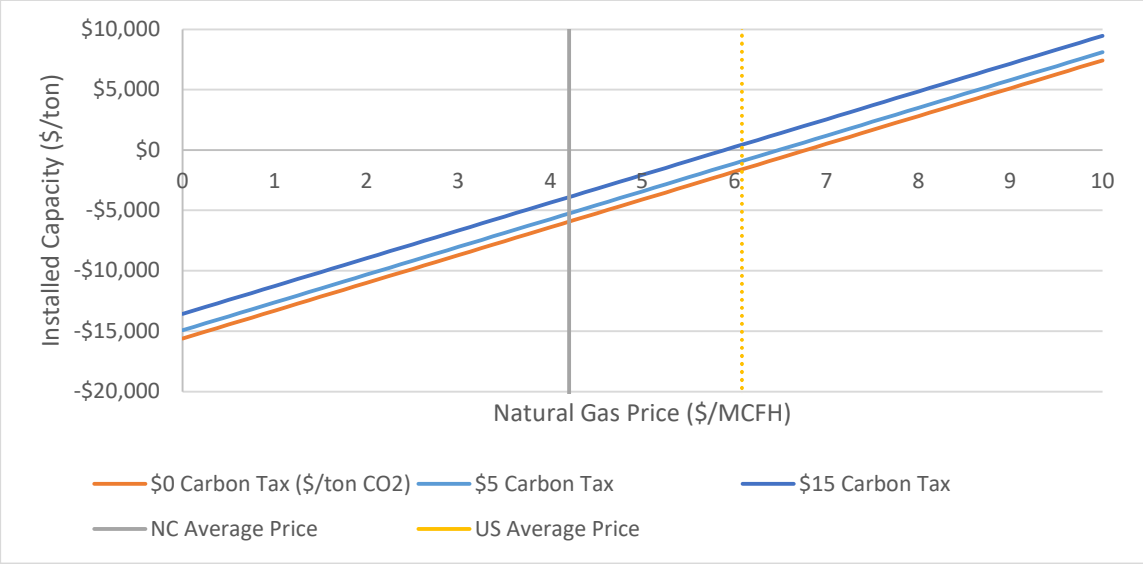

Figure 38. Breakeven Price for an Electric Lime Kiln at Plant A with Carbon Taxes.

5.5.2 Plant B

In this cost analysis, Plant B benefits by creating an overgeneration of electricity due to the steam demand. This means the price of electricity generation is not included in the cost analysis. Plant B also consumes more natural gas and produces less lime than Plant A, which means savings will be realized at lower breakeven costs. In Figure 39, the breakeven price reaches $10,000/ton capacity at just before $2/MCFH, which is well below the national average. The installation of the SMR will be significant capital investment, however, those costs are not included in this analysis because it assumes that the plant has already decided to install the SMR.

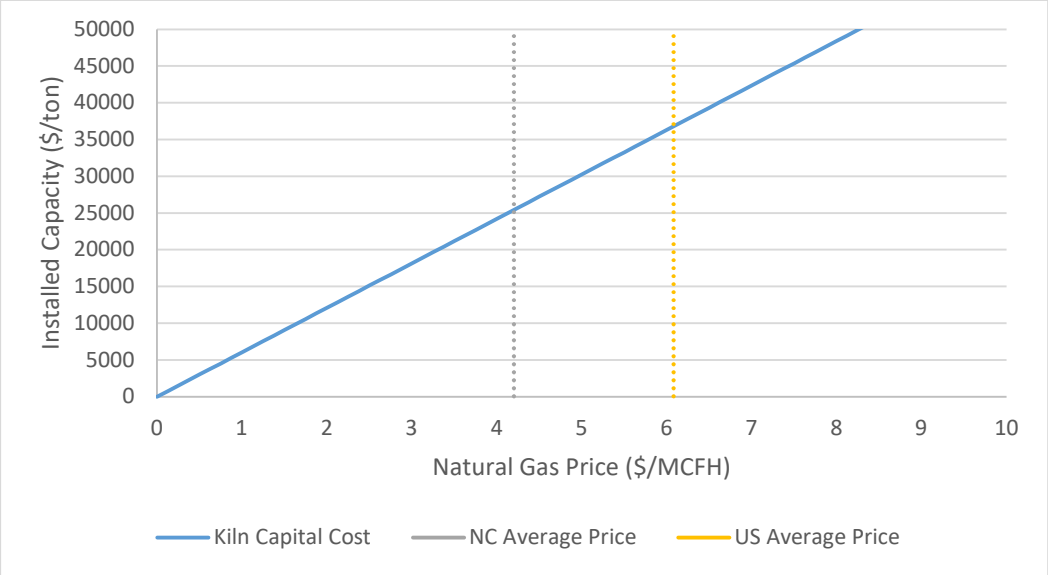

Figure 39. Breakeven Price for a Lime Kiln at Plant B.

One way for both mills to utilize excess electricity while increasing sustainability is to invest in carbon sequestration. Although the methods above describe how carbon dioxide emissions can be eliminated from fuel use, there are still emissions from the lime causticizing itself. Current methods of carbon capture at the source require separating carbon dioxide from other gases, compressing it, and transferring it to an isolated location. This method is often dismissed due to the energy costs required for its operation, however, electricity generated by the SMR on-site could help decrease these costs

5.6 Conclusion

This study presents a steady-state configuration of two plants with steam and electricity provided by a NuScale small modular reactor. The purpose of this study is to determine a suitable replacement for natural gas lime kilns to eliminate all carbon emissions from fossil fuels used in plant operation. An analysis of several renewable options shows that electric lime kilns are the best solution to meet the plant's demands of 24-hour operation, operating temperatures, and minimal changes to the existing process and structures.

The steady-state models estimate the steam required by the SMR to maintain steam quality within the plant. Plant A is a large plant that produces most of its steam from wood waste and black liquor recovery boilers. Only one module is required to make up the steam from the natural gas, but a second module would be required to account for the demand from the addition of electric lime kilns. The cost analysis shows that it would not be economical to use electric lime kilns unless the price of natural gas greatly increased. However, the plant could see future savings, or make-up for the extra costs by selling electricity back to the grid through a PPA with the local utility.

Plant B produces most of its steam from natural gas and requires 5 modules to make up this steam. This leaves the plant generating more electricity than it needs to operate. In this case, the electric lime kiln is truly the best option, since only the capital costs contribute to the breakeven cost of change. Plant B could also utilize a PPA to increase savings from the SMR. For both plants, savings could increase in the future if the price of natural gas changes drastically, or carbon taxes are implemented.

Chapter 6: Dynamic Demonstration of a Pulp and Paper Mill Coupled to an SMR

6.1 Background

Developing a dynamic model of the plant is integral to determining the performance of the SMR when demands change throughout the plant.

A dynamic model was developed using Dymola, a software which uses the Modelica framework. The model is initialized based on the steady-state models created in Chapter 4. Dymola and HYSYS are based on different mathematical models. HYSYS uses mass and energy conservation to solve for a single state of a system. Dymola uses momentum conservation to solve for time dependent states within a system. Between the two software packagess, it is possible to design consistent steady-state models, but they will not solve for exactly the same resulting values. This is intended to be a low fidelity model of the plant, illustrating the potential electric and steam demands from the SMR when demands change within the plant. This gives a realistic idea of the appropriate size of the SMR and thermal storage.

The barrier to creating a higher fidelity model is that only high-level operation data was provided by the plants. Conditions and demands within the plant are varied with the use of PI controllers. It would be impossible to create a physically accurate system with the data available. The model presented here satisfies the functional requirements for this analysis.

6.2 Plant B

Plant B consists of three steam sources that feed into a single turbine. Each source is controlled in the model by its enthalpy flow rate in Watts. The nominal values of the bark boiler and black liquor recovery boiler are based on the steady-state data provided by Plant B. These sources are considered constant because their output is based on the chemical recovery process, which remains consistent even if steam demands change.

Based on the steady-state analysis in HYSYS, Plant B is utilizing 5 SMR modules for a maximum steam flow of 1.33 million lb/hr steam (167 kg/s). The steady-state steam flow required from the SMR is 1.10 million lb/hr (186 kg/s). Increasing process steam flow from the SMR will decrease electricity production in the SMR and increase electricity production within the plant. Decreasing process steam flow from the SMR will increase electricity production in the SMR and decrease electricity production within the plant. The steam properties of each of the three steam sources are listed in Table 5.

Table 5. Steam Conditions of Process Steam Sources.

Source	Temperature (°C)	Pressure (bar)	Steady-State Flow Rate (kg/s)	h (kJ/kg)
SMR	260	28.6	138.5	2,892.70
Bark Boiler	371	28.6	7.245	3,168.05
Recovery Boiler	371	28.6	82.53	3,168.05

Based on trends within the plant, turbine intake can vary between 40% and 110% of the steady-state intake. Flows can change based on demands for MP and LP steam, as well as variation in the electricity purchase price. At steady state, the total steam demand from all 3 sources is 228 kg/s, so the steam demand could vary between 91 kg/s and 251 kg/s. If the bark boiler and RB boiler sources remain constant at 89.78 kg/s, the SMR would vary between 1.5 and 161 kg/s. It is probably not feasible to have 1.5 kg/s steam flow rate directly from the SMR, but if instead steam is diverted from the nominal flow rate to send only 1.5 kg/s to the turbine, this low flow rate becomes a possibility.

It's important to note that the SMR source is at a lower temperature than the other sources and has a lower specific enthalpy than the original natural gas source. Increased flow from the SMR results in slightly decreased heat to the rest of the system. To solve this, a PI

controller is placed on either the MP or LP steam line to control the total enthalpy (mass flow rate times specific enthalpy) provided rather than mass flow rate.

6.2.1 Case 1: Baseline Plant Operations

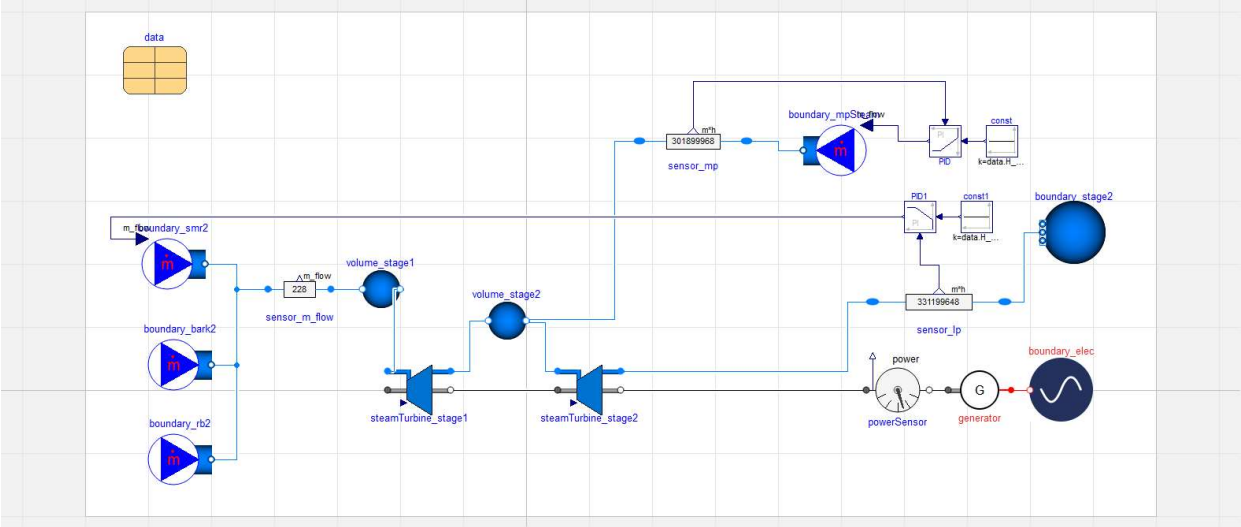

Figure 40. Model of the Baseline Case of Plant B.

The first case solves for steady-state operation as based on the heat demands calculated in the steady-state HYSYS model. The PID controller on the MP steam offtake adjusts the MP steam mass flow rate to meet the steady-state heat demand. The controller cannot simply adjust for mass flow rate because changes in the SMR flow rate changes the specific enthalpy of the entire steam system. The sensor measures the specific enthalpy of the stream times the mass flow rate to indicate a total heat output. Although this is not a physical sensor, it serves the purpose in this simplifies model to adjust the flow rate based on changes in the steam specific heat.

The PID control on the SMR outlet controls the mass flow rate of the SMR based on the heat demand of the LP stream. This ensures that the SMR puts out the proper mass flow rate to meet the demands and steam conditions of the entire system, rather than controlling the flow rate

based on a condition sooner in the system. With this set-up, the SMR should solve closely to the steady-state HYSYS model.

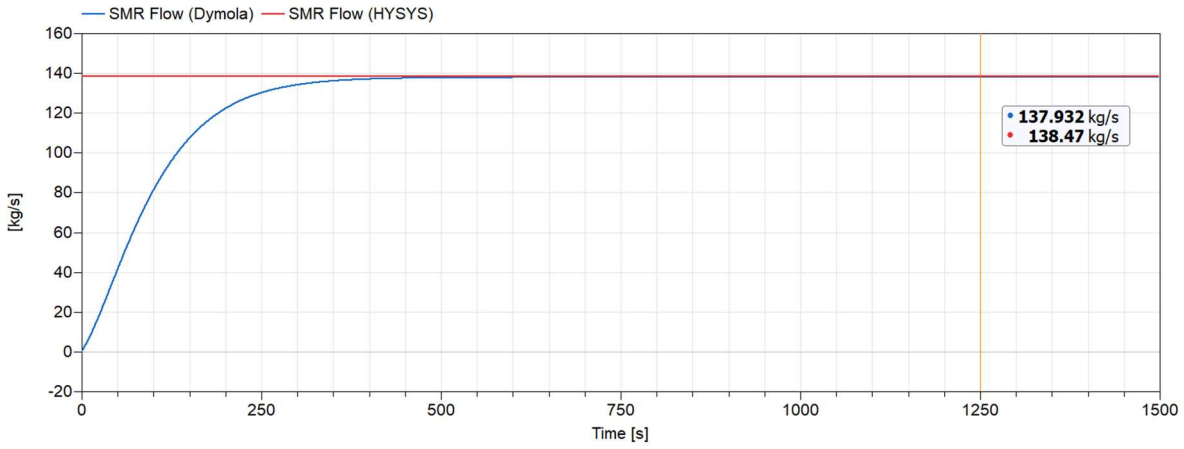

Figure 41. Comparison of Steady-State SMR Mass Flow Rates Calculated by Dymola and HYSYS.

Once the model reaches steady-state, the Dymola model solves for the steady-state SMR flow of 137.9 kg/s, which is slightly higher than the HYSYS mass flow rate of 138.5, but less than 1% error. It takes the model about 500 seconds to reach steady-state, and about 1000 seconds for the flow rate to stabilize completely.

The other value that can help verify the model is the turbine electric output. The steady-state HYSYS model solved for the steady-state power output of the plant as 54.77 MW. At 54.11 MW solved in the Dymola model, the error is negligible.

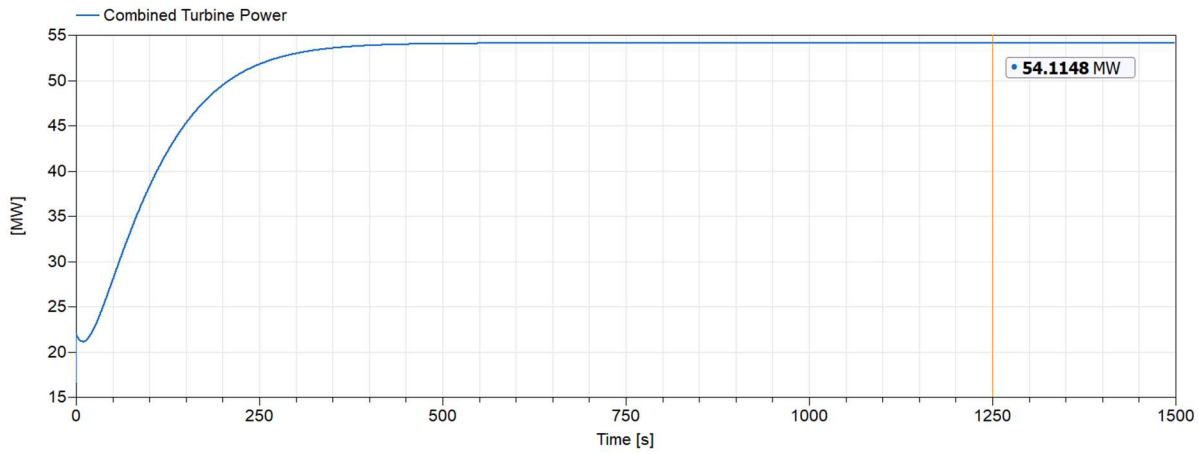

Figure 42. Steady-state Combined Turbine Power for Plant B.

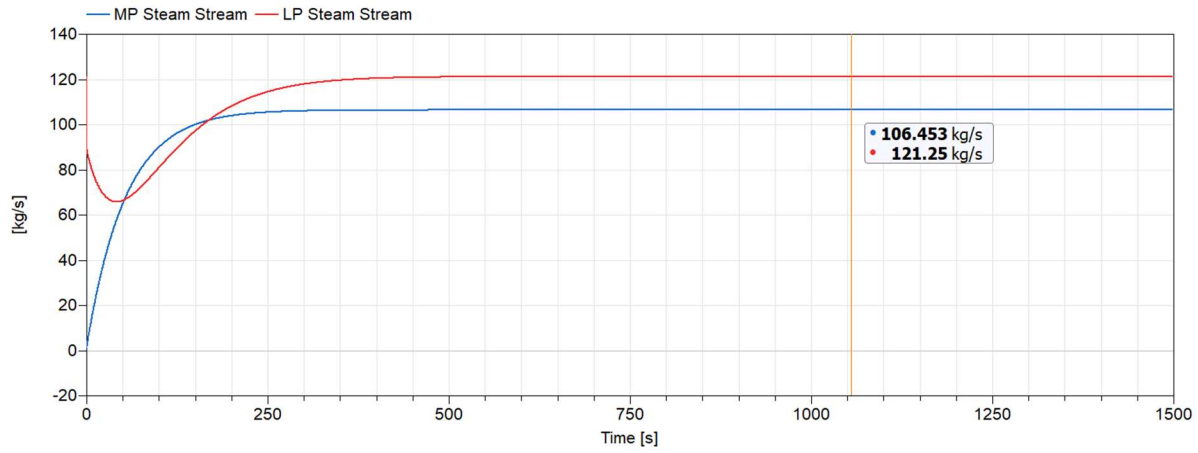

Figure 43. Steam Mass Flow Demand in the MP and LP Streams.

It is also necessary to establish steady-state mass flow rates for the MP and LP steam outlets in the Dymola model. In Figure 43, the LP Steam reaches steady-state at 121.3 kg/s, and the MP steam reaches steady-state at 106.5 kg/s.

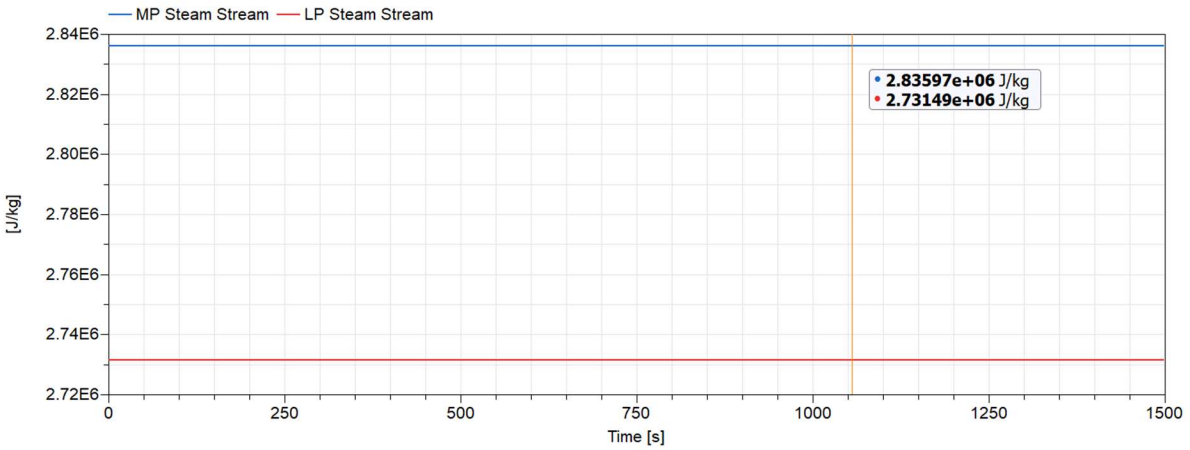

Figure 44. Specific Enthalpy of the MP and LP Steam Streams.

Shown in Figure 44, at steady-state, the LP steam is saturated with a specific enthalpy of 2,731 kJ/kg and the MP steam is superheated with a specific enthalpy of 2,836 kJ/kg. Notice that both steam flow specific enthalpies are constant due to the boundary conditions of constant enthalpy at the outlets.

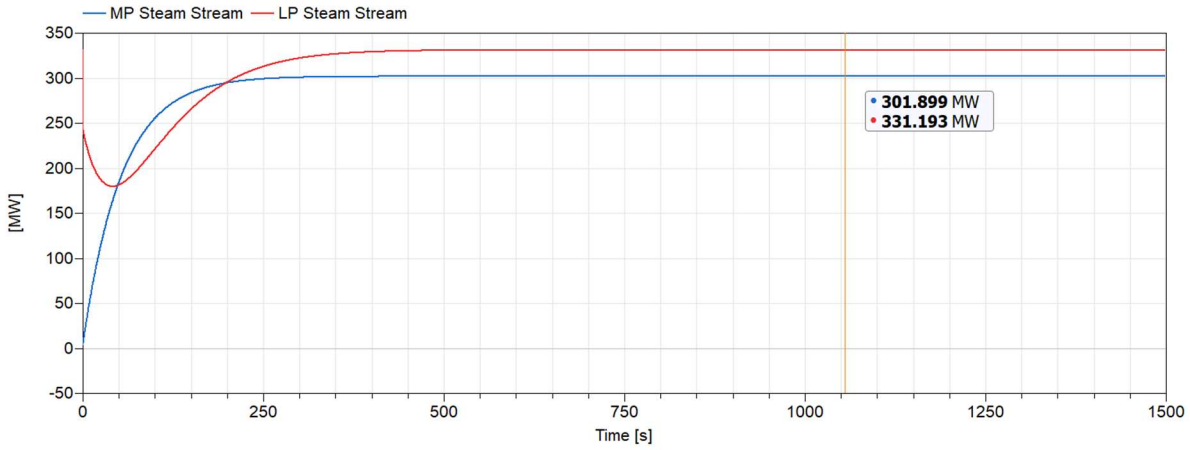

Figure 45. Heat Demand at the MP and LP Steam Outlets.

Figure 45 shows the heat flow for both streams controlled by PID controllers. The LP stream is set to require 331.2 MW heat flow. The MP stream requires 301.9 MW of heat flow. These values are based on the original steady-state model of the plant presented in Chapter 5.

6.2.2 Case 2: Heat demand changes, no limit on SMR flow rates

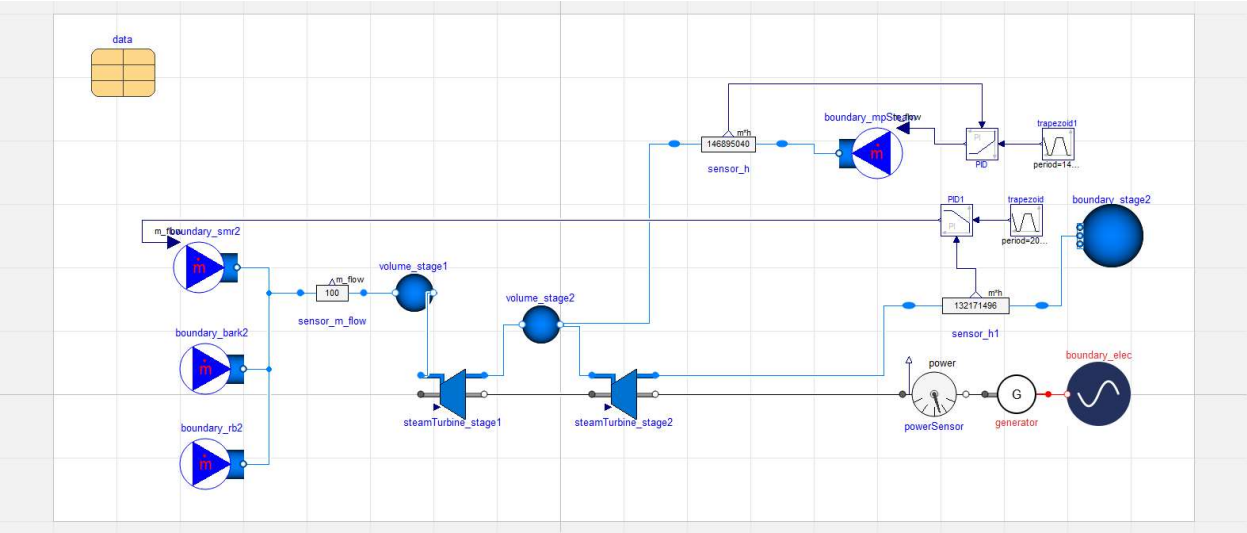

Figure 46. Case 2 Model Built in Dymola.

In this case, the SMR flow rate is dependent on the demand of the LP steam, with the MP steam demand controlled independently. Figure 46 shows the case model built in Dymola. There are no flow limits on the SMR, and it is assumed to change according to the demand. This is not a sustainable control strategy for the SMR. Constantly changing the steam rate off the SMR adds risks of disrupting the reactor.

The demand specified for each steam stream is a trapezoid signal, which differs for each stream to create a quasi-random distribution of the infinite demand scenarios. The main scenarios to study here for the purpose of determining the range of steam needed in the system are: the MP and LP streams are both at maximum demand, and the MP and LP Streams are both at minimum demand. Table 6 shows the demand source curve parameters for both streams.

Table 6. Trapezoidal Heat Demand Source Signals for Plant B.

Parameter	LP Steam	MP Steam
Amplitude	[LP Steam Nominal Heat Demand]*1.1 – [LP Steam Nominal Heat Demand]*0.4	[MP Steam Nominal Heat Demand]*1.1 – [MP Steam Nominal Heat Demand]*0.4
Rising (s)	2000	4000
Width (s)	6000	5000
Falling (s)	8000	3000
Period (s)	20000	14000
Nperiod	-1 (inf)	-1 (inf)
Offset	[LP Steam Nominal Heat Demand]*0.4	[MP Steam Nominal Heat Demand]*0.4
startTime (s)	1000	1500

In Figure 47, the SMR requires 160.7 kg/s of steam flow when both demands are at their maximum. The nominal flow rate is 137.9 kg/s for this system. Despite both demands only being 10% higher, the SMR steam flow requirement is 17% higher than the nominal flow rate.

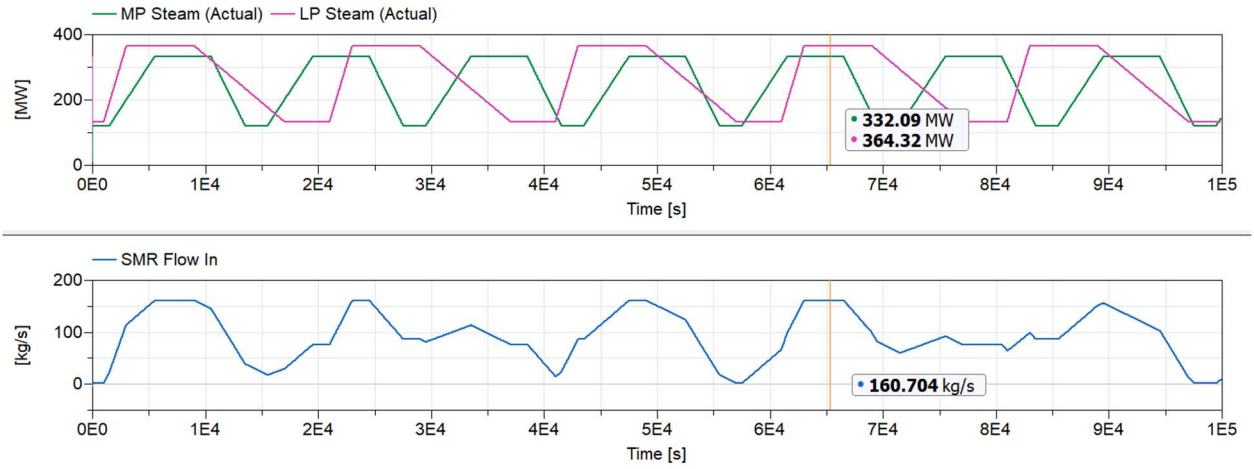

Figure 47. SMR Steam Demand Versus Heat Demands at Highest Point.

As shown in Figure 48, when both demands are at the lowest, the demand from the SMR is very small, 1.3 kg/s. This is an impossible scenario unless some steam was taken off either of the other steam streams to meet the demand exactly. The SMR steam demand here is 99% lower

than the nominal steam demand when the heat demand for each stream is 40% below the nominal.

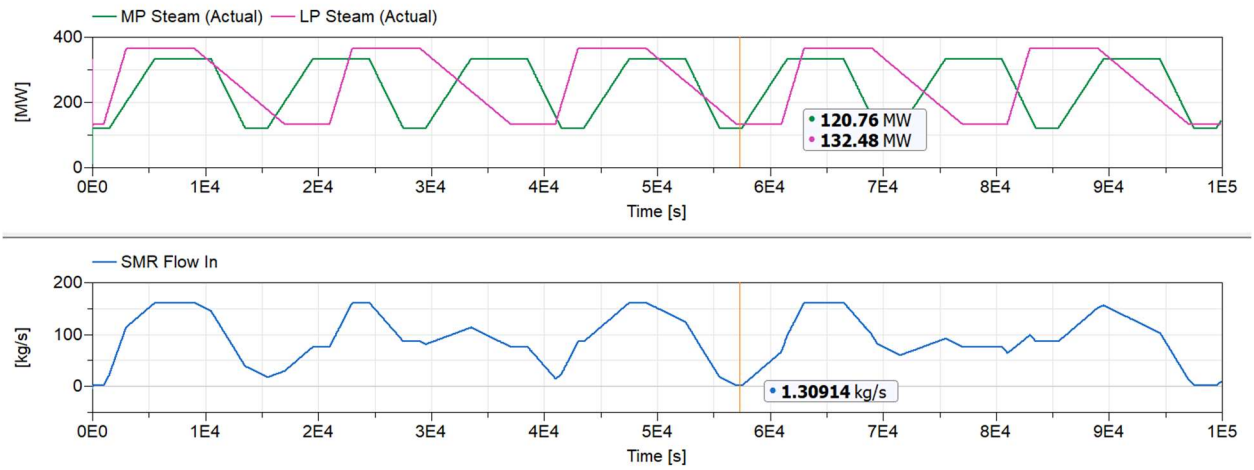

Figure 48. SMR Steam Demand Versus Heat Demands at Lowest Point.

One interesting consequence of this control scheme is that the LP steam actual heat supply does not match up exactly with the demand when the LP steam demand is changing. There are two reasons for this. The first reason is that the control response is slower for the LP stream than the MP stream because the MP mass flow is controlled directly from the turbine outlet, while the LP stream mass flow is controlled by the SMR at the beginning of the system. This means that while the MP steam demand and actual flow match up exactly, it is more difficult for the LP stream to maintain an equilibrium while the SMR flow changes. The other reason is that as the MP steam demand changes, the SMR steam flow rate must also change, which changes the specific enthalpy of the steam stream. With the specific enthalpy and the required mass flow rate changing consistently, it's difficult for the controls to reach an equilibrium. Figure 46 shows the differences in demand of the LP steam stream, as well as the specific enthalpy of the stream at each time. The specific enthalpy is constant in the LP steam because of the boundary condition, but it does change the mass flow rate through the MP steam

stream, and therefore the mass flow rate of the LP stream changes the total heat through the LP stream. Overall this doesn't make a significant difference in the system's ability to meet demands.

One way that this can be mitigated is by increasing the gain on the PID controller connected to the LP steam stream. Figure 49 shows the resulting curves with a gain of 1, and Figure 50 shows the curve with a gain of 10. While the gain of 10 matches more closely, a gain of 1 is a more realistic picture of the result of an actual response from a control system to a changing demand. For the purposes of this study, the two points of interest are when all the demands are at the highest and all demands are at their lowest. The two timestamped points collected match closely with the demand curves, so it can be assumed that most of the important results listed here are unaffected by the gain change.

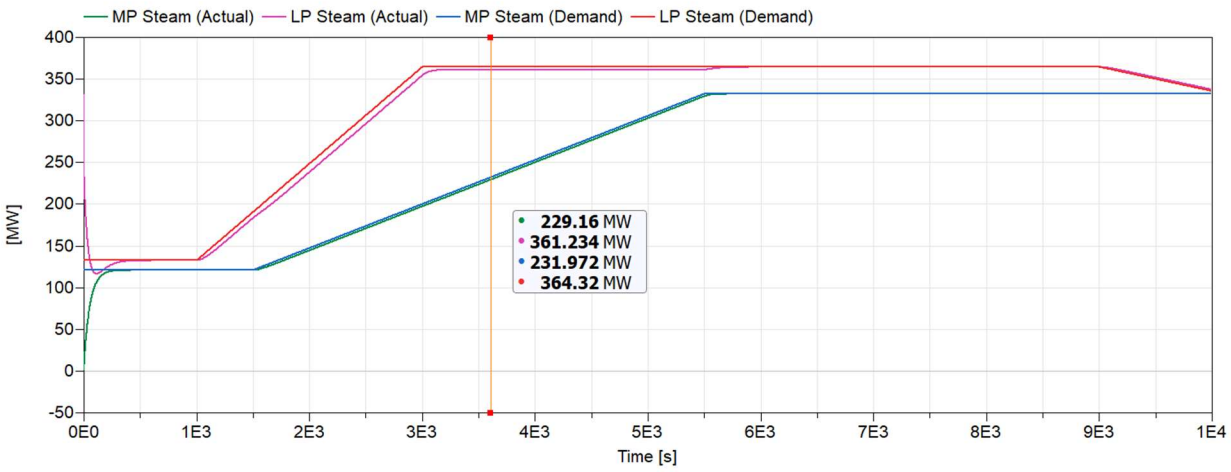

Figure 49. Resulting Heat Out Curves with a PID Gain of 1.

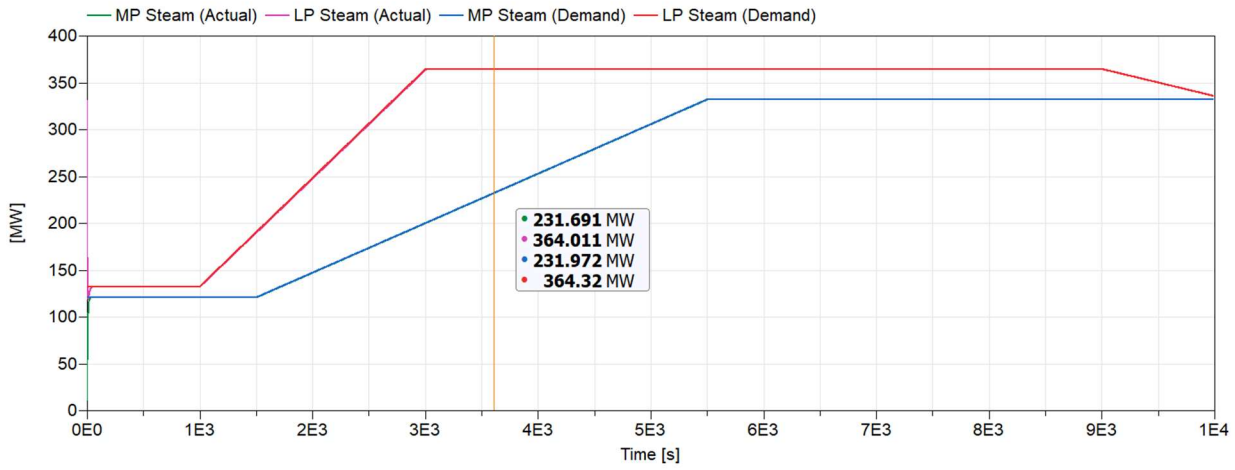

Figure 50. Resulting Heat Out Curves with a PID Gain of 10.

As mentioned before, the specific enthalpy of the source steam changes depending on the amount of SMR steam that is mixed in. In Figure 51, the small deviations in specific enthalpy are seen compared to the SMR mass flow into the system. At the highest mass flow in, the specific enthalpy of the resulting stream is at its lowest, although it does not greatly affect the properties of the superheated steam.

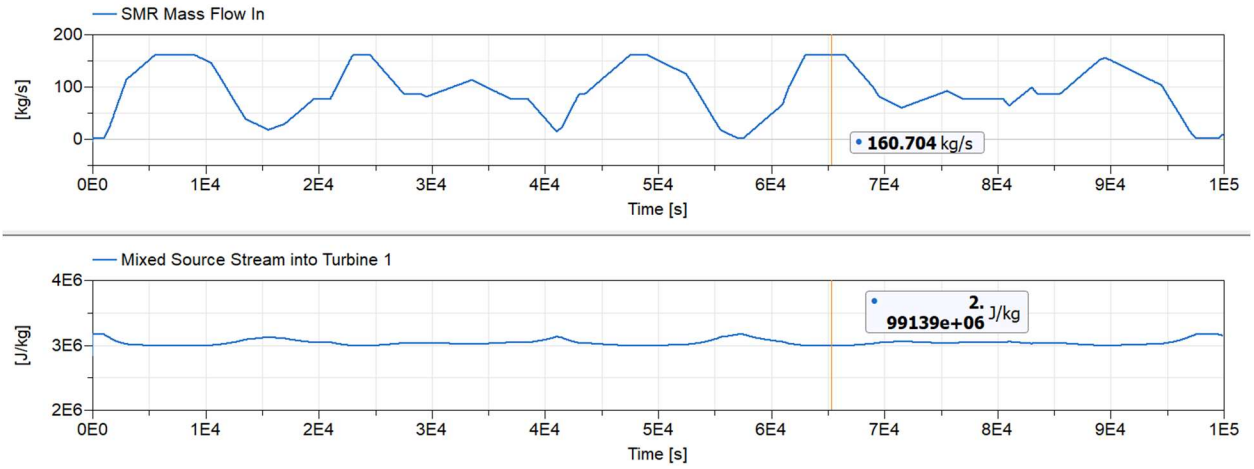

Figure 51. Specific Enthalpy Changes in the Mixed Steam Source Stream.

The last thing to look at are the changes in turbine power of the system. The electricity generated by the plant varies from 17.9 MW (Figure 52) at the minimum SMR flow rate to 60.7 MW (Figure 53) at the highest SMR rate. This is a wide range of power levels that may impact the electricity needed from other sources to maintain the plants operation.

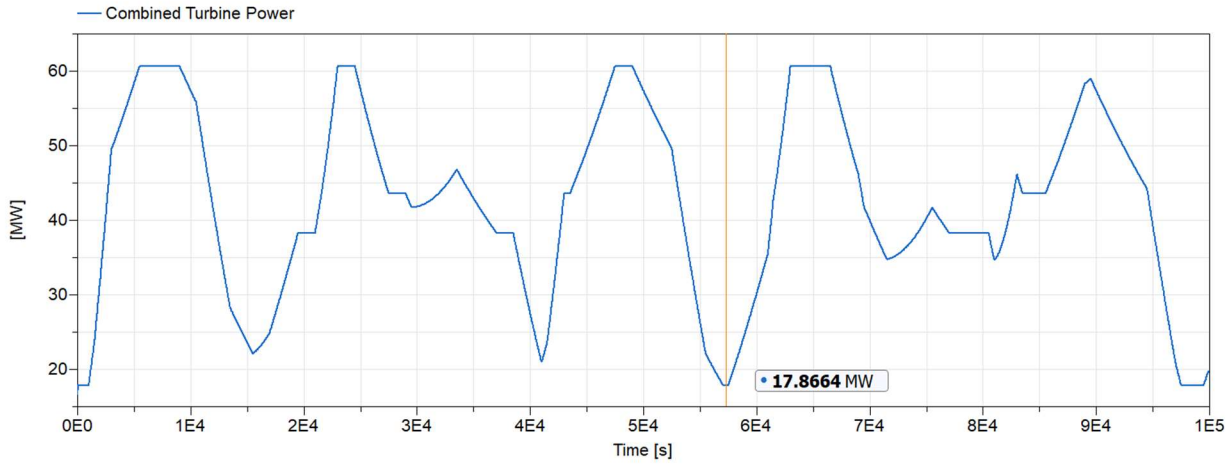

Figure 52. Minimum Combined Turbine Power in Case 2.

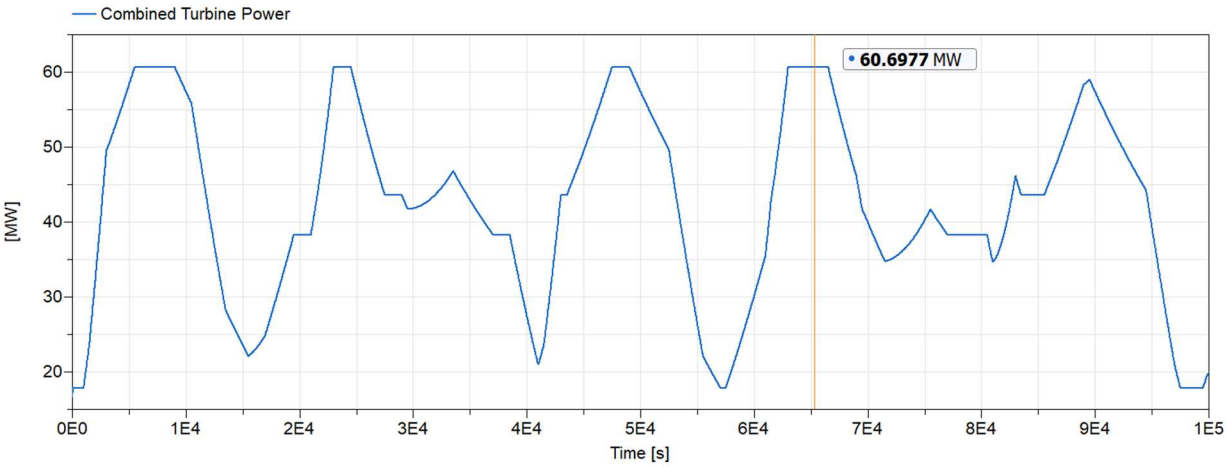

Figure 53. Maximum Combined Turbine Power in Case 2.

6.2.3 Case 3: SMR Nominal Flow Rate

The purpose of this case is to determine the heat that is wasted or the deficit of heat when the SMR stays at the nominal flow rate all the time. The best way to operate the SMR is to keep the steam offtake consistent and allow the reactor to operate in steady-state. However, this is not sustainable for the system since the demand is not always constant.

Figure 54 shows the set up for Case 3. The MP is controlled by the same signal as the previous cases. The LP steam stream is not controlled and will take any steam that is not required by the MP stream. The previous LP stream signal is included to compare the energy the LP stream received compared to what it actually requires. The difference shows the amount of energy that is wasted or still needed. The SMR steam source is set to the steady-state nominal rate of 137.9 kg/s.

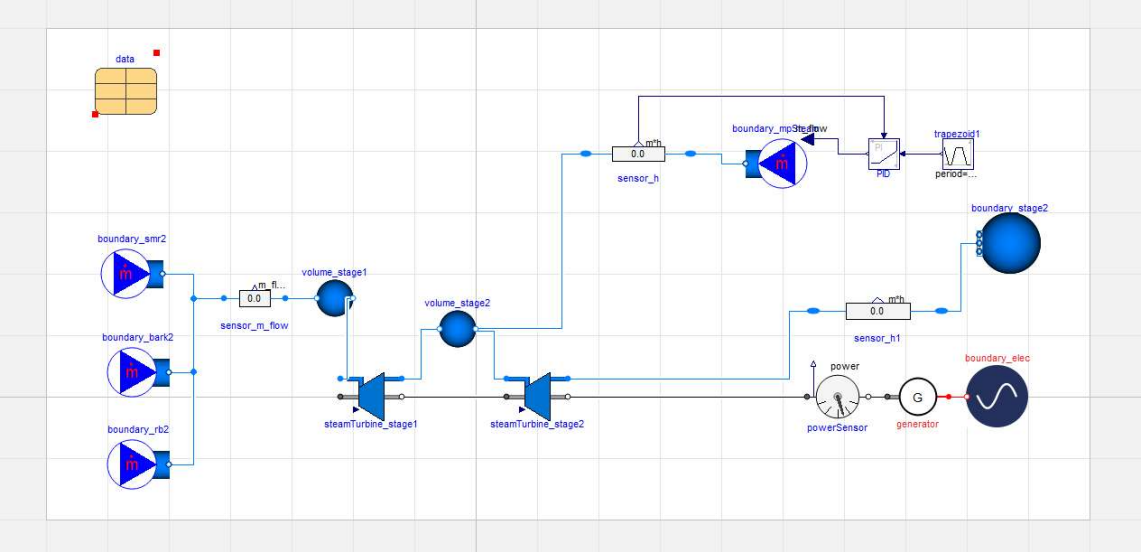

Figure 54. Case 3 Model in Dymola.

Figure 55 compares the actual heat received by each stream compared to the demand. The MP actual and demand curves are identical, because that is the only stream that is controlled. The actual LP steam heat is the reverse of the MP steam demand. When the red curve is above

the blue curve, it is a place where there is a deficit in the heat going to the LP stream. When the blue curve is above the red curve, it is a surplus of heat. There are only small areas in which there is a deficit of steam because the demand can only go 10% above the nominal, but where there is a surplus of heat there is a large spike, because the demand can be down to 40% of the nominal. This results in a lot of wasted heat produced by the SMR and not used by the system. In the case of surplus heat, about 373 MWth are produced but not used by the system. This heat would then be vented either to a condenser, or off the roof of the facility. In the case of a deficit, the system needs an additional 62.2 MWth.

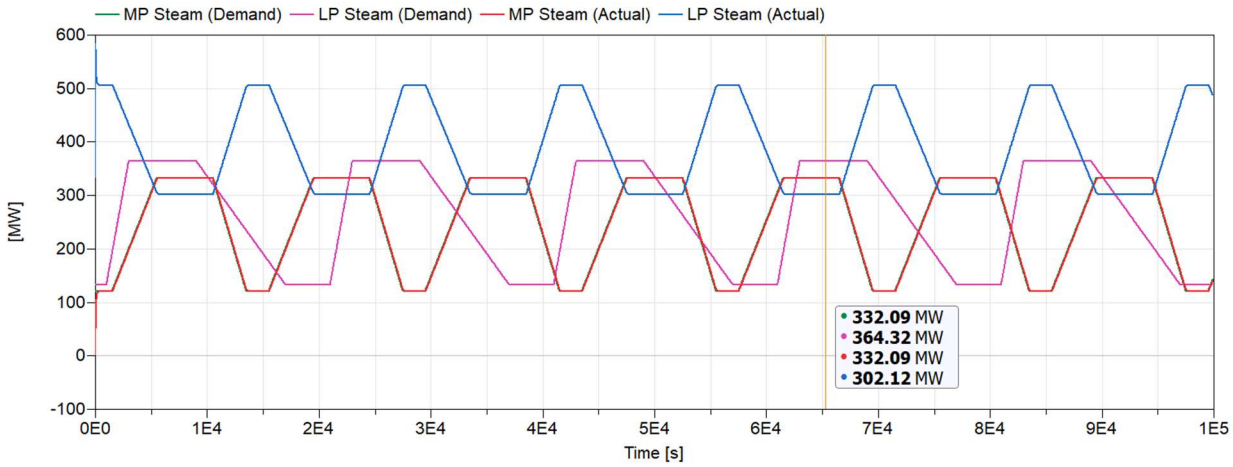

Figure 55. Heat Deficit When Demands are at Maximum in Case 3.

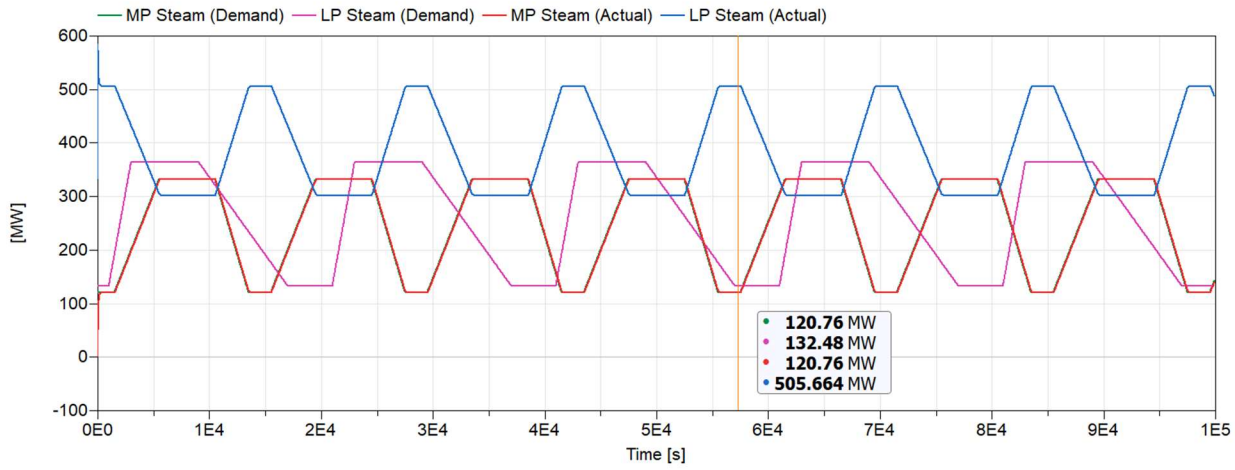

Figure 56. Heat Surplus when Demands are at Minimum in Case 3.

Figure 57 and Figure 58 show the power produced in the turbines for this case. As opposed to Case 2, the range of turbine power is much smaller. There is a consistent amount of steam going through the first turbine, which helps to provide more power. The steam going through the second turbine has a smaller variation because it takes any steam not required by the MP stream.

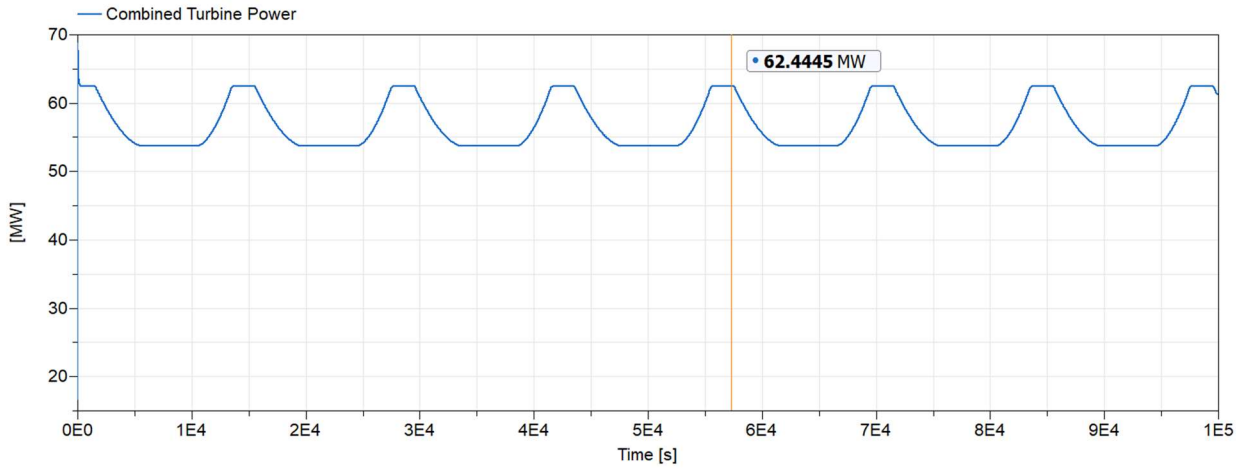

Figure 57. Maximum Combined Turbine Power in Case 3.

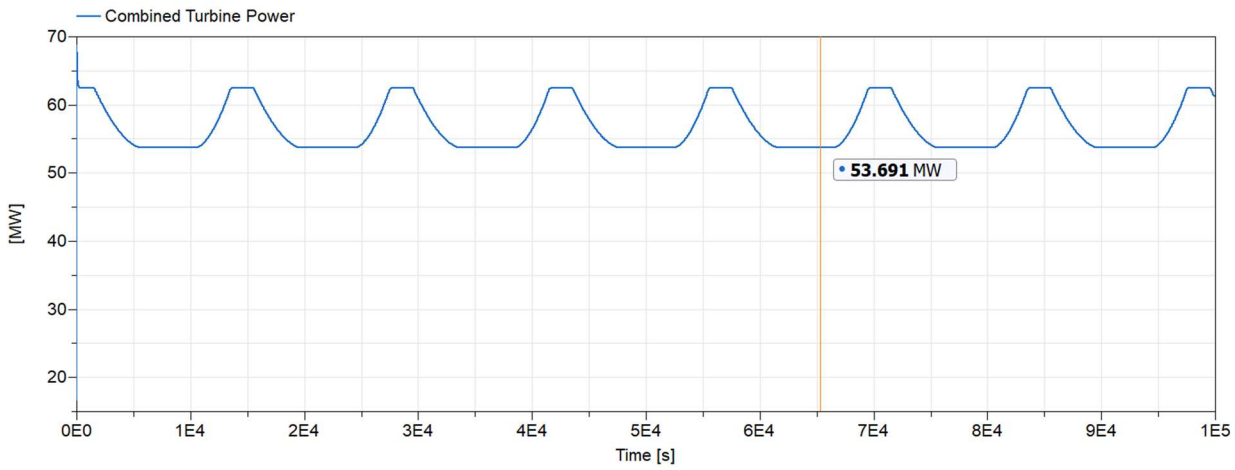

Figure 58. Minimum Combined Turbine Power in Case 3.

Although having a consistent power production by the turbines is good for creating a steady-state operation, the large surplus of steam during times of low demand decreases the efficiency of the entire system. Even more concerning is the deficit of steam during times of high demand. This will cause disruptions in the process or damage quality control.

If the SMR flow rate cannot constantly change, but the nominal flow rate isn't appropriate for most of the scenarios, a good way to increase the efficiency and performance of the system is to add energy storage. There are several ways that this can be implemented.

6.2.4 Steam Accumulator Design

Steam peaking can occur with short-term, frequent peaks, or heavy and long-term. Peak demands can cause problems within batch processing industries, with heavy demands lasting an hour or more. However, peaking is typically not frequent, occurring once a week or once a day during start-up. Boilers are typically sized for average demand rather than peak demand, because an oversized boiler can cost a facility efficiency, space, and money. In the case of an SMR, achieving a "right-size" boiler has been shown in the previous chapter to be difficult. Rather, the steam demand is sized with by the proportion of steam and electricity needed from the modules.

Although the SMR can provide the additional steam needed for long-term or short-term peaking, abrupt changes in demand are difficult to handle and can reduce the health of the system over time. A steam accumulator can react quickly to a short-term change in demand, or cushion the load changes in the SMR if a long-term change in demand is needed [77].

Steam accumulators are the most appropriate means of providing clean, dry steam instantaneously. The volume of the accumulator is based on the storage required to meet a peak demand. The data available from the plants gives the average peak steam flow at about 110% of the nominal steam demand. There is no information regarding the frequency or duration of these peaks, however, because pulp and paper production is a batch process, these peaks can be assumed to be infrequent and typically long in duration.

Steam mass flow during the peak is based on the steam flow required as well as the duration of discharge. If $\dot{m}_{peak}$ is the mass flow rate above nominal in kg/hr [77]:

$$\dot{m}_{cycle} = \frac{\dot{m}_{peak} * 60\ min}{Duration\ of\ Peak\ (minutes)}$$

Calculating the steam storage required is a similar method, using the duration of each cycle and the mass flow at the peak [77].

$$m_{storage/cycle} = \frac{\dot{m}_{peak} * Duration\ of\ Cycle\ (\text{min})}{60\ min/hr}$$

The mass and volume of water storage required in the steam accumulator can be determined from the design pressure (P2) and fully charged pressure (P1) of the steam accumulator, and the steam flow required during peaking [77].

$$m_l = \frac{h_{fg@P2} * m_s}{(h_{f@P1} - h_{f@P2})}$$

Where m_l is the mass of water storage required in the accumulator and m_s is the steam storage capacity, or the mass of steam required during the accumulator discharge.

The volume of the accumulator is determined using the specific volume of saturated water at the fully charged pressure. Typically, liquid water makes up 90% of the total volume [77].

$$V_{tank} = 1.1 * v_{water} * m_l$$

For a typical manufacturing application, a steam accumulator would be recommended because of the ease of integration with the rest of the system. However, there would be some challenges with sizing the accumulator if the plant does not have a regular pattern of steam peaking. It is still an option that any plant should explore. In this specific case, keeping with the goals of the JUMP program, a two-tank sensible heat storage system will be designed and used for the dynamic model.

6.2.5 Two-Tank Sensible Heat Storage Design

Another option for providing additional steam to the process is through sensible heat storage. In this case, the sensible heat storage is modeled after the storage system being explored for the JUMP secondary side. This is a two-tank system with Therminol 66 as the heat transfer fluid. During times of low demand, steam can be redirected to an intermediate heat exchanger which passes heat to a thermal fluid which is then stored in a "hot tank" until additional steam is needed. During times of high steam demand, the thermal fluid passes through a steam generator with feedwater on the other side. The feedwater could be preheated by other process steam before passing through the steam generator to increase efficiency. Figure 59 shows the design of the simplified two tank system.

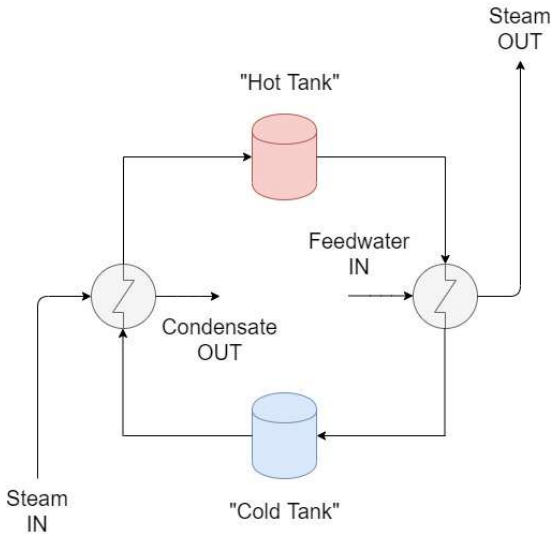

Figure 59. System Design of a Two-Tank Sensible Heat Storage System.

The steam out can be designed for peaking on either the MP or LP streams and could be placed at any point in the stream. The first step to designing the thermal storage system is estimating how much heat will need to be stored. In both plants, the maximum steam demand through the turbines is 110% of the steady-state demand. We can simulate this increase with the Dymola model by increasing the nominal heat demand for the MP and LP steam by 10%.

The specific enthalpy of the SMR source is 2,892.68 kJ/kg and 3,168.04 kJ/kg for the bark source. The steam provided by the thermal energy storage system (TESS) cannot be greater than that. The specific enthalpy of saturated steam at atmospheric pressure is 2,675 kJ/kg, so the source cannot feasibly be lower than that. By linking a mass flow source of steam to the rest of the Modelica model with a set specific enthalpy, the heat demand from that source can be estimated and changes to the overall system function can be explored.

It's important to note that in the same way that the SMR causes changes to the mass flow rate requirements within the plant because of its difference in specific enthalpy from the other sources, the TESS can also cause mass flow rate changes because of its specific enthalpy

difference. Although a design specific enthalpy must be chosen to account for losses within the heat exchanger, a low stream enthalpy could change other properties within the steam streams.

First, Table 7 shows the changes to the entire steam system if the TESS steam source is connected to the rest of the streams before the first turbine.

Table 7. Changes to Steam System with Addition of TESS Steam Source Before First Turbine.

TESS h (kJ/kg)	TESS $\dot{m}$ (kg/s)	Q (kJ/s)	Q difference from 3000 kJ/kg	Plant Power (MW)
3000	22.80	68411		61.2
2950	22.80	67271	1.67%	61.0
2900	22.80	66130	3.33%	60.7
2850	22.80	64991	1.72%	60.5
2800	22.80	63850	3.45%	60.2
2750	22.80	62710	5.17%	60.0
2700	22.80	61570	6.90%	59.7

Next, Table 8 shows the changes to the entire steam system if the TESS steam source is connected to the stream after the first turbine but before the MP steam stream.

Table 8. Changes to Steam System with Addition of TESS Steam Source after First Turbine.

TESS h (kJ/kg)	TESS $\dot{m}$ (kg/s)	Q (kJ/s)	Q difference from 3000 kJ/kg	Plant Power (MW)
3000	22.80	68412		55.1
2950	22.80	67272	1.67%	55.1
2900	22.80	66132	3.33%	55.0
2850	22.80	64991	5.00%	55.0
2800	22.80	63851	6.67%	54.9
2750	22.80	62711	8.33%	54.9
2700	22.80	61571	10.00%	54.9

The difference in the mass flow rate and heat rate rate required change by less than 1% and 10% or less respectively between 3,000 kJ/kg and 2,700 kJ/kg steam. It's likely that the insignificant changes in the required mass flow rate are due to specific enthalpy boundary conditions in the model, although when this method was repeated with a temperature boundary rather than specific enthalpy boundary on the LP steam turbine, the mass flow rate changed by less than 1%. The change in specific enthalpy only makes a small change in the turbine power output. This shows that any reasonable specific enthalpy within this range can be chosen without making a significant impact on the system, however, the overall plant power generation changes by about 5 MW. The nominal plant power is around 55 MW, so adding the TESS before the first turbine increases the nominal plant power. Because Plant B is already over generating electricity, there is no reason to send this steam through the first turbine and generate more electricity. In this case, the TESS will be placed after the first turbine to slightly decrease the size requirements for the tanks and give more design flexibility since the nominal pressure after the first turbine is greatly reduced.

Because pulp and paper processing is a batch process, it's likely that the TESS will need to operate over a long period of time rather than short, repeated intervals. Extended demand increases (greater than 4 hours) would require an increase in production from one of the three steam sources, but the TESS would allow plenty of time for the plant to operate normally while long-term changes are made. Likely, the increase in steam generation would come from the SMR, since the steam is readily available, although it would decrease the overall electricity generation of the plant.

After the first turbine, the steam properties are 9.6 bar and 202°C with a specific enthalpy of 2835 kJ/kg. The output steam conditions from the TESS could be higher than that, but it

would only slightly affect the mass flow rate requirements and result in an oversized steam generator.

The amount of total heat needed to be stored in the tank is estimated by multiplying the Q flow required (kJ/s) by the duration that the TESS will be in use. Table 9 shows the estimated heat requirements for the TESS placed after the first turbine.

Table 9. Heat Output Estimates for TESS Based on Discharge Time.

h (kJ/kg)	$\dot{m}$ (kg/s)	Q (kW)	30 min discharge Q (kJ)	1 hr (kJ)	2 hr (kJ)	4 hr (kJ)
2900	22.80	66,131.60	1.309e8	2.619e8	5.238e8	1.048e9
2835	22.80	64,646.51	1.280e8	2.560e8	5.120e8	1.024e9
2700	22.80	61,570.80	1.219e8	2.438e8	4.876e8	9.753e8

It has been shown that differences in the steam outlet conditions from the TESS do not significantly change the overall stream conditions within the plant.

A simple heat exchanger design can estimate if the steam output conditions specified are feasible, and to size the storage system. To simplify the model, it is assumed that the steam from the TESS is at the same conditions as the current stream. In this case, it is at the same conditions as the medium pressure steam. Feedwater is passed through the steam generator inlet at 82°C and pumped to the desired outlet pressure. 82°C is a typical temperature of processed condensate return. The inlet and outlet steam conditions for the steam generator are listed in Table 10.

Table 10. Conditions of Inlet and Outlet Conditions of Water in Steam Generator.

Steam Generator	Temperature (°C)	Pressure (bar)	h (kJ/kg)	Condition
Feedwater Inlet	82	9.63	344.07	Subcooled liquid
Steam Outlet	202	9.63	2,835.24	Superheated Steam

The Therminol conditions on the steam generator side of the TESS are unknown but can be set to achieve the desired design. The restraint on the Therminol inlet temperature, or hot tank temperature, is the inlet temperature of the steam on the IHX side, 260°C. The hot tank temperature must be less than 260°C to maintain a temperature difference across the IHX. To determine an optimum design, hot tank temperatures of 240, 230 and 220°C are used.

The outlet condition of the Therminol, or cold tank temperature, is unknown, and will be based on other design conditions within the heat exchanger. Because the temperature is not known, and because the water undergoes a phase change within the heat exchanger, it is best to calculate the rest of the conditions with the e-NTU method. The e-NTU calculates heat exchanger conditions based on the effectiveness of the heat exchanger, ε, or the ratio of the actual heat transferred vs the maximum possible heat transfer.

$$\varepsilon = \frac{\dot{Q}}{\dot{Q}_{max}}$$

The quantity C_{min} is used to find the maximum heat transfer. C_{min} is the smallest value found when multiplying the mass flow rate by the heat capacity of the cold side (subscript c) and the hot side (subscript h).

$$C_c = m_c c_{p,c}$$
$$C_h = m_h c_{p,h}$$
$$C_{min} = \min\left(C_c, C_h\right)$$

Because the mass flow rate of Therminol is unknown, C_h can't be calculated. However, water has an infinite heat capacity when undergoing a phase change, so C_h is automatically assigned as C_{min}.

The actual heat transfer rate is the heat transfer rate required to achieve the desired steam outlet conditions in the steam generator. The heat transfer rate can be calculated simply using the mass flow rate on the steam side and the change in enthalpy. It's been established that the

thermal storage system will have to operate at a maximum for a long period time, therefore the steam mass flow rate design condition is set to 22.8 kg/s, which is calculated by Dymola in the previous section.

$$\dot{Q} = \dot{m}\Delta h = \left(22.8\frac{kJ}{s}\right)(2{,}835.24 - 344.07)\frac{kJ}{kg} = 56{,}448\ kJ/s$$

The effectiveness of the heat exchanger can also be calculated by a ratio of the inlet and outlet temperatures on each side of the heat exchanger. The outlet temperature of Therminol is unknown, however, it can be calculated if an effectiveness is chosen for the heat exchanger. The effectiveness 0.85 is used as a conservative, yet typical effectiveness value of a boiler.

$$\varepsilon = \frac{T_{h,in} - T_{h,out}}{T_{h,in} - T_{c,in}}$$

$T_{h,out}$ calculated for each design condition at $\varepsilon = 0.85$ are tabulated in Table 11.

Table 11. Therminol Hot and Cold Tank Temperatures with Calculated Average Heat Capacity.

$T_{h,in}$ (°C)	$T_{h,out}$ (°C)	C_p, ave (kJ/kg-K)
220	102.7	2.06
230	104.2	2.08
240	105.7	2.10

The mass flow rate of Therminol required can be calculated using an energy balance and the average C_p calculated in Table 12.

$$\dot{Q} = \varepsilon\left(\dot{m}C_p\right)_{hot}(T_{h,in} - T_{c,in})$$

Table 12. Mass Flow Rate of Therminol Based on Hot Tank Temperature.

$T_{h,in}$ (°C)	$\dot{m}$ (kg/s)
220	233.6
230	215.7
240	200.2

The heat transfer calculations using the average Cp can be verified by using the change in enthalpy of the Therminol.

$$Q = \dot{m}(h_{105.7} - h_{240}) = 200.2 * (203.1 - 484.7) = -56{,}376$$

$$Error = \frac{Q_{Cp} - Q_h}{Q_h} = \frac{56{,}448 - 56{,}376}{56{,}448} = 0.001\%$$

The relationship of the Cp of Therminol to temperature is approximately linear, so the error is very small at 0.001%.

On the IHX side, the steam from the SMR also undergoes a phase change, therefore the Therminol is C_{min}, although this time it on the cold side. We can calculate the effectiveness without knowing the outlet temperature of the steam, determining whether the design calculated on the steam generator side is feasible for the IHX side. Table 13 uses the effectiveness equation to determine the effectiveness on the SMR side.

Table 13. Effectiveness of IHX Based on Therminol Hot Tank Temperature.

$T_{h,in}$ (°C)	ε, IHX
220	0.75
230	0.81
240	0.87

These are all reasonable values for effectiveness and show that it would be unlikely to use a hot tank temperature above 240°C to create a conservative design. Moving forward in the design, 240°C will be used as the hot tank temperature, since it allows the most heat transfer to the Therminol on the SMR side while still maintaining a conservative effectiveness value.

The mass flow rate on the SMR side will fluctuate based on demands in the plant, and the maximum steam mass flow rate through the IHX can be estimated by subtracting the SMR steam flow rate at the lowest demands from Case 2, 1.5 kg/s, from the nominal steam demand, 137.9

kg/s, giving an estimated maximum steam flow rate of 136.4 kg/s. The mass flow rate of Therminol on this side can also fluctuate to maintain the desired heat transfer across the heat exchanger, although the temperature difference must remain the same between the hot and cold tanks. To make sure that the design remains feasible, an outlet temperature of water can be assigned for the steam side.

The outlet temperature of steam determines the size of the heat exchanger. A larger heat exchanger will extract more heat from the steam and raise the efficiency of the system, and a smaller one will extract less heat and require more steam to charge the TESS. The decision in sizing can be based on the desired length of time for the system to fully charge. In this case, it is assumed that steam peaks will be long and infrequent, so there could be a few hours to a few days between peaks. Additionally, in a system sized to produce peak steam for several hours, if multiple peaks occur during a short period of time, the system would not need to fully recharge between each peak. If the charge time for the system is extended, a smaller heat exchanger would save on cost and space in the plant.

The heat transfer that must occur is based on the time to full discharge, and the total heat stored in the tank at full charge. The actual heat transfer that occurs on the steam generator side is 56,448 kJ/s, as calculated previously. Table 14 estimates the mass of Therminol and tank volume required to achieve each discharge time using a hot tank temperature of 240°C, in which the density of liquid Therminol is 856 kg/m^3.

Table 14. Therminol Mass Storage and Tank Volume Based on Discharge Time.

Time to Discharge	30 min	1 hour	2 hour	4 hour
Total Mass Flow (kg)	3.60e5	7.21e5	1.44e6	2.88e6
Minimum Tank Volume (m^3)	245	490	980	1,960
Heat Storage (kJ)	1.02e8	2.03e8	4.06e8	8.13e8

Using a set outlet temperature for steam gives the actual heat transfer on the Therminol side, calculated from the change in enthalpy of the steam. Because the mass flow rate is variable, the total heat transfer is also variable. The mass flow rate can be calculated by the e-NTU method. The steam flow rate for Plant B can theoretically vary from 0 kg/s to 138 kg/s, based on the steady-state data.

Table 15 estimates the total heat transfer based on the SMR steam flow rate and the steam outlet temperature. In an ideal design, the steam will exit the IHX as a subcooled liquid. An outlet temperature of 5°C is not likely achievable, but it is included to compare the heat transfer and Therminol flow rate required if energy is extracted from the steam until it is almost solid.

Table 15. Total Heat Transfer from Steam to Therminol Based on Steam Outlet Temperature and Flow Rate.

T outlet (°C)	5	50	100	150
Δh (kJ/kg)	2,880.36	2,692.39	2,482.98	2,270.4
Steam Flow (kg/s)	Total Heat Transfer (kJ)			
0	0	0	0	0
10	28,804	26,924	24,830	22,704
20	57,607	53,848	49,660	45,408
30	86,411	80,772	74,489	68,112
40	115,214	107,696	99,319	90,816
50	144,018	134,620	124,149	113,520
60	172,822	161,543	148,979	136,224
70	201,625	188,467	173,809	158,928
80	230,429	215,391	198,638	181,632
90	259,232	242,315	223,468	204,336
100	288,036	269,239	248,298	227,040
110	316,840	296,163	273,128	249,744
120	345,643	323,087	297,958	272,448
130	374,447	350,011	322,787	295,152
140	403,250	376,935	347,617	317,856

Using the total heat transfer and the e-NTU method, the mass flow rate of Therminol can be required at each steam flow rate and outlet temperature. In Table 16, the Therminol hot tank temperature used is 240°C to estimate the mass flow rate of Therminol on the SMR side based on the outlet temperature and mass flow rate of the SMR steam.

$$\dot{Q} = \varepsilon\left(\dot{m}C_p\right)_{hot}(T_{h,in} - T_{c,in})$$

Table 16. Therminol Mass Flow Rate Based on Steam Outlet Temperature and Flow Rate.

T outlet (°C)	5	50	100	150
Δh (kJ/kg)	2,880.36	2,692.39	2,482.98	2,270.4
Steam Flow (kg/s)	Therminol Mass Flow Rate (kg/s)			
0	0.0	0.0	0.0	0.0
10	102.2	95.5	88.1	80.5
20	204.3	191.0	176.2	161.1
30	306.5	286.5	264.2	241.6
40	408.7	382.0	352.3	322.1
50	510.9	477.5	440.4	402.7
60	613.0	573.0	528.5	483.2
70	715.2	668.5	616.5	563.8
80	817.4	764.1	704.6	644.3
90	919.6	859.6	792.7	724.8
100	1,021.7	955.1	880.8	805.4
110	1,123.9	1,050.6	968.9	885.9
120	1,226.1	1,146.1	1,056.9	966.4
130	1,328.3	1,241.6	1,145.0	1,047.0
140	1,430.4	1,337.1	1,233.1	1,127.5

Because the steam flow rate is variable, there is no way to estimate an exact charging time for the TESS. However, a range can be given based on the lowest and highest possible charge times based on the range of steam flow rates.

If the steam flow rate through the IHX is a constant 10 kg/s, Table 17 gives the charge time in hours based on the discharge capacity of the hot tank.

$$Charge\ Time = \frac{m_{tank}}{\dot{m}_{therminol@steam\ flow}}$$

Table 17. TESS Charge Time Based on Discharge Capactity and Steam Outlet Temperature at 10 kg/s Steam.

Steam outlet temperature (°C)	Discharge Time (hr)			
	0.5	1	2	4
5	0.98	1.96	3.92	7.84
50	1.05	2.10	4.19	8.38
100	1.14	2.27	4.54	9.09
150	1.24	2.49	4.97	9.94

If the steam flow rate through the IHX is a constant 138 kg/s, Table 18 gives the charge time in hours based on the discharge capacity of the hot tank.

Table 18. Charge time TESS Charge Time Based on Discharge Capactity and Steam Outlet Temperature at 138 kg/s Steam.

Steam outlet temperature (°C)	Discharge Time (hr)			
	0.5	1	2	4
5	0.07	0.12	0.24	0.49
50	0.08	0.13	0.26	0.52
100	0.08	0.14	0.28	0.57
150	0.09	0.16	0.31	0.62

The maximum charge time for any of the designs is about 10.5 hours, which is very reasonable for a batch process system. The actual charge time is likely to be much lower because the steam flow rate will vary over time to be higher than 10 kg/s.

The discharge times can be verified by comparing the heat transfer of Therminol to the actual heat transfer in the system. To charge a 4-hour capacity system with an outlet temperature of 150°C at 10 kg/s steam flow:

$$\dot{Q}_{actual,water} = \dot{m}(h_{150} - h_{260}) = \left(10\frac{kg}{s}\right) * \left(-2270.4\frac{kJ}{kg}\right) = -22704\ kJ/s$$

$$\dot{Q}_{actual,therminol} = \dot{m}(h_{240} - h_{105.7}) = \left(80.54\frac{kg}{s}\right) * \left(281.6\frac{kJ}{kg}\right) = 22680\ kJ/s$$

$$Error = \frac{22704 - 22680}{22704} = 0.001\%$$

$$\Delta t_{charg} = \frac{Q_{charge}}{Q_{therminol}} = \frac{8.13e8\ kJ}{22704\ kJ/s} = 37306\ s = 9.95\ hours$$

$$Error = \frac{9.94 - 9.95}{9.94} = -0.001\%$$

The final design is proposed below, using charging steam from the SMR. The purpose of the TESS is to assist the SMR with peak steam loads and allow time to increase steam demand in the SMR if a long-term increase is expected. Additionally, it serves to capture the excess heat generated by the SMR when the demand is low, without requiring changes in SMR steam flow, and increasing the overall efficiency of the system. A system that is too small or charges too quickly will not serve one or both of those two purposes. The proposed design includes 4 hours of steam discharge capacity, with a steam outlet temperature of 150°C. The increased outlet temperature will give a longer charging time and reduce the area required in the heat exchanger. Condensate exiting the IHX could be used to preheat the feedwater entering the steam generator. The tank volume in the design is the approximate volume of Therminol increased by 10% because some mass will always be flowing through the system. Figure 60 shows the final design of the two-tank system.

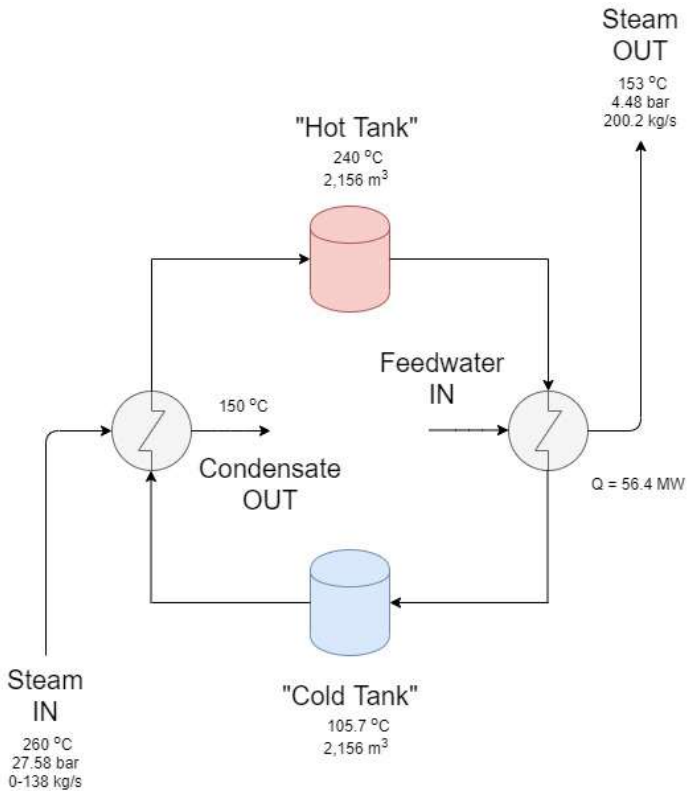

Figure 60. Design of Two-Tank Sensible Heat Storage System.

6.2.6 Case 4: Charging the Thermal Storage System

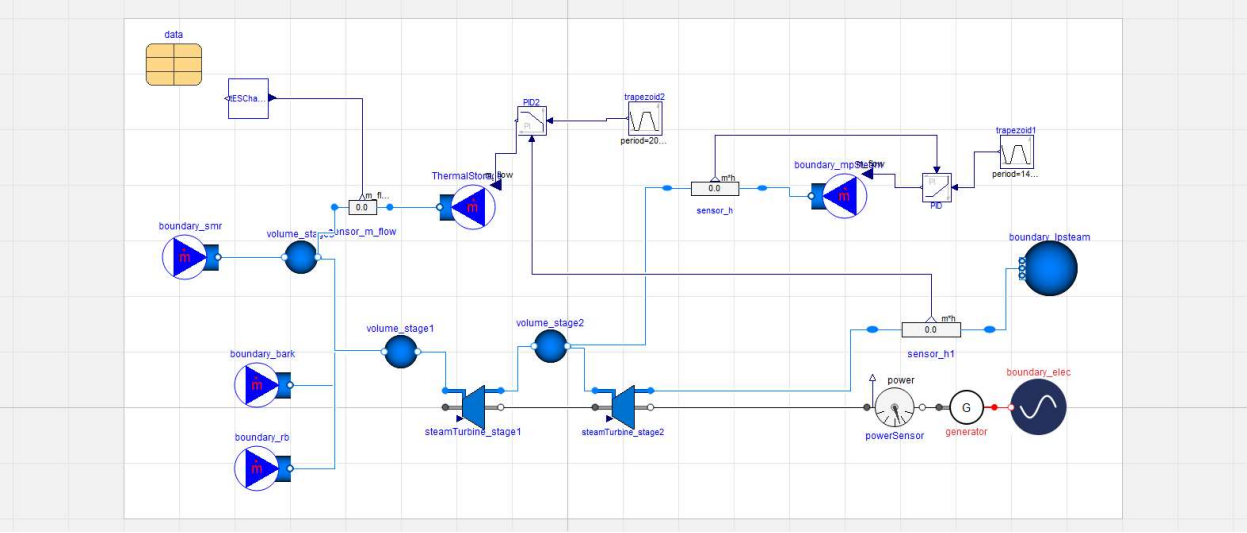

Figure 61. Case 4 Model in Dymola.

Figure 61 shows the set up for the charging thermal storage system. The SMR is set to the nominal mass flow rate, and the thermal storage system is controlled by the LP steam stream to pull steam out before the first turbine if there will be a surplus of steam. The storage system is charged with Therminol using a simple code which uses the relationship between steam mass flow rate and Therminol mass rate developed in the previous section.

The TES block receives a real input from the flow rate into the Thermal Storage system. The maximum amount of Therminol that can be stored in the block is 2.88 million kg, based on the mass of Therminol needed to discharge the system for the specified time. If the amount of Therminol contained in the block is less than the maximum, the block calculates the amount of Therminol that has entered based on the mass flow rate of the steam using the equation in Figure 62. This equation is calculated by fitting a linear curve to the Therminol flow rates in Table 16. If the TES system is full, no additional Therminol will be added, and the steam entering the Thermal Storage System is assumed to be vented.

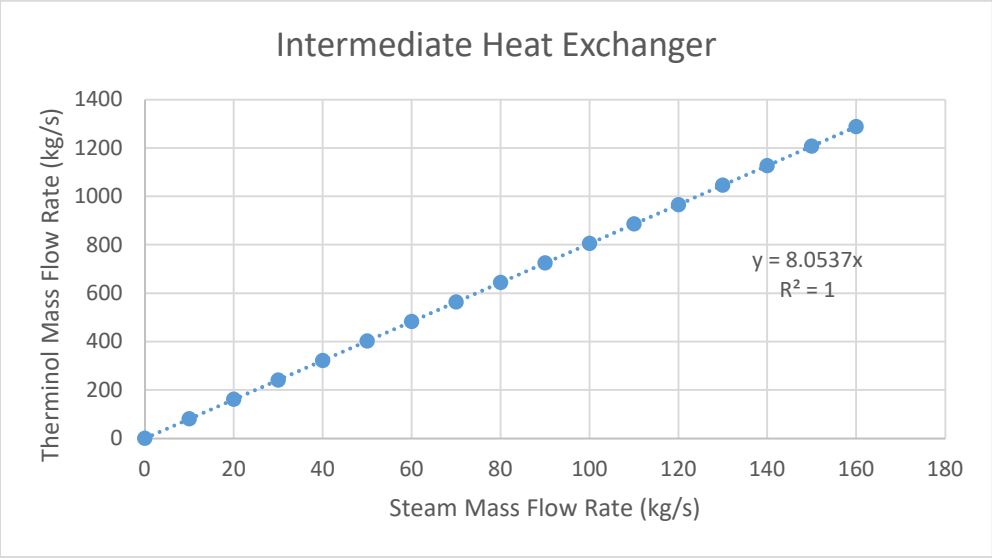

Figure 62. Curve Fit of Therminol Flow Rate Versus Steam Flow Rate in the IHX.

The first step is verifying that the model is working correctly to charge the system. Table 14 shows that the calculated time to discharge a system with a steam outlet temperature at 150°C with 4 hour capacity is 9.94 hours. If the mass flow rate of the Thermal storage block is set to 10 kg/s, the system shows the time for charging.

Figure 63 shows that at a constant 10 kg/s, the system is fully charged around 3.58e4 seconds, or 9.44 hours, giving a less than 1% error. It also verifies that the mass flow rate into the thermal storage system is a constant 10 kg/s.

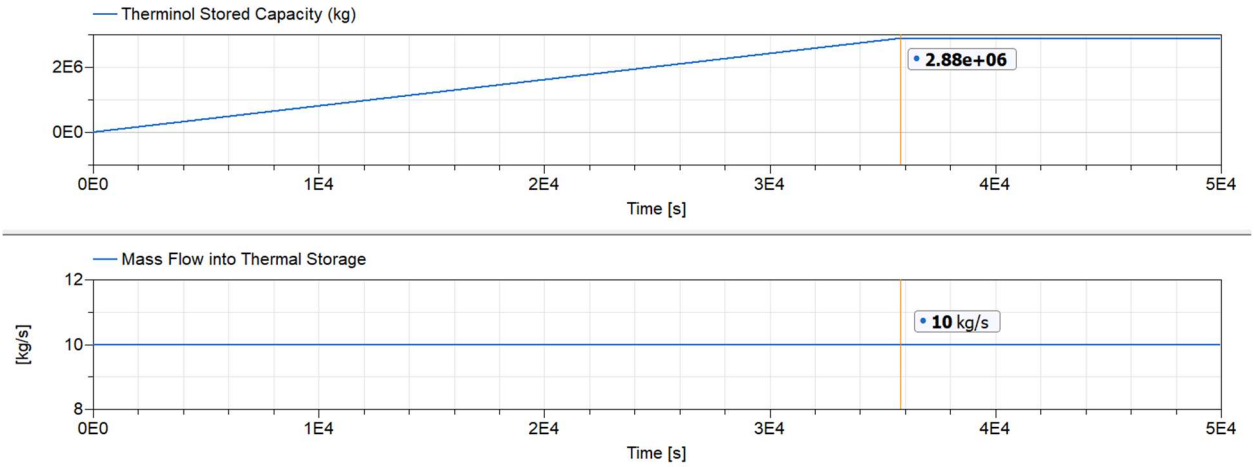

Figure 63. Charge Time for the TESS at 10 kg/s Steam.

The demand curves for both are set to go down to the minimum demand, but not above the nominal demand, in which case the storage system would be discharged.

Table 19. Trapezoidal Source Demand Curve for Case 4.

Parameter	LP Steam	MP Steam
Amplitude	[LP Steam Nominal Heat Demand] – [LP Steam Nominal Heat Demand]*0.4	[MP Steam Nominal Heat Demand] – [MP Steam Nominal Heat Demand]*0.4
Rising (s)	2,000	4,000
Width (s)	6,000	5,000
Falling (s)	8,000	3,000
Period (s)	20,000	14,000
Nperiod	-1 (inf)	-1 (inf)
Offset	[LP Steam Nominal Heat Demand]*0.4	[MP Steam Nominal Heat Demand]*0.4
startTime (s)	1,000	1,500

Using this demand curve, the thermal storage system is fully charged around 3,925 seconds, or 1.09 hours. Figure 64 shows the current tank capacity vs the instantaneous mass flow rate of steam into the thermal storage system. 1.09 hours is a short charging time for a system that will remain at nominal or below nominal flow rate for most of the time. More energy could be harvested if the tank capacity was bigger, but this would increase the expense and size. This is unnecessary discharge capacity is already very large, especially if the plant does not need the full peaking load for the entire duration of discharge.

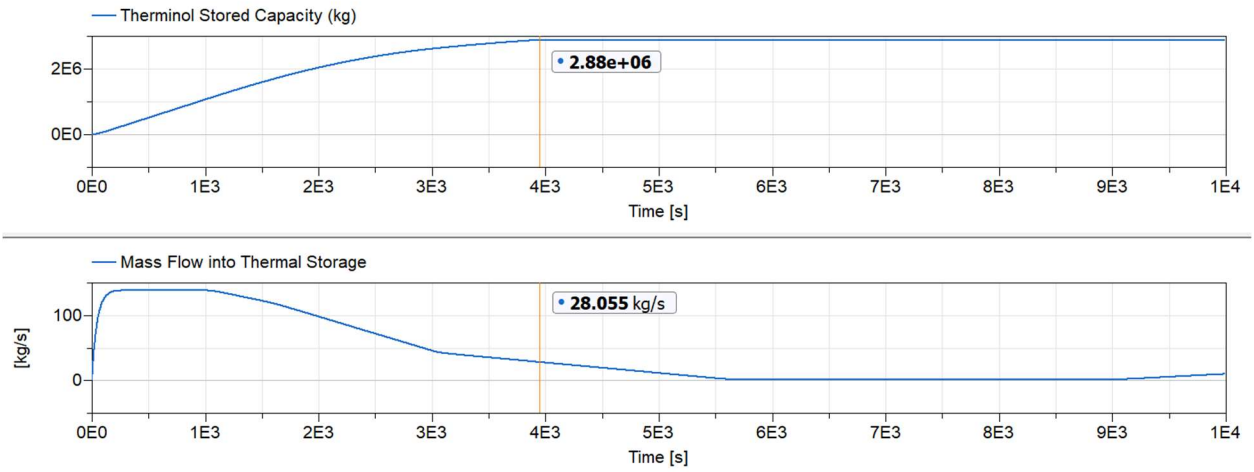

Figure 64. Charged Therminol Mass and Steam Mass Flow Rate Into the TESS.

Figure 65 and Figure 66 show the maximum flow rate and minimum flow rate possible into the thermal storage system. The maximum flow rate occurs when the MP and LP steam demands are both at the lowest. In this case, all the SMR steam is diverted to the storage system. The smallest mass flow rate is 1.5 kg/s when the demand is nominal. Theoretically, this should be 0, since the SMR is designed for a steam flow that meets the nominal demands. As the maximum flow rate into the SMR, the TES is diverting slightly more than the nominal SMR flow rate. The error here of 0.2 kg/s can be attributed to slight differences in conditions when altering the model.

It is important to note that this is a simplistic model, and there will always be some mass flow through the heat exchangers, especially as the system begins to lose heat to its environment.

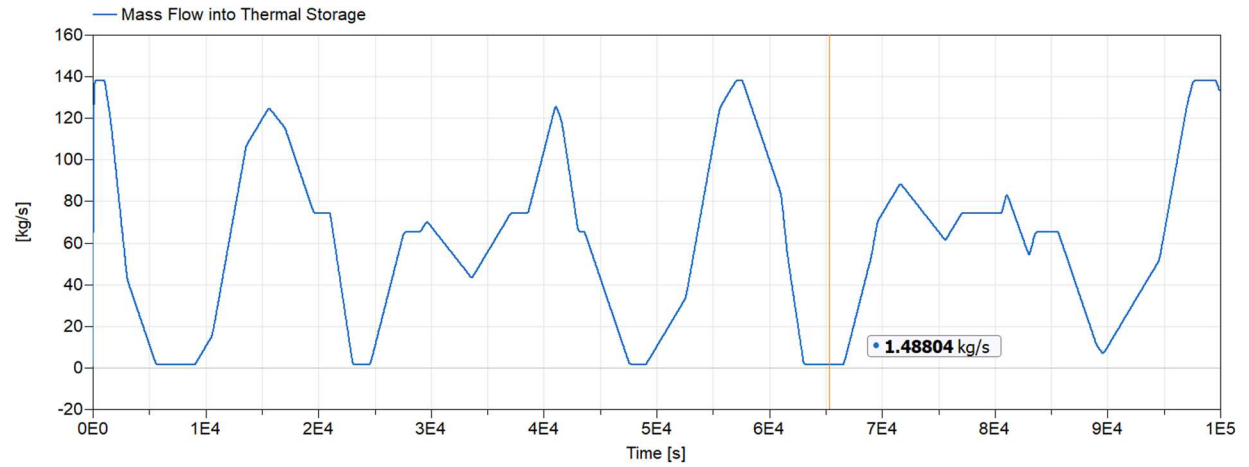

Figure 65. Steam Flow Into the Thermal Storage When Both Demands are at Nominal.

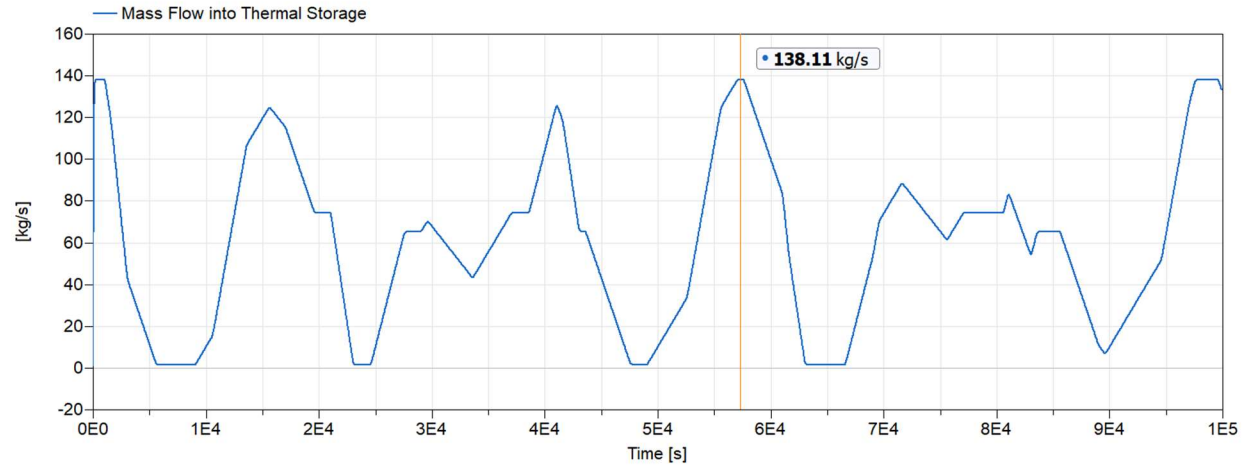

Figure 66. Steam Flow into Thermal Storage when Both Demands are at Minimum.

Figure 67 and Figure 68 show the minimum and maximum power production for the turbines in this case. The range is quite extreme, from 18 to 54 MW. A quick shift from one to the other would be difficult for the plant from an operation standpoint, but because the steam flow already shifts in regular operation, it could still be feasible to maintain this range.

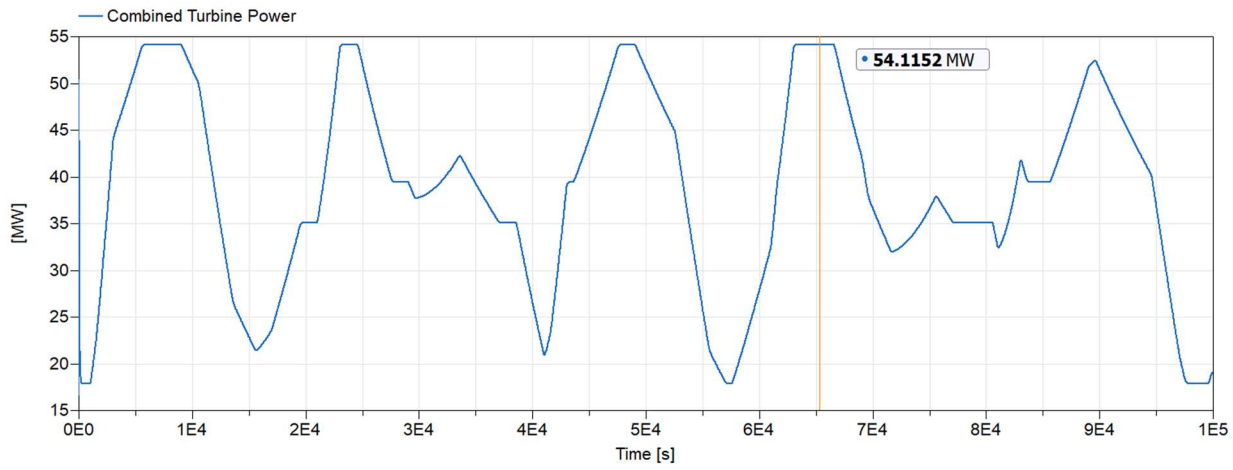

Figure 67. Maximum Combined Turbine Power in Case 4.

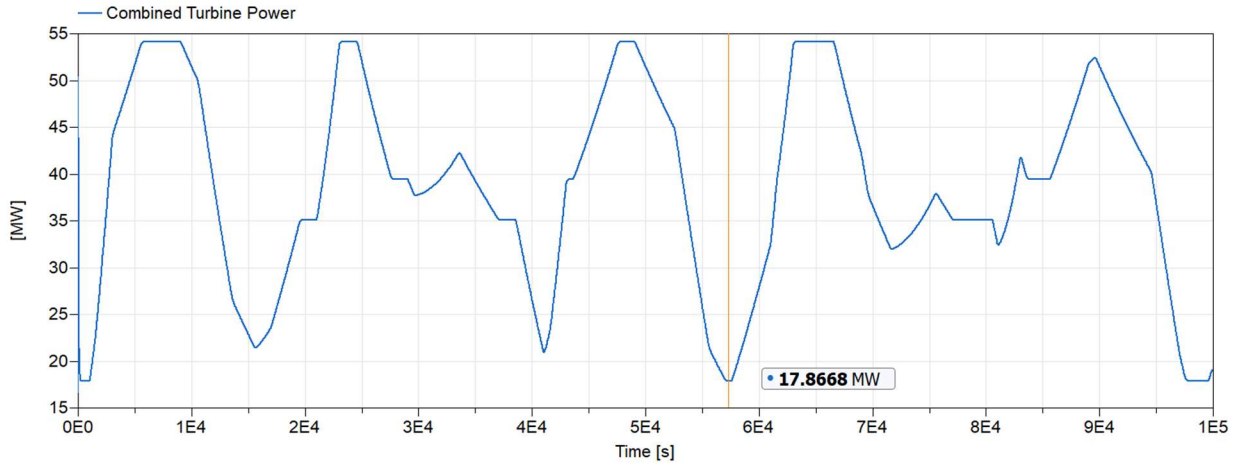

Figure 68. Minimum Combined Turbine Power in Case 4.

6.2.7 Case 5: Discharging

The discharging TES block operates similarly to the charging block. A mass flow source is connected after the first turbine stage with a fixed specific enthalpy to match the steam exiting the turbine. The mass flow rate is controlled by the demand curve of the LP steam stream. An additional control must be added in this case to stop the thermal storage system from discharging if it is empty. A Boolean switch checks the tank capacity via a real output from the TES clock. If

the tank capacity is less than or equal to 0, no steam is discharged. Otherwise, the demand curve can pass through to control the discharge steam.

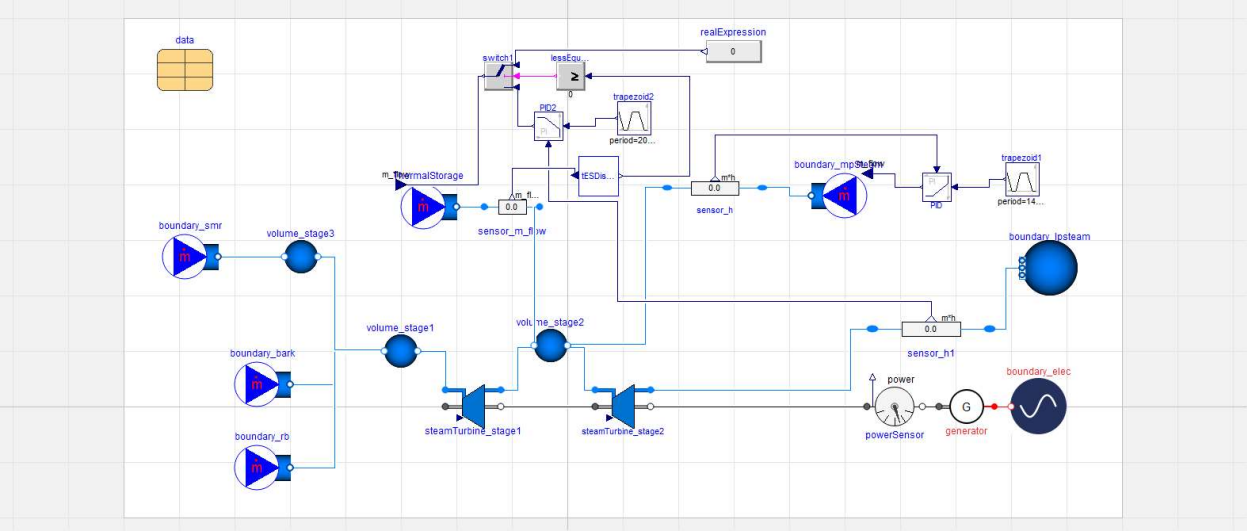

Figure 69. Case 5 Model in Dymola.

The TES block calculates the mass of Therminol used during the discharging process using the equation in Figure 70. The linear relationship is calculated from the heat transfer needed in the steam generator to bring the steam to the correct conditions depending on the mass flow rate of steam. This is based on calculations in the previous section.

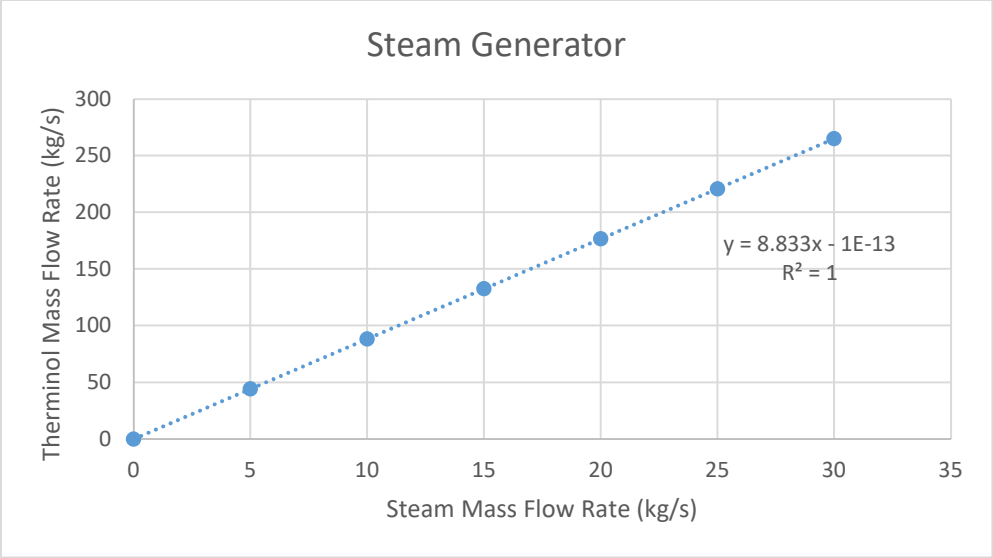

Figure 70. Curve Fit of Therminol Flow Rate Versus Steam Flow Rate in the Steam Generator.

The thermal storage system is sized to discharge steam at 22.8 kg/s with a specific enthalpy of 2,835 kJ/kg when both the MP and LP steam streams are at 110% demand. As shown in Figure 71, when both demand streams are set to 110% of the nominal heat demand, the system reaches steady-state with a constant discharge mass flow rate of 22.8 kg/s, as designed.

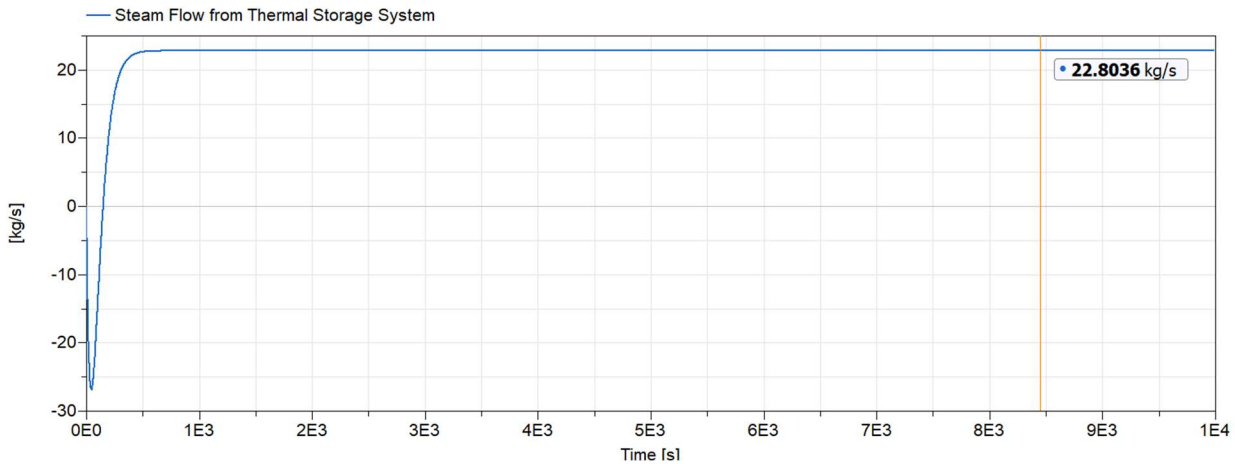

Figure 71. Steam Mass Flow Rate from the Thermal Storage System at Maximum Demand.

According to Figure 72, at the maximum demand for both streams, the system fully discharges at about 14,400 seconds, or exactly 4 hours. Overall, the simplified system gives a good representation of the design. Figure 72 also confirms that the TES stops discharging steam when the Therminol is fully discharged.

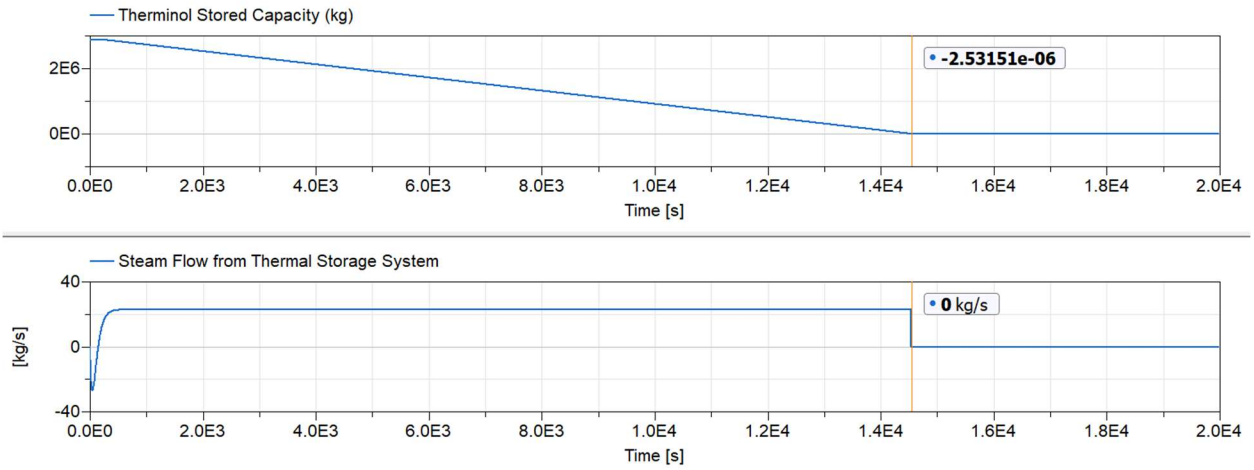

Figure 72. Discharge Time for TESS When Demands are at Maximum

The demand curves are adjusted to go between the steady-state demand and the maximum demand. It will not go below the steady-state demand because in that case, the thermal storage system would be charged.

Table 20. Trapezoidal Source Demand Curve for Case 5.

Parameter	LP Steam	MP Steam
Amplitude	[LP Steam Nominal Heat Demand]*1.1 – [LP Steam Nominal Heat Demand]	[MP Steam Nominal Heat Demand]*1.1 – [MP Steam Nominal Heat Demand]
Rising (s)	2000	4000
Width (s)	6000	5000
Falling (s)	8000	3000
Period (s)	20000	14000
Nperiod	-1 (inf)	-1 (inf)
Offset	LP Steam Nominal Heat Demand	MP Steam Nominal Heat Demand
startTime (s)	1000	1500

Similarly to the verification case, the maximum flow rate of steam from the steam generator is 22.7 kg/s. The lowest theoretical flow rate is 0 kg/s when the system is fully discharged.

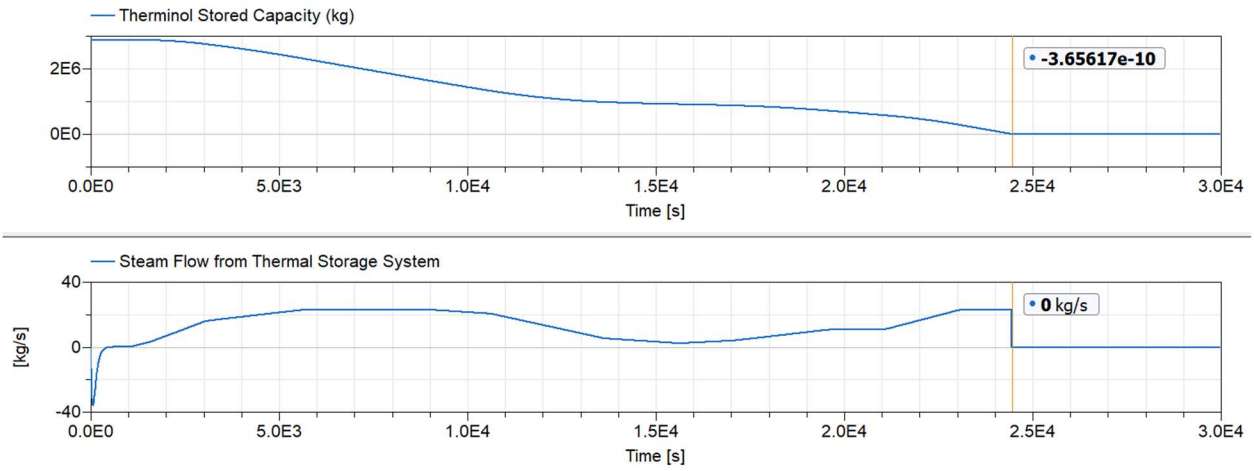

Figure 73. Actual Therminol Steam Output and Discharge Time for Case 5.

Using this demand curve, the system discharges in 23,800 seconds, or 6.6 hours. When the system is not discharging at the maximum for the entire time, it can accommodate much

longer peaks. This is a good amount of time to keep the system steady for the plant to adjust for a longer-term increase in demand.

The MP steam demand curve and actual heat input is almost exact, but the LP heat curve has some discrepancies, similar to previous cases. Overall, the thermal storage system is able to accommodate the increase in demand for a long period of time. Once the storage system is fully discharged, the LP steam will have a large deficit in steam supply.

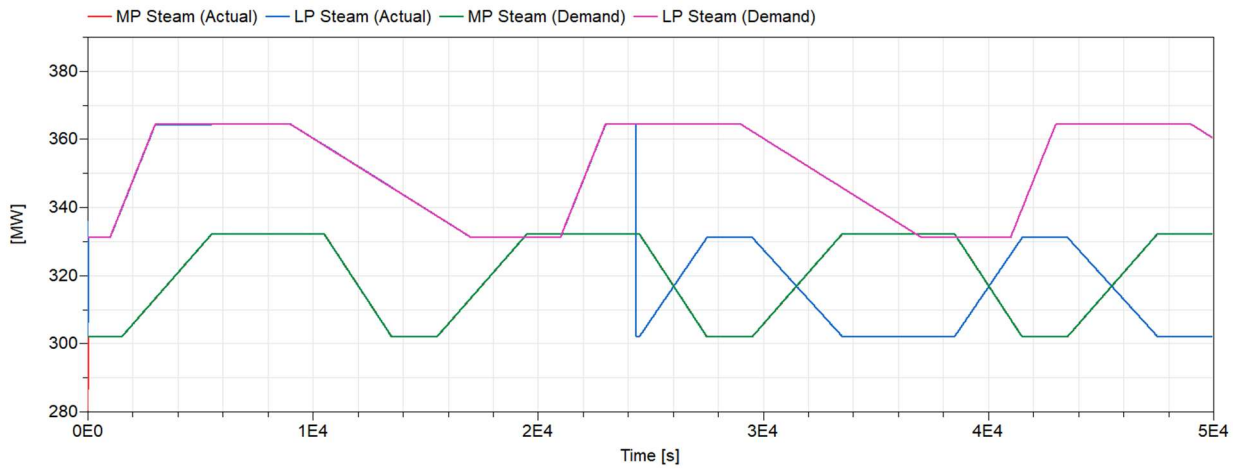

Figure 74. Case 5 Demand Curves Versus Actual Heat Out Before and After TESS Assistance.

When both streams are at their maximum demand and the TES is at maximum discharge, the power is 55 MW (Figure 75). Note that this is lower than the maximum power in both Case 2 and Case 3, because the discharge steam is not sent through a turbine. At no discharge, the power is 54.1 MW. The SMR is still providing the nominal flow rate, but the power increases because the thermal storage system increases the steam through turbine 2. The power output of the turbines varies very little, even after the storage system stops discharging. This is good for the steady-state operation of the plant.

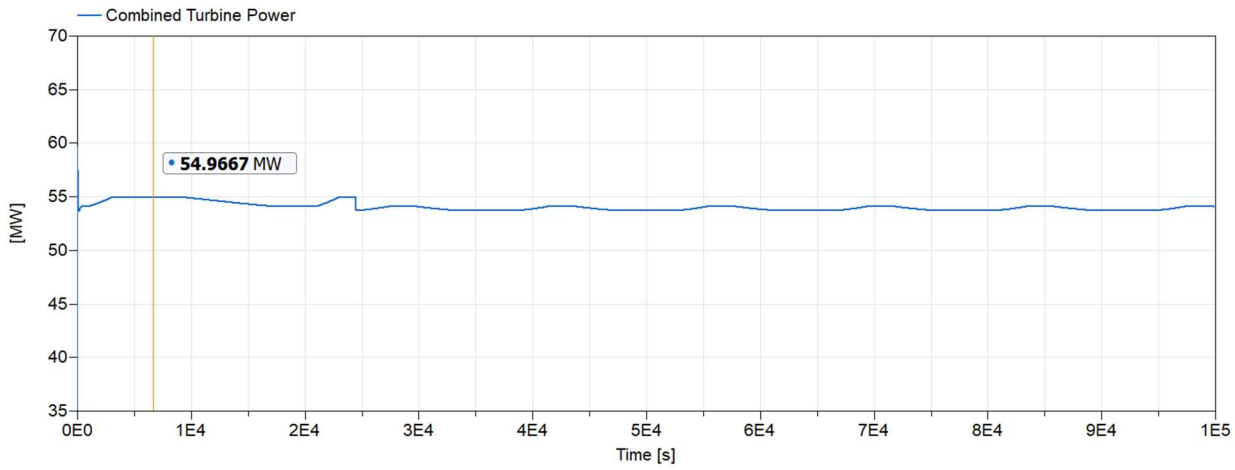

Figure 75. Combined Turbine Power when Demands are at Maximum with TESS Assistance.

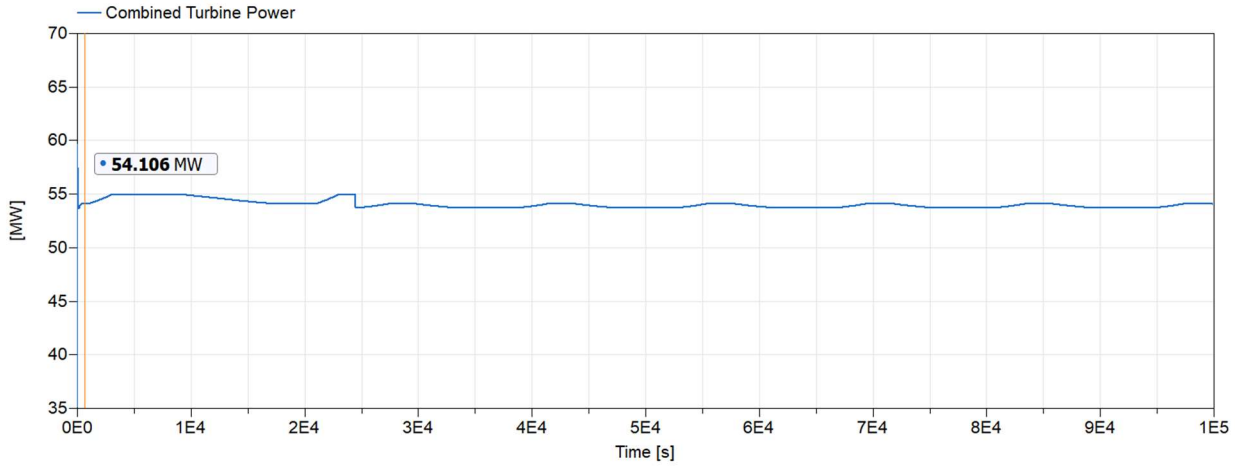

Figure 76. Combined Turbine Power when Demands are at Minimum with TESS Assistance.

6.3 Plant A

Plant A consists of four steam sources that feed into two turbines. Each source is controlled in the models by its heat flow rate in Watts. The nominal values of the bark boiler and black liquor recovery boilers are based on the steady-state data provided by Plant A. These sources are considered constant because their output is based on the chemical recovery process, which remains consistent even if steam demands change.

Based on the steady-state analysis, Plant A is utilizing 1 SMR Modules for a maximum steam flow of 265,923 lb/hr (33.5 kg/s) steam. The steady-state steam flow required is 142,200 lb/hr (17.9 kg/s). Increasing steam flow from the SMR will increase electricity production within the plant. Decreasing steam flow from the SMR will increase electricity production in the SMR and decrease electricity production within the plant.

Based on trends within the plant, turbine intake can vary between 40% and 110% of the steady-state intake. Flows can change based on demands for MP and LP steam, as well as variation in the electricity purchase price. At steady-state, the total steam demand from all 4 sources is 1.53 million lb/hr (193 kg/s), so the steam demand could vary between 612,000 and 1.68 million lb/hr (77.1-212 kg/s). If the bark boiler and RB boiler sources remain constant, this means the SMR would vary between 0 and 150,000 lb/hr (0-18.9 kg/s) .

It's important to note that the SMR source is at a lower temperature than the other sources, and has a lower specific enthalpy than the original natural gas source. Increased flow from the SMR results in slightly decreased heat to the rest of the system. To solve this, a PI controller is placed on either the MP or LP steam line to control the total enthalpy (mass flow rate times specific enthalpy) provided rather than mass flow rate.

6.3.1 Case 1: Baseline Plant Operations

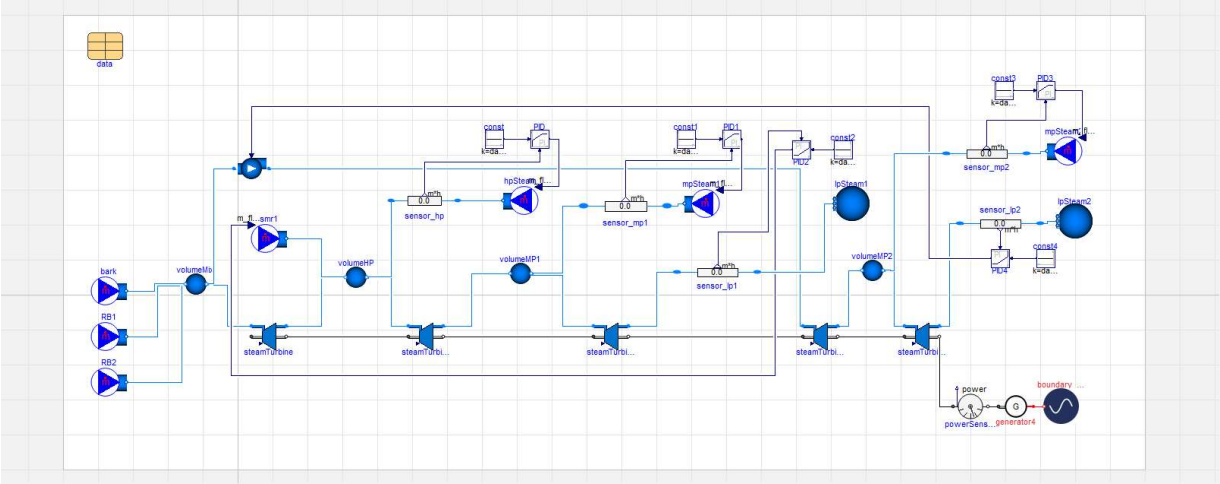

Figure 77. Baseline Model of Plant A Built in Dymola.

The baseline model for Plant A is very similar in terms of operation to Plant B. The main difference is that the RB and Bark steam sources are split between two turbines, which feed separate MP and LP steam streams. The first turbine also feeds a high pressure steam stream. As in the Plant B model, each steam source is controlled by the total heat demand, the specific enthalpy of the stream times the mass flow rate. The LP stream on turbine 1 (LP1) demand controls the SMR output, and the LP stream on turbine 2 (LP2) controls the amount of steam diverted off the original steam sources into turbine 2. All 5 turbine stages are connected to produce a combined turbine electricity generation for the plant.

The first results needed for verification of the model are the steady-state mass flow outputs of the HYSYS model and the Dymola Model. Figure 78 shows the steady-state flow rate calculated from the HYSYS model and the flow rate from Modelica. As with plant B, the results are slightly different, with an error of 2.5%. The increase of error from Plant B is likely due to the amount of controlled variables in this model. With more controlled variables, there is more risk for variation from rounding errors and differences in calculation methods.

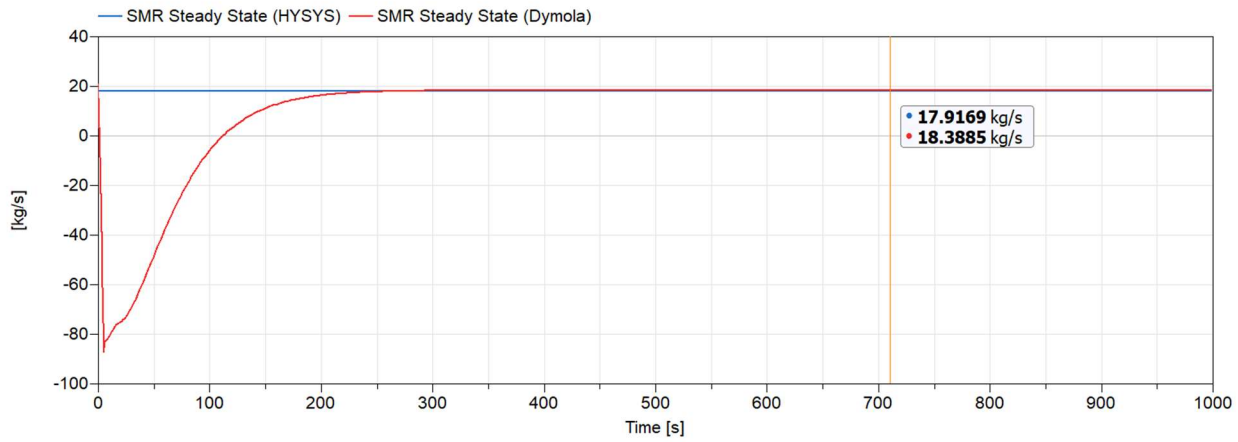

Figure 78. SMR Steady-State Steam Flow Calculated by Dymola and HYSYS.

The other verification point is the combined turbine power of the plant. The HYSYS model calculated the steady-state power as 84.8 MW, while in Figure 79 the Dymola model calculated a power of 89.4 MW resulting in a 5.4% difference. The main reason for this is the difference in the way turbine calculations are done in the two programs. HYSYS uses the Peng-Robinson equation of state for fluid calculations in the turbine, while the Dymola turbine component uses Stodola's Law.

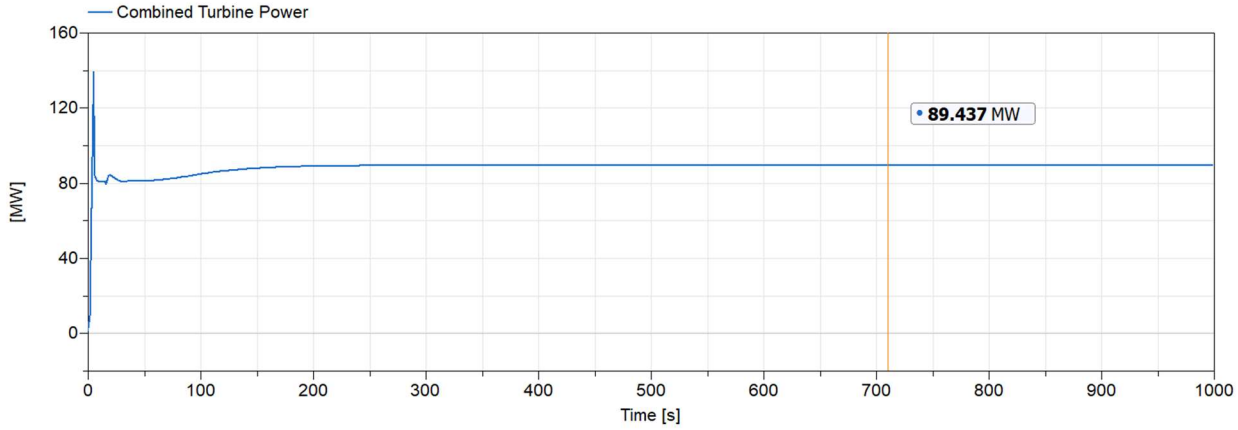

Figure 79. Steady-State Combined Turbine Power for Plant A.

The mass flow rate (Figure 80) and specific enthalpy (Figure 81) of each stream can also be verified and will help determine the streams causing the large difference. The specific enthalpy can be specified for each stream in the model to try and reduce variations.

Table 21 shows the resulting mass flow rate has an insignificant error, showing that the heat rate calculated for each stream in both models is the same.

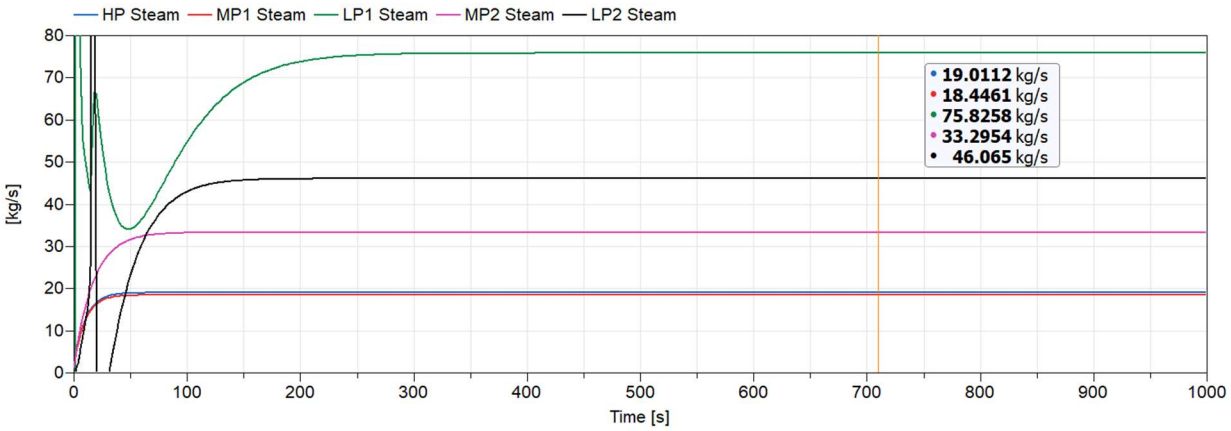

Figure 80. Steady-State Mass Flow Rates for Each Steam Stream.

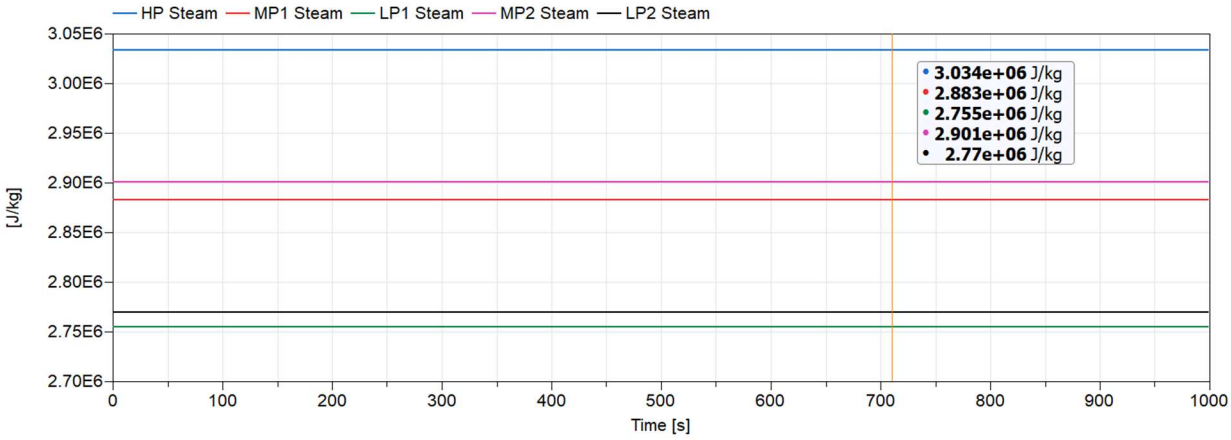

Figure 81. Specific Enthalpy of Each Steam Stream in Plant A.

Table 21. Comparison of HYSYS and Dymola Steady-State Models.

	Specific Enthalpy (kJ/kg)			Mass Flow (kg/s)		
	HYSYS Model	Dymola Model	Difference	HYSYS Model	Dymola Model	Difference
HP Steam	3,034	3,034	0%	19.01	19.01	0%
MP Steam 1	2,883	2,883	0%	18.44	18.45	0.05%
LP Steam 1	2,755	2,755	0%	75.80	75.83	0.04%
MP Steam 2	2,901	2,901	0%	33.29	33.30	0.03%
LP Steam 2	2,779	2,779	0%	46.04	46.07	0.07%

6.3.2 Case 2: Steam Demand Changes, No SMR Flow Limits

In the second case, the steam demand fluctuates without setting flow limits on the SMR, it is simply controlled by the steam demand of the LP1 stream. The model first runs in steady state to initialize the model, then the steam demand can fluctuate. Figure 82 shows the complete model set-up for this case.

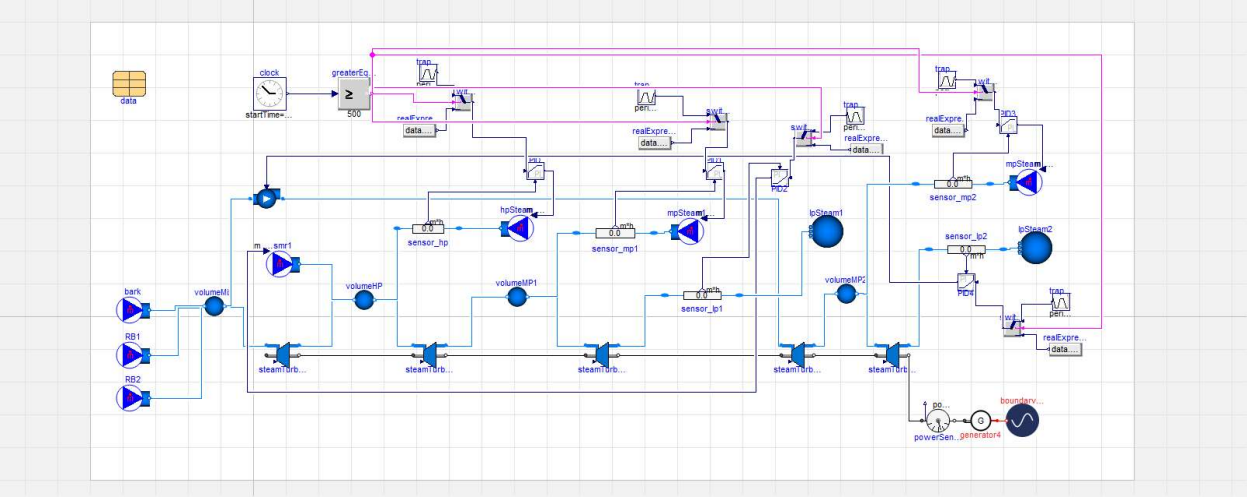

Figure 82. Case 2 Model in Dymola.

The steam demand for all cases versus the actual heat rate is very similar, with only small differences in the two LP streams. The differences can be minimized by increasing the gain in

the controllers to allow a faster response time, but in a model like this one with many controlled variables, the gain can only be increased so much before it restricts the calculation in the model. Figure 83 shows that even at a higher gain, there are still places where the actual calculation differs from the desired demand.

Table 22. Trapezoidal Heat Demand Source Curve for Case 2 and 3.

Parameter	HP Steam	MP1 Steam	LP1	MP2	LP2
Amplitude	[HP Steam Nominal Heat Demand]*1.1 – [HP Steam Nominal Heat Demand]*0.4	[MP1 Steam Nominal Heat Demand]*1.1 – [MP1 Steam Nominal Heat Demand]*0.4	[LP1 Steam Nominal Heat Demand]*1.1 – [LP1 Steam Nominal Heat Demand]*0.4	[MP2 Steam Nominal Heat Demand]*1.1 – [MP2 Steam Nominal Heat Demand]*0.4	[LP2 Steam Nominal Heat Demand]*1.1 – [LP2 Steam Nominal Heat Demand]*0.4
Rising (s)	500	350	500	800	400
Width (s)	750	700	700	750	600
Falling (s)	600	500	500	1200	250
Period (s)	3000	2500	2000	3000	1500
Nperiod	-1 (inf)	-1 (inf)	-1 (inf)	-1 (inf)	-1 (inf)
Offset	[HP Steam Nominal Heat Demand]*0.4	[MP1 Steam Nominal Heat Demand]*0.4	[LP1 Steam Nominal Heat Demand]*0.4	[MP2 Steam Nominal Heat Demand]*0.4	[LP2 Steam Nominal Heat Demand]*0.4
startTime (s)	500	500	500	500	500

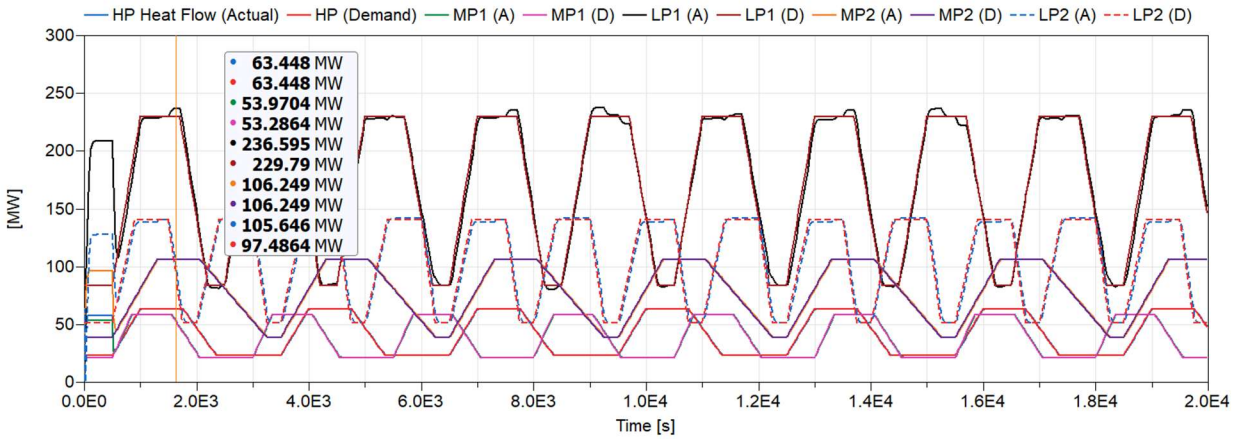

Figure 83. Heat Out Demand Curves Versus Actual Model Calculations.

At the highest possible gain, the approximate largest errors in each stream are in Table 23.

Table 23. Heat Out Error at Maximum Deviation from Demand.

	HP	MP1	LP1	MP2	LP2
Demand	63.45	53.2864	229.79	106.249	97.4864
Actual Output	63.45	53.9704	236.595	106.249	105.646
Error	0%	1.3%	2.9%	0	7.7%

In a more detailed study of the effects of these steam changes on the system, these errors could be very significant. In this study, however, there are only two major points of interest: the point where all streams are at the maximum demand, and all streams are at the minimum demand.

At the two points identified, the errors are very small, meaning the data collected at these two points is accurate up to the accuracy of the model itself. Figure 84 shows the selected point where all demands are at the maximum. Table 24 shows the corresponding error.

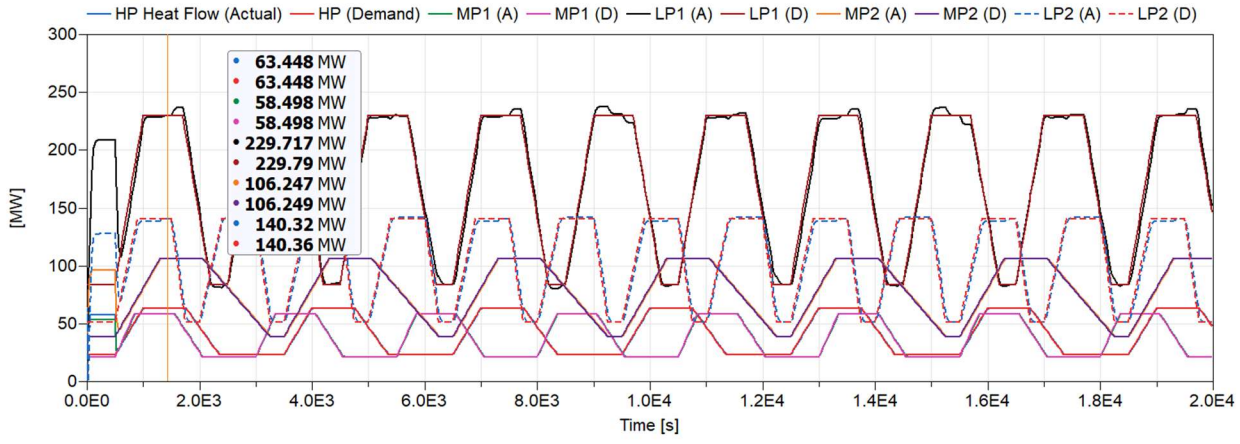

Figure 84. All Streams at Maximum Demand.

Table 24. Error at Maximum Demand Point.

	HP	MP1	LP1	MP2	LP2
Demand	63.45	58.45	229.72	106.25	140.36
Actual Output	63.45	58.45	229.79	106.25	140.32
Error	0%	0%	0.03%	0%	0.03%

Figure 85 shows the selected point at which all streams are at the minimum demand.

Table 25 shows the corresponding error.

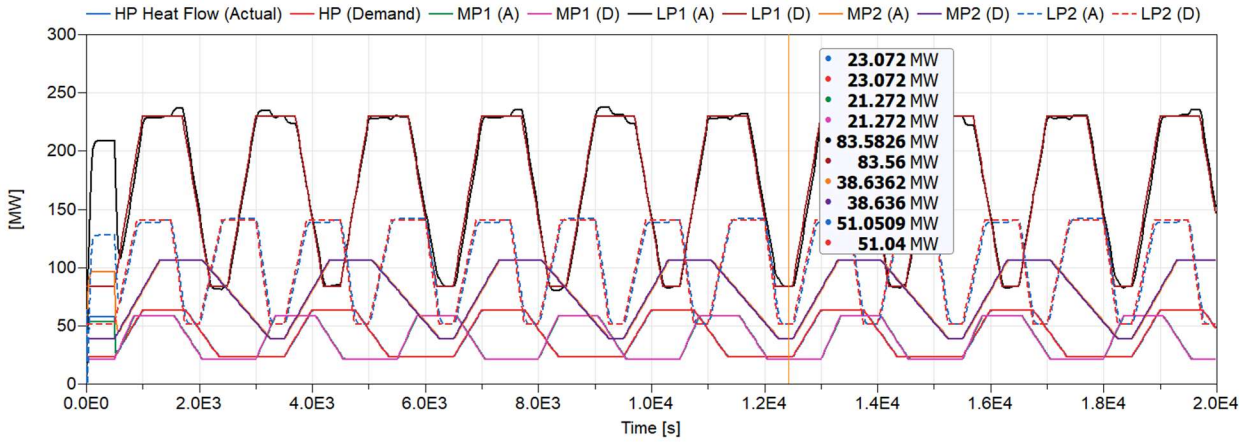

Figure 85. Demand Curves Versus Actual Heat Ouput for All Streams at Minimum Demand.

Table 25. Error at Minimum Demand Point.

	HP	MP1	LP1	MP2	LP2
Demand	23.07	21.27	83.56	38.64	51.04
Actual Output	23.07	21.27	83.58	38.64	51.05
Error	0%	0%	0.03%	0%	0.02%

It is easily shown that this in an unrealistic case. When the steam demand for all streams is at the lowest, the SMR stream has a reverse flow of 97 kg/s, which would be detrimental but also physically impossible for the system. Even if the SMR was removed, the plant is still generating a large surplus of steam when the demands are at their lowest.

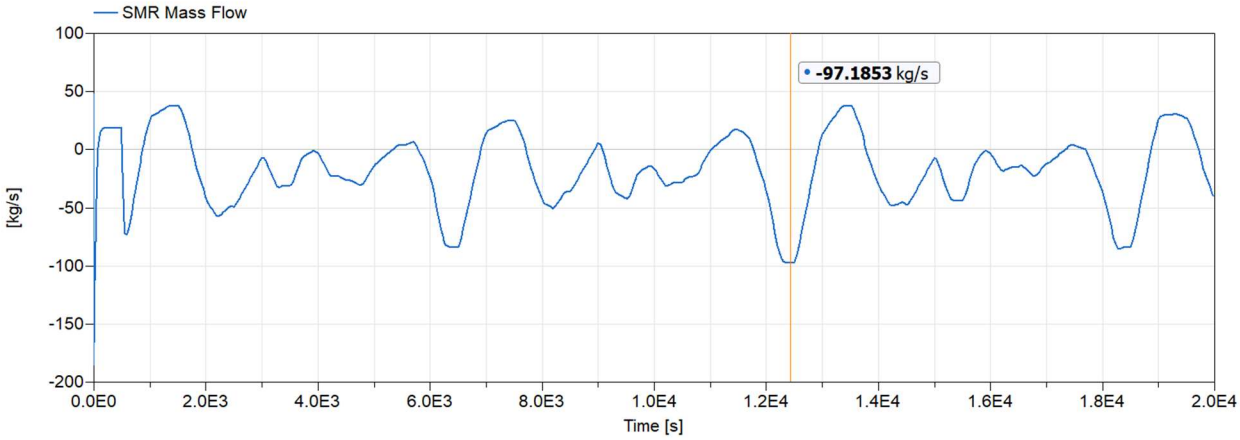

Figure 86. SMR Steam Flow When all Demands are at Minimum.

From Figure 87, when all streams are at the highest demand, the steam flow required from the SMR to meet the demands is 37.6 kg/s, more than double the steady-state steam requirement. Although this is a good estimate for the possible maximum demand needed from the SMR, the negative flow rates that are generated from this case make this configuration impossible.

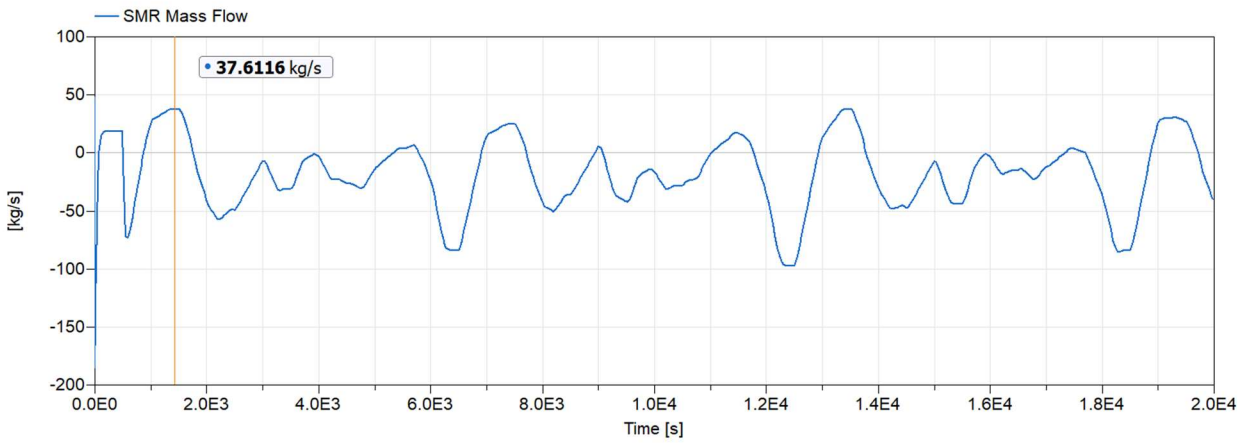

Figure 87. SMR Steam Flow When All Demands are at Maximum.

While the steady-state requirement is too high for times of lowest demand in the plant, it is also well below the necessary steam to meet the highest demands.

By looking at the mass out of each stream to meet the heat demands in Figure 88, it shows how great the demands of LP1 are compared to the rest of the streams. LP1 has a 40% higher mass demand than LP2, the next highest stream demand. It also has the largest range of heat demands. The demand range of LP1 is likely the largest contributor to the swings of SMR demand as the heat demands for each stream change.

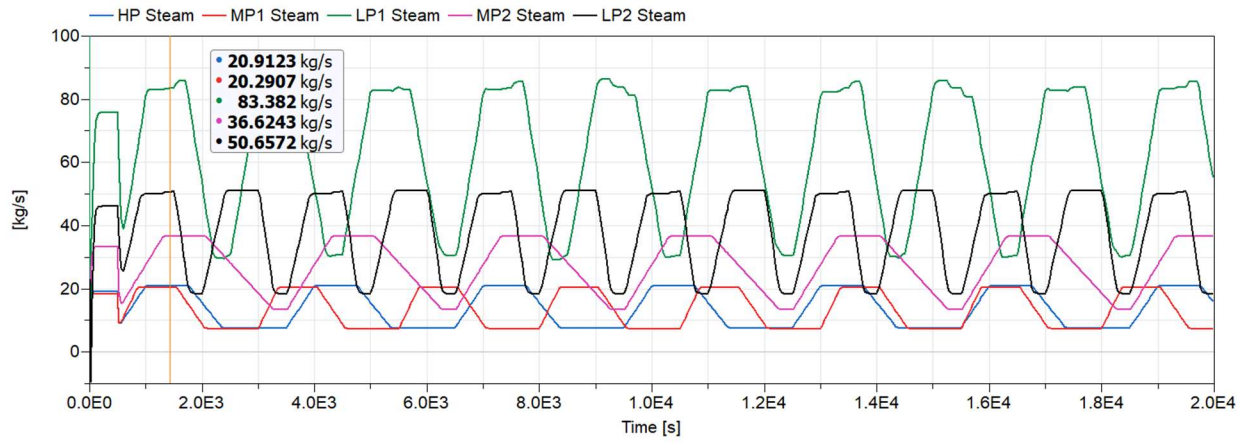

Figure 88. Steam Demand of Each Stream in Case 2.

One last point of discussion is the change in specific enthalpy of the stream due to addition of the SMR steam supply, which is shown in Figure 89. Because of how small the mass contribution of the SMR steam is compared to the other steam sources, the effect is not as great as it is in Plant B, but there is still a small difference that can be measured.

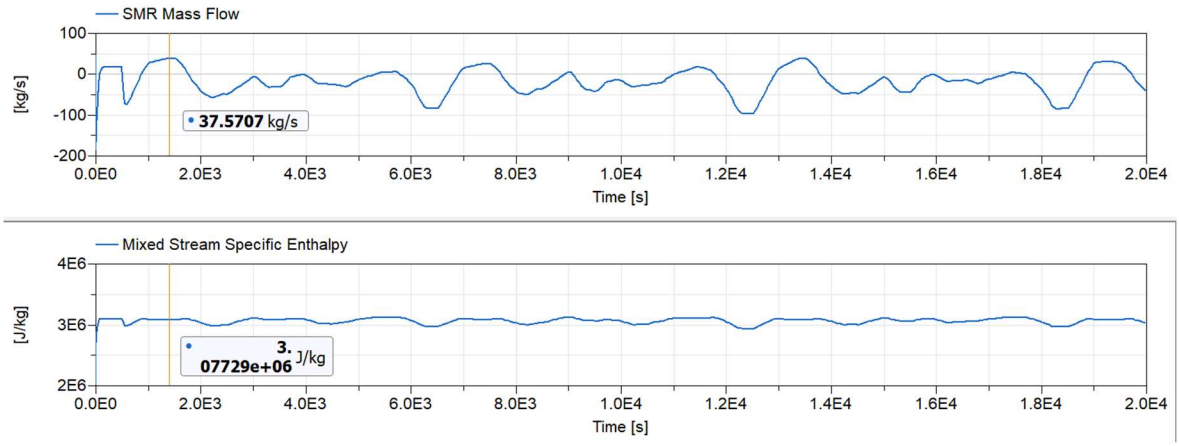

Figure 89. Specific Enthalpy of Steam Flow Versus SMR Flow Rate.

6.3.3 Case 3: Demands change, SMR remains at steady state

In Case 3, the model in Figure 90 initializes using the demand values from Case 2, then the SMR operates at the steady-state flow rate.

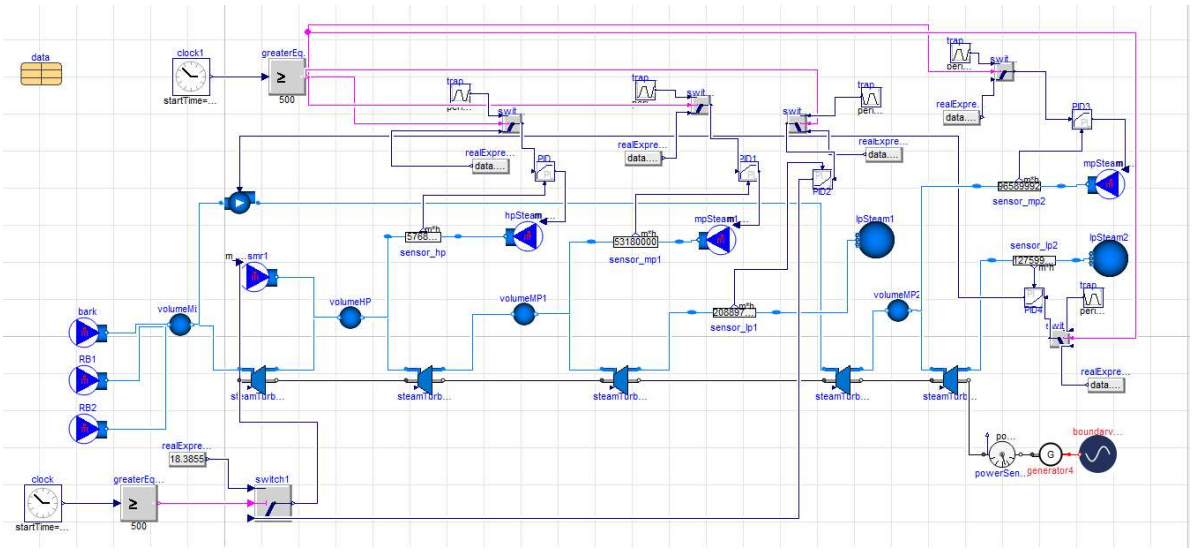

Figure 90. Case 3 Model for Plant A in Dymola.

In Figure 91, all the actual heat outputs from the stream except for LP1 match the demand curve closely, since they are controlled elsewhere in the model. By comparing the LP1 actual curve against the demand curve, we can estimate the amount of heat wasted or needed to meet the total demand of the plant when the SMR runs at steady state. We also know from Case 2 that LP1 has the largest individual impact on demand swings in the plant. Case 3 uses the same demand curve as Case 2.

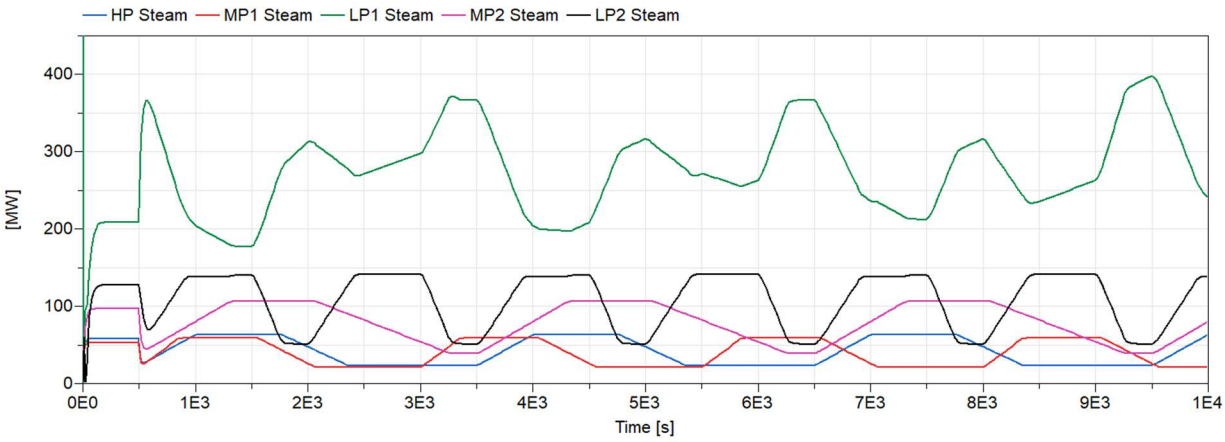

Figure 91. Actual Heat Out for All Streams in Case 3.

In Figure 92, the demands of all streams are at their highest (110% of nominal), while the SMR runs at the steady-state flow rate. At this point, the heat deficit in the plant is 53 MW. The combined turbine plant power is 88.4 MW (Figure 93), which is close to the steady-state plant value of 89 MW. Although the SMR cannot meet the demands of the plant, it is good that the turbine power has small variations because it helps the steady operation of the plant.

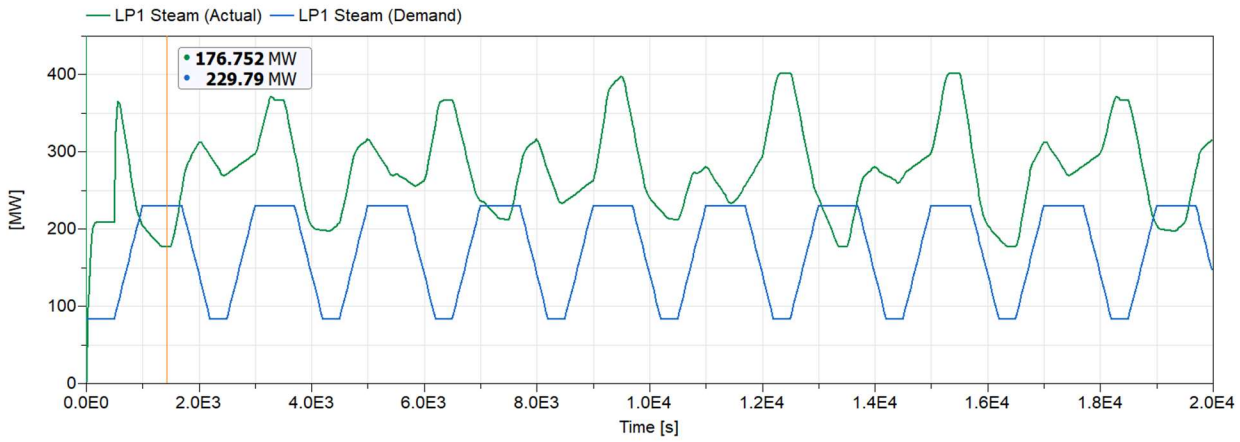

Figure 92. LP1 Heat Demand Curve Versus Actual Output When All Demands are at Highest Point.

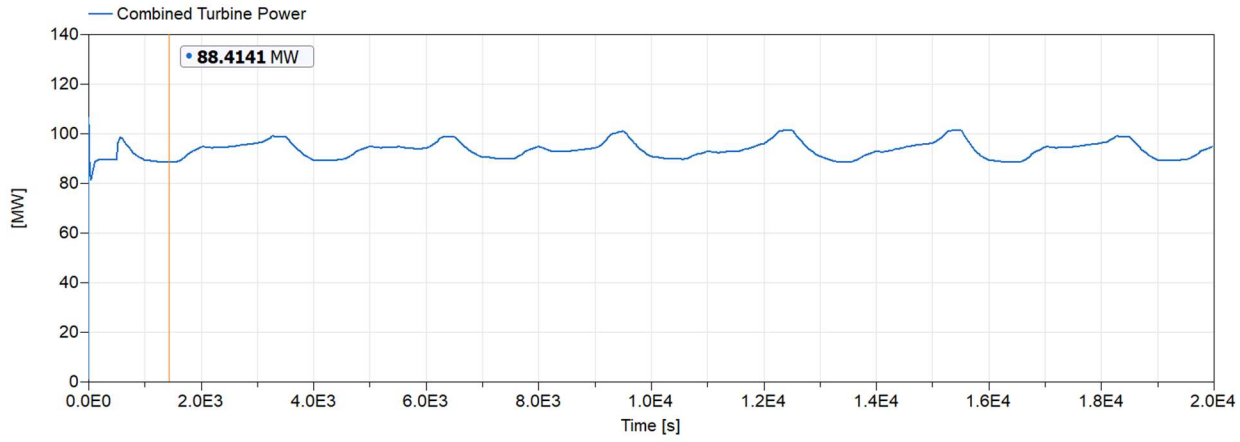

Figure 93. Combined Turbine Power When All Demands are at Highest Point.

When all the demands are at the lowest in Figure 94, the plant produces a surplus of 318 MW heat. The combined turbine power is 101 MW (Figure 95), which is much higher than the

steady-state power value. Although keeping the SMR at the steady-state value sometimes increases the turbine power of the plant, which decreases the amount of electricity the plant must buy to meet its electricity demands, the wasted heat is decreasing the efficiency of the plant, and the periods when the steady-state rate from the SMR cannot meet the demands will cause issues for production and quality within the plant.

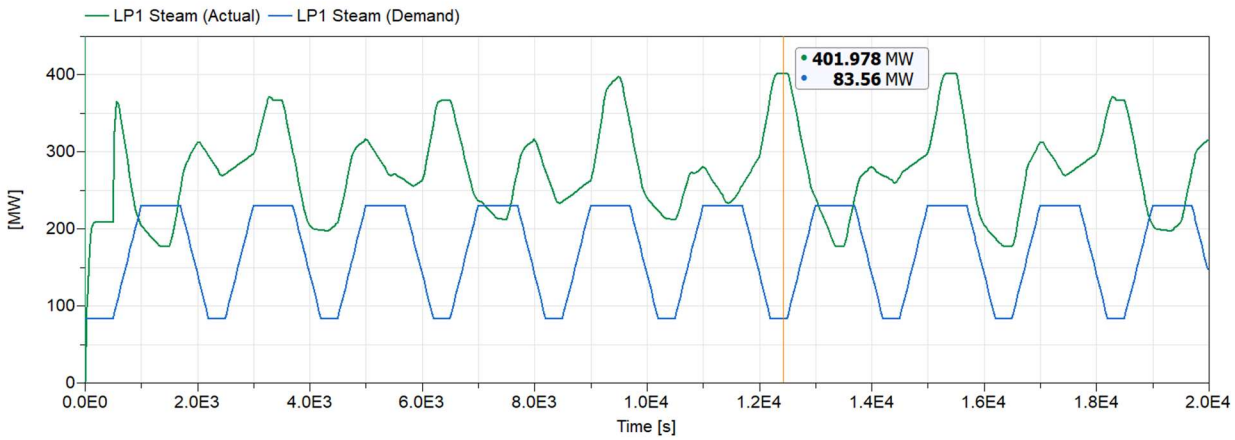

Figure 94. LP1 Heat Demand Curve Versus Actual Output When All Demands are at Lowest Point.

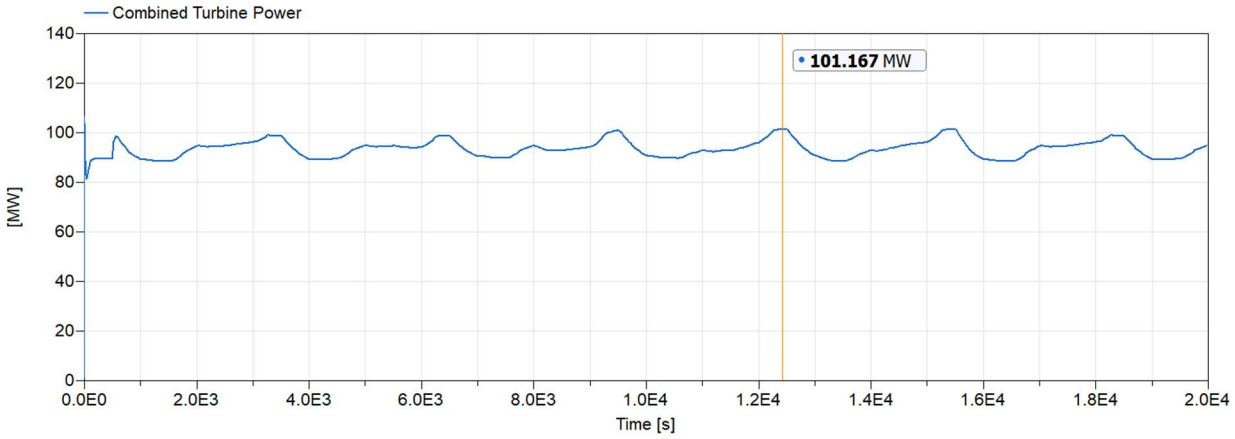

Figure 95. Combined Turbine Power When All Demands are at Lowest Point.

Although it is best for the operation of the SMR to keep it at the steady-state value all the time, this nominal value does not meet the needs of the plant all the time, in terms of demand and

efficiency. One way to improve the economics and performance of the SMR with the plant is to incorporate a thermal energy storage system.

6.3.4 Thermal Energy Storage Design

From Plant B, it has been shown that slight differences in the steam outlet conditions from the TESS do not significantly change the overall stream conditions within the plant. For continuity, the outlet conditions of the TESS are assumed to be the same as the stream it connects to. However, there are still options for the placement of the charging and discharging points of the system.

Unlike Plant B, the SMR is included as a source mid-stream, rather than at the beginning. There is also a split of the initial steam source into two separate turbines. At 103 bar and 507°C, it is not necessary to use this high energy steam as a charging source for thermal storage. Using this as the source will also greatly reduce the power from the first turbine stage 1, which is needed because the steady-state SMR and turbine power are about 12 MW below the needed power, as shown in Chapter 5.

It would not be effective to take the steam off the SMR only. The SMR is only providing a steady-state mass flow of about 18 kg/s, and Case 2 showed that when all the streams are at minimum demand, the SMR source has a reverse flow. Taking steam off only the SMR source would mean that even if all the steam from the SMR was diverted to the storage system, there would still be a surplus of steam flow into the rest of the system, decreasing the overall efficiency of the plant.

The most effective stream for the TESS to charge from is where the SMR and original steam stream is combined, and the HP steam is taken off. This will allow the TES system to take off as much steam as needed to meet the demands of the HP, MP1 and LP1 streams.

There are three possible places for the TESS discharge stream. The first would be discharging into the MP2 or LP2 streams. While this would be possible, it is not necessary because the model is already controlled to take all the needed steam for Turbine 2 off the Bark and Recovery steam sources, and the demands are met at all levels. The other reason that this is unnecessary is that we are trying to integrate the SMR and storage while making the minimum changes to the system as possible. In the current system design, only the T1 stream is affected by the SMR. If the thermal storage were to discharge into the T2 stream, there would need to be changes to both turbines rather than just one.

The second and third options are after the second Turbine 1 stage (MP1 Stream) or after the third Turbine 1 stage (LP1 Stream). Using the model with all streams set to the maximum demand (1.1 times the nominal) a steam source is added before and after the third turbine stage. The resulting steady-state requirements are listed in Table 26.

Table 26. Discharge Steam Results Before and After Third Turbine Stage

	Temp. (C)	Spec. Enthalpy	Req. Mass Flow From TESS	Total Heat Out	Resulting Turbine Power
MP1 Stream	225.3	2,878	19.75	56,841	90.4
LP1 Stream	153.0	2,755	19.23	53,012	88.6

In both streams, the required mass flow is almost exactly the same. This indicates that the current stream has enough heat to accommodate the MP1 stream, so the mass flow in is to meet the demands for the LP1 stream. However, the resulting heat input at both points has a 6.7% difference. The major resulting difference between the two is the total turbine power is higher on

the MP1 stream by 2 MW. While this is good for the plant, the LP steam still provides close to the expected, steady-state turbine power of 89.4 MW.

While extra power production for plant A would be helpful to account for the 8 MW of electricity deficit in steady-state, the extra heat that is transferred and stored in order to release steam at the MP1 conditions would require larger, more expensive heat exchangers and storage. Discharging the TESS into the LP1 stream is more practical from a cost/benefit perspective. It will also require less changes to the system because the discharge steam will not be injected until after the turbine, and be used in only one stream.

A simple heat exchanger design can estimate if the steam output conditions specified are feasible, and to size the storage system. To simplify the model, it is assumed that the steam from the TESS is at the same conditions as the low pressure steam from turbine 1. Feedwater is passed through the steam generator inlet at 82°C and pumped to the desired outlet pressure.

Table 27. Feedwater Conditions in the Steam Generator

Steam Generator	Temperature (°C)	Pressure (bar)	h (kJ/kg)	Condition
Feedwater Inlet	82	4.48	343.7	Subcooled liquid
Steam Outlet	153	4.48	2,755	Superheated Steam

The conditions on the steam generator side of the TESS are unknown but can be set to achieve the desired design. The restraint on the Therminol inlet temperature, or hot tank temperature, is the inlet temperature of the steam on the IHX side, 313°C, which is higher than the SMR steam source alone due to mixing with the bark and recovery boiler sources. The hot tank temperature must be less than 313°C to maintain a temperature difference across the IHX, however, it can be much lower because the outlet temperature requirement on the steam side is

only 153°C. To determine an optimum design, hot tank temperatures of 240, 260 280, and 290°C are used.

The outlet condition of the Therminol, or cold tank temperature, is unknown, and will be based on other design conditions within the heat exchanger. Because the temperature is not known, and because the water undergoes a phase change within the heat exchanger, it is best to calculate the rest of the conditions with the e-NTU method. This method is described in Section 6.2.5.

Because the mass flow rate of Therminol is unknown, C_h can't be calculated. However, water has an infinite heat capacity when undergoing a phase change, so C_h is automatically assigned as C_{min}.

The actual heat transfer rate is the heat transfer rate required to achieve the desired steam outlet conditions in the steam generator. The heat transfer rate can be calculated simply using the mass flow rate on the steam side and the change in enthalpy. It's been established that the Thermal storage system will have to operate at a maximum for a long period time, therefore the steam mass flow rate design condition is set to 19.2 kg/s, which was calculated by Dymola in Table 26.

$$\dot{Q} = \dot{m}\Delta h = \left(19.2\frac{kg}{s}\right)(2{,}755.5 - 343.7)\frac{kJ}{kg} = 46{,}399\ kJ/s$$

The effectiveness of the heat exchanger can also be calculated by a ratio of the inlet and outlet temperatures on each side of the heat exchanger. $T_{h,out}$ calculated for each design condition at $\varepsilon = 0.85$ are tabulated below.

Table 28. Average C_p From Resulting Inlet and Outlet Temperatures.

$T_{h,in}$ (°C)	$T_{h,out}$ (°C)	Cp, ave (kJ/kg-K)
240	105.7	2.10
260	108.7	2.14
280	111.7	2.18
290	113.2	2.21

The mass flow rate of Therminol required can be calculated using an energy balance and the average Cp calculated above.

Table 29. Required Maximum Therminol Mass Flow Rate**.**

$T_{h,in}$ (°C)	$\dot{m}$ (kg/s)
240	164.5
260	143.3
280	126.5
290	118.7

The heat transfer calculations using the average C_p can be verified by using the change in enthalpy of the Therminol.

$$Q = \dot{m}(h_{105.7} - h_{240}) = 164.5 * (203.1 - 484.7) = -46{,}328$$

$$Error = \frac{Q_{Cp} - Q_h}{Q_h} = \frac{46{,}399 - 46{,}328}{46{,}399} = 0.002\%$$

The relationship of the C_p of Therminol to temperature is approximately linear, so the error is very small.

On the IHX side, the steam from the SMR also undergoes a phase change, therefore the Therminol is Cmin, although this time it on the cold side. We can calculate the effectiveness without knowing the outlet temperature of the steam, determining whether the design calculated on the steam generator side is feasible for the IHX side.

Table 30. Resulting Efficiency of IHX from Therminol Hot Tank Temperature.

$T_{h,in}$ (°C)	E, IHX
240	0.65
260	0.74
280	0.84
290	0.88

With the higher steam inlet temperature on the IHX side, and the lower steam outlet temperature on the steam generator side, there is an opportunity to use smaller and less effective heat exchangers in exchange for less overall efficiency of the TESS. This could increase the charge time which may be practical for a plant that only peaks once a day or less. With 0.85 effectiveness on the steam exchanger side, Table 30 shows medium effectiveness values with lower Therminol hot tank temperatures like 240°C, which is used as the hot tank temperature in Plant B. These are all reasonable values for effectiveness, but keeping consistent with an effectiveness of about 85%, we will use a hot tank temperature of 280°C for future calculations.

The mass flow rate on the SMR side will fluctuate based on demands in the plant, which could be as high as 116 kg/s flowing through the IHX. The mass flow rate of Therminol on this side can also fluctuate to maintain the desired heat transfer across the heat exchanger, although the temperature difference must remain the same between the hot and cold tanks. To make sure that the design remains feasible, an outlet temperature of water can be assigned for the steam side.

The heat transfer that must occur is based on the time to full discharge, and the total heat stored in the tank at full charge. The actual heat transfer that occurs on the steam generator side is 46,399 kJ/s, as calculated previously. These numbers use a hot tank temperature of 280°C.

Table 31. Design of TESS at 280°C.

Time to Discharge	30 min	1 hour	2 hour	4 hour
Total Mass Flow (kg)	2.28e5	4.5e5	9.11e5	1.82e6
Density of Hot Tank Therminol (kg/m^3)	825	825	825	825
Minimum Tank Volume (m^3)	276	552	1,104	2,207
Heat Storage (kJ)	8.35e7	1.67e8	3.34e8	6.68e8

For size comparison, calculations for a Therminol hot tank temperature of 240°C is in Table 32. Although the Therminol density is higher at the lower temperature, there is a 25% increase in tank volume from the Therminol stored at 280°C. Also, the same amount of heat transfer is required despite the Therminol being at a lower temperature, so more area will be required in the heat exchanger to get the steam to the required outlet temperature. The benefit of a lower hot tank temperature is that there will be less heat loss to the environment. These are all factors that can be considered by a facility when determining an optimal design.

Table 32. Design of TESS at 240°C.

Time to Discharge	30 min	1 hour	2 hour	4 hour
Total Mass Flow (kg)	2.96e5	5.92e5	1.18e6	2.37e6
Density of Hot Tank Therminol (kg/m^3)	856	856	856	856
Minimum Tank Volume (m^3)	346	692	1,384	2,768
Heat Storage (kJ)	8.35e7	1.67e8	3.34e8	6.68e8

Using a set outlet temperature for steam gives the actual heat transfer on the Therminol side, calculated from the change in enthalpy of the steam. Because the mass flow rate is variable, the total heat transfer is also variable. The mass flow rate can be calculated by the e-NTU method. The steam flow rate for plant A can vary from 0 kg/s to 113 kg/s. In an ideal design, the steam will exit the IHX as a subcooled liquid.

Table 33. Heat Transfer Required Per Steam Mass Flow Rate in IHX.

T outlet (°C)	5	150	200	250
Δh (kJ/kg)	3009.44	2399.54	2180.32	164.61
Steam Flow (kg/s)	Total Heat Transfer (kJ)			
0	0	0	0	0
10	30,094	23,995	21,803	1,646
20	60,189	47,991	43,606	3,292
30	90,283	71,986	65,410	4,938
40	120,378	95,982	87,213	6,584
50	150,472	119,977	109,016	8,230
60	180,566	143,972	130,819	9,877
70	210,661	167,968	152,622	11,523
80	240,755	191,963	174,426	13,169
90	270,850	215,959	196,229	14,815
100	300,944	239,954	218,032	16,461
110	331,038	263,949	239,835	18,107
113	349,095	278,347	252,917	19,095

Note that with a steam outlet temperature of 250°C, the steam does not condense. This would be an ineffective design because the greatest heat transfer happens during the phase change. Using the total heat transfer and the e-NTU method, the mass flow rate of Therminol can be required at each steam flow rate and outlet temperature. In Table 34, the Therminol hot tank temperature used is 280°C.

Table 34. Therminol Mass Flow Rate Required Per Steam Flow Rate in IHX.

T outlet (°C)	5	150	200	250
Δh (kJ/kg)	3009.44	2399.54	2180.32	164.61
Steam Flow (kg/s)	Mass Flow Rate of Therminol (kg/s)			
0	0	0	0	0
10	82	65	59	4
20	164	131	119	9
30	246	196	178	13
40	328	262	238	18
50	411	327	297	22
60	493	393	357	27
70	575	458	416	31
80	657	524	476	36
90	739	589	535	40
100	821	655	595	45
110	903	720	654	49
120	928	740	672	51

Because the steam flow rate is variable, there is no way to estimate an exact charging time for the TESS. However, a range can be given based on the lowest and highest possible charge times based on the range of steam flow rates.

If the steam flow rate through the IHX is a constant 10 kg/s, Table 35 gives the charge time in hours based on the discharge capacity of the hot tank.

$$Discharge\ Time = m_{tank}/\dot{m}_{therminol@steam\ flow}$$

Table 35. Charge Time for Plant A TESS at 10 kg/s Steam Flow.

Steam outlet temperature (°C)	Discharge Time (hr)			
	0.5	1	2	4
5	0.77	1.54	3.08	6.16
150	0.97	1.93	3.86	7.73
200	1.06	2.13	4.25	8.50

Table 36 shows the charge time if the steam flow rate is a constant 113 kg/s.

Table 36. Charge Time for Plant A TESS at 113 kg/s Steam Flow.

Steam outlet temperature (°C)	Discharge Time (hr)			
	0.5	1	2	4
5	0.07	0.14	0.27	0.55
50	0.09	0.17	0.34	0.68
100	0.09	0.19	0.38	0.75

The maximum charge time for any of the designs is about 8.50 hours, which is very reasonable for a batch process system. The actual charge time is likely to be much lower because the steam flow rate will vary over time to be higher than 10 kg/s.

The discharge times can be verified by comparing the heat transfer of Therminol to the actual heat transfer in the system. To charge a 4-hour capacity system with an outlet temperature of 150°C at 10 kg/s steam flow:

$$\dot{Q}_{actual,water} = \dot{m}(h_{150} - h_{260}) = \left(10\frac{kg}{s}\right) * \left(-2{,}400\frac{kJ}{kg}\right) = -24{,}000\ kJ/s$$

$$\dot{Q}_{actual,therminol} = \dot{m}(h_{280} - h_{105.7}) = \left(65.48\frac{kg}{s}\right) * \left(-378.3\frac{kJ}{kg}\right) = 24{,}771\ kJ/s$$

$$Error = \frac{24{,}000 - 24{,}771}{24{,}000} = 0.03\%$$

$$\Delta t_{charge} = \frac{Q_{charg}}{Q_{thermino}} = \frac{6.68e8\ kJ}{24{,}000\ kJ/s} = 37{,}306\ s = 7.73\ hours$$

$$Error = \frac{7.73 - 7.73}{7.73} = 0\%$$

The final design is proposed in Figure 96, using charging steam from the combined source stream after the first Turbine 1 stage. The proposed design includes 4 hours of steam discharge capacity, with a steam outlet temperature of 200°C. The increased outlet temperature will give a longer charging time and reduce the area required in the heat exchanger. Condensate exiting the IHX could be used to preheat the feedwater entering the steam generator. The tank volume in the design is the approximate volume of Therminol increased by 10% because some mass will always be flowing through the system.

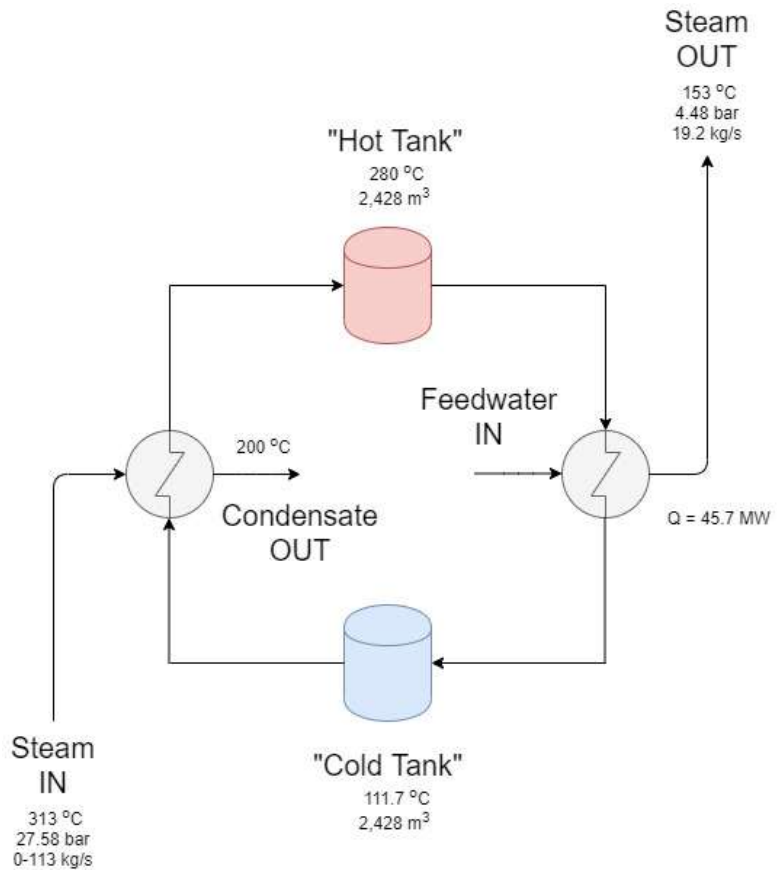

Figure 96. Proposed Thermal Energy Storage System for Plant A.

6.3.5 Case 4: Charging the Thermal Storage System

The model for case 4 in Figure 97 first initializes in steady state before switching the demand control for LP1 to the thermal energy storage system. The TESS diverts steam from the mixed source stream (SMR, RB and Bark) before the HP steam stream. When steam goes through the TESS, the charging block calculates the amount of Therminol that would pass through to complete the heat transfer using the calculations in Figure 98. This equation is calculated by fitting a linear curve to the Thermiol flow rates in Table 34. Once the TESS has the maximum amount of Therminol stored, the steam that goes through the TESS is assumed to be vented instead.

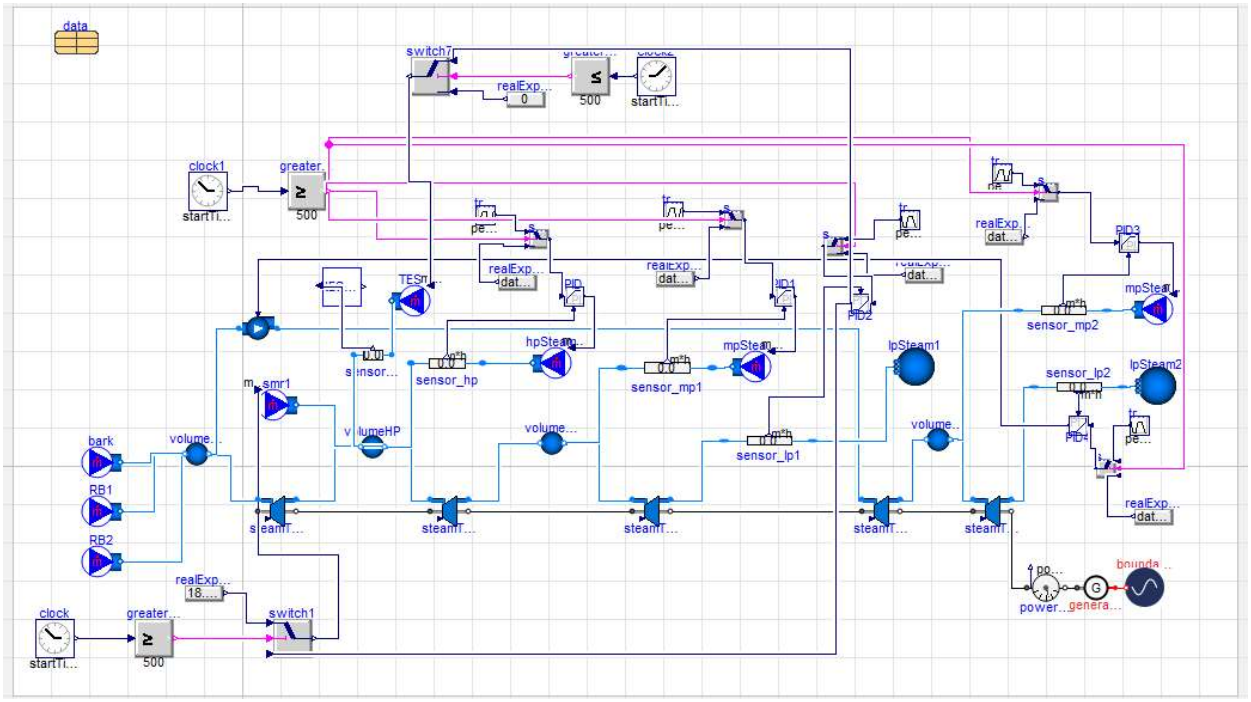

Figure 97. Case 4 Model for Plant A.

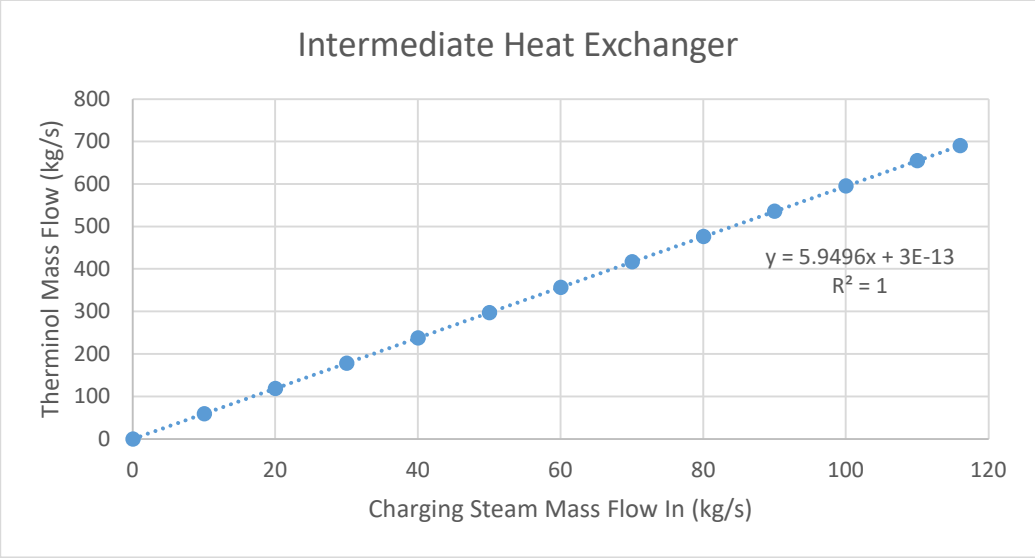

Figure 98. Intermediate Heat Exchanger Therminol-Steam Flow Relationship.

The first step is verifying the function of the TESS blocks. According to the analysis in the previous section, if there is a constant 10 kg/s into the TESS, it will take 8.5 hours to fully charge the system. In the model, the system charges in 30,650 seconds (beginning charge at 500 seconds), or 8.51 hours. The simplified model of the thermal storage system is a good representation of the actual design.

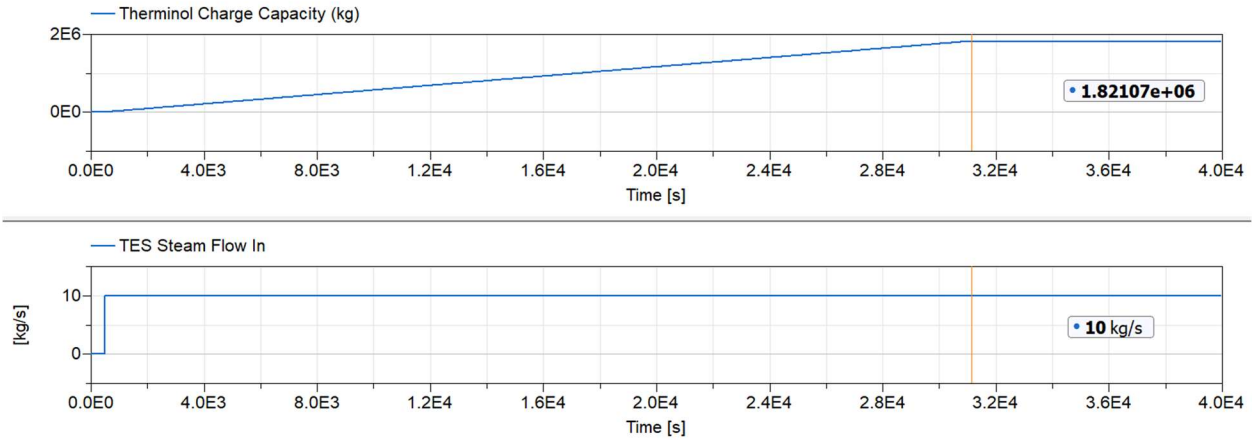

Figure 99. Model Verification for the Plant A TESS Block.

The other point that can be verified is that the TESS diverts 0 kg/s of steam when all the streams are at their steady state demands in Figure 100. When we apply the case 4 loads in Figure 100, the steam flow into the TESS is 0.04 kg/s, essentially 0. In reality, there will always be some steam flowing through the TESS to keep heat circulating and make up for heat loss in the Therminol tank to the environment.

The demand source curve used for Case 4 is in Table 37. The difference from the curve in Cases 2 and 3 is that the demand only varies from the lowest point to the nominal point.

Table 37. Trapezoidal Demand Source Curve For Case 4.

Parameter	HP Steam	MP1 Steam	LP1	MP2	LP2
Amplitude	[HP Steam Nominal Heat Demand] – [HP Steam Nominal Heat Demand]*0.4	[MP1 Steam Nominal Heat Demand] – [MP1 Steam Nominal Heat Demand]*0.4	[LP1 Steam Nominal Heat Demand] – [LP1 Steam Nominal Heat Demand]*0.4	[MP2 Steam Nominal Heat Demand] – [MP2 Steam Nominal Heat Demand]*0.4	[LP2 Steam Nominal Heat Demand] – [LP2 Steam Nominal Heat Demand]*0.4
Rising (s)	500	350	500	800	400
Width (s)	750	700	700	750	600
Falling (s)	600	500	500	1200	250
Period (s)	3000	2500	2000	3000	1500
Nperiod	-1 (inf)	-1 (inf)	-1 (inf)	-1 (inf)	-1 (inf)
Offset	[HP Steam Nominal Heat Demand]*0.4	[MP1 Steam Nominal Heat Demand]*0.4	[LP1 Steam Nominal Heat Demand]*0.4	[MP2 Steam Nominal Heat Demand]*0.4	[LP2 Steam Nominal Heat Demand]*0.4
startTime (s)	500	500	500	500	500

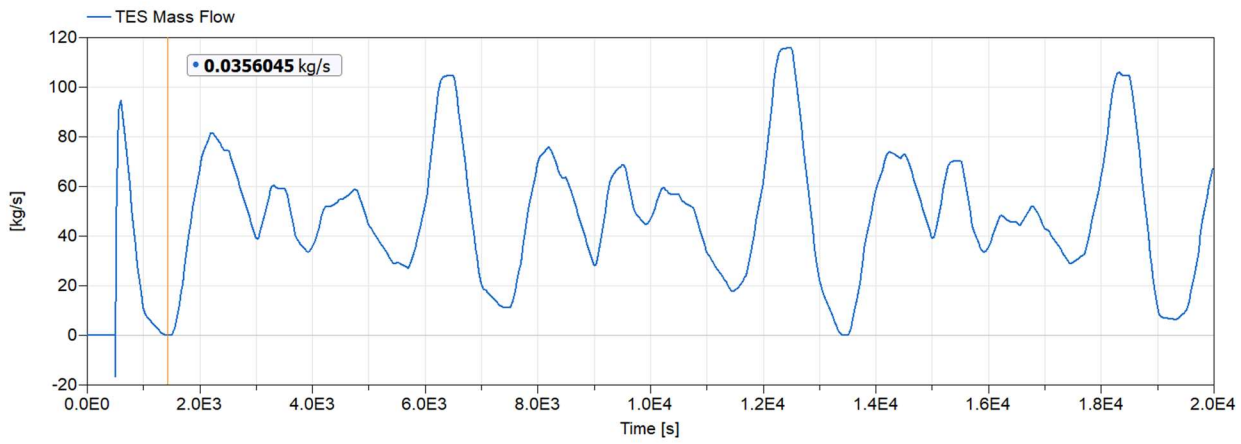

Figure 100. Steam Fow Into the TESS at Nominal Demands.

When all the demands are at their lowest, the TESS diverts 116 kg/s of steam, as shown in Figure 101. This diversion increases the overall efficiency of the plant, and allows the heat generated by the plant to be used during times of higher demand via the TESS.

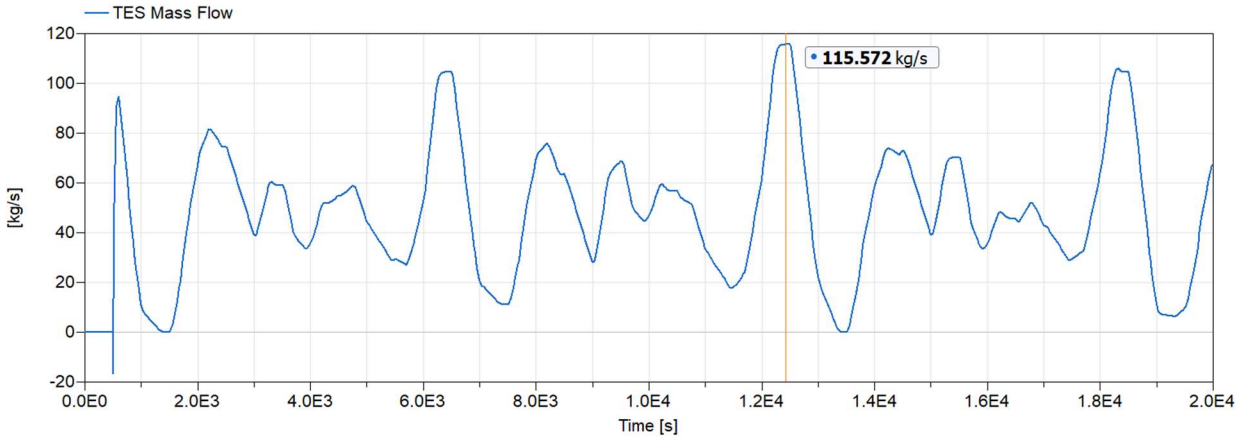

Figure 101. Steam Flow Into TESS When All Demands are at Lowest.

Figure 102 shows how the steam into the TESS changes in relation to the heat out for each stream. When the curves are not all either at the lowest or nominal demand, the flow in is in the range of 50 kg/s.

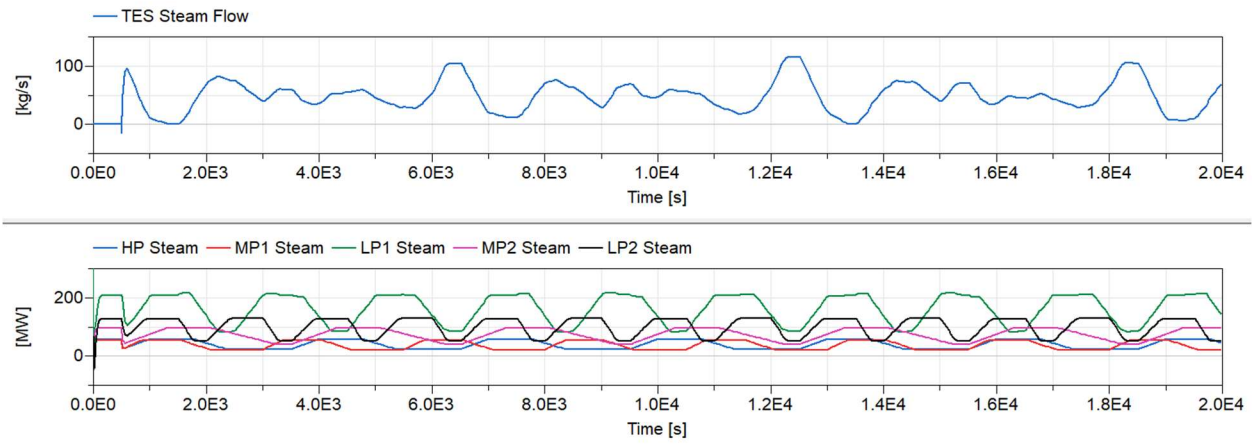

Figure 102. Steam Flow Into TESS Versus Demand Curves.

Using these specific demand curves, Figure 103 shows the charge time for the TESS. The system is fully charged at 6,200 seconds (beginning charging at 500 seconds), or 1.7 hours. This is much quicker than the charge time calculated during verification. The charge time will vary based on the actual demands within the plant.

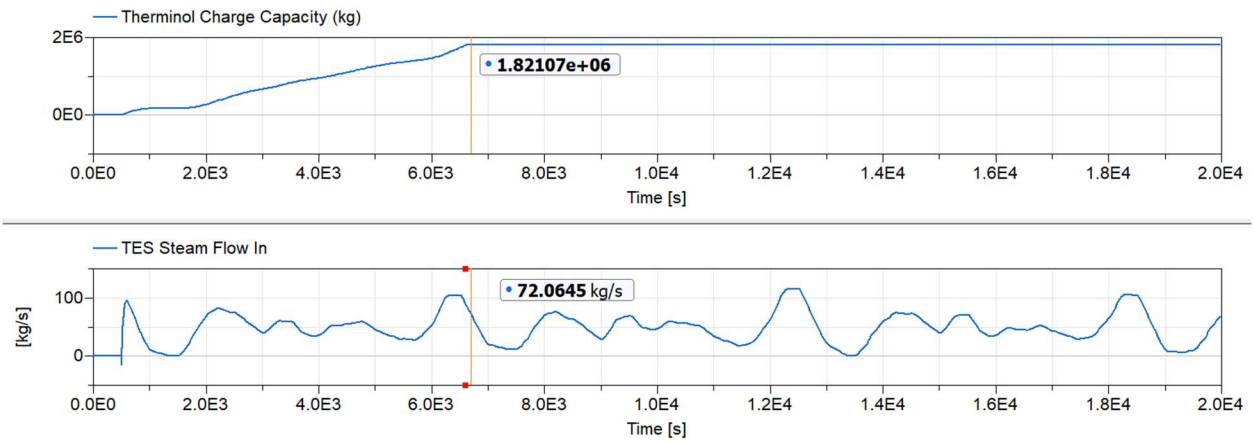

Figure 103. Charge Time and Instantaneous Mass Flow for TESS Using Case 4 Demand Curve.

From Figure 104 and Figure 105, the plant power varies between 89.4 MW when all the streams are at their steady-state demands, and 82.3 MW when the streams are at their lowest

demands, and the TESS is diverting the maximum amount of steam. This range is smaller than the range in Case 2.

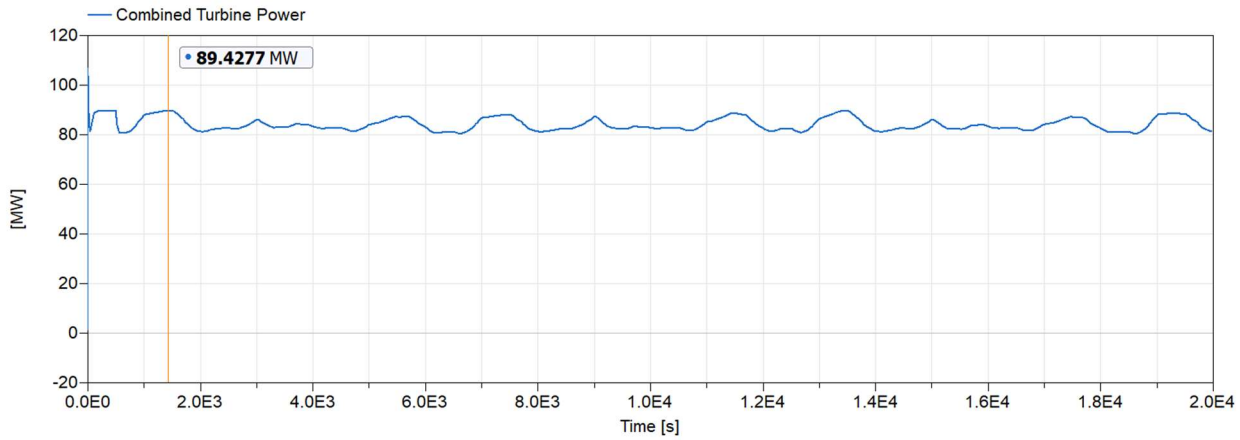

Figure 104. Combined Turbine Power When All Demands are at Maximum.

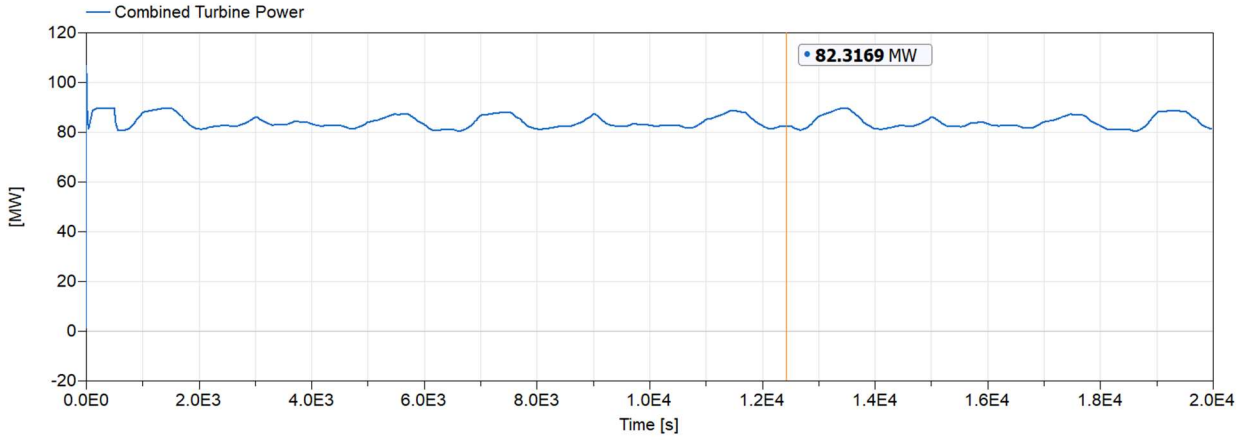

Figure 105. Combined Turbine Power in Plant A When all Demands are at Minimum.

6.3.6 Case 5: Discharging the Thermal Storage System

This model in Figure 106 is similar to the others in that it first initializes in steady-state. The TESS injects into the LP1 stream directly. When steam goes through the TESS, the charging block calculates the amount of Therminol that would pass through to complete the heat transfer using the calculations in Figure 107. The linear relationship is calculated from the heat transfer

needed in the steam generator to bring the steam to the correct conditions depending on the mass flow rate of steam. Once the TESS has the maximum amount of Therminol stored, the steam that goes through the TESS is assumed to be vented instead.

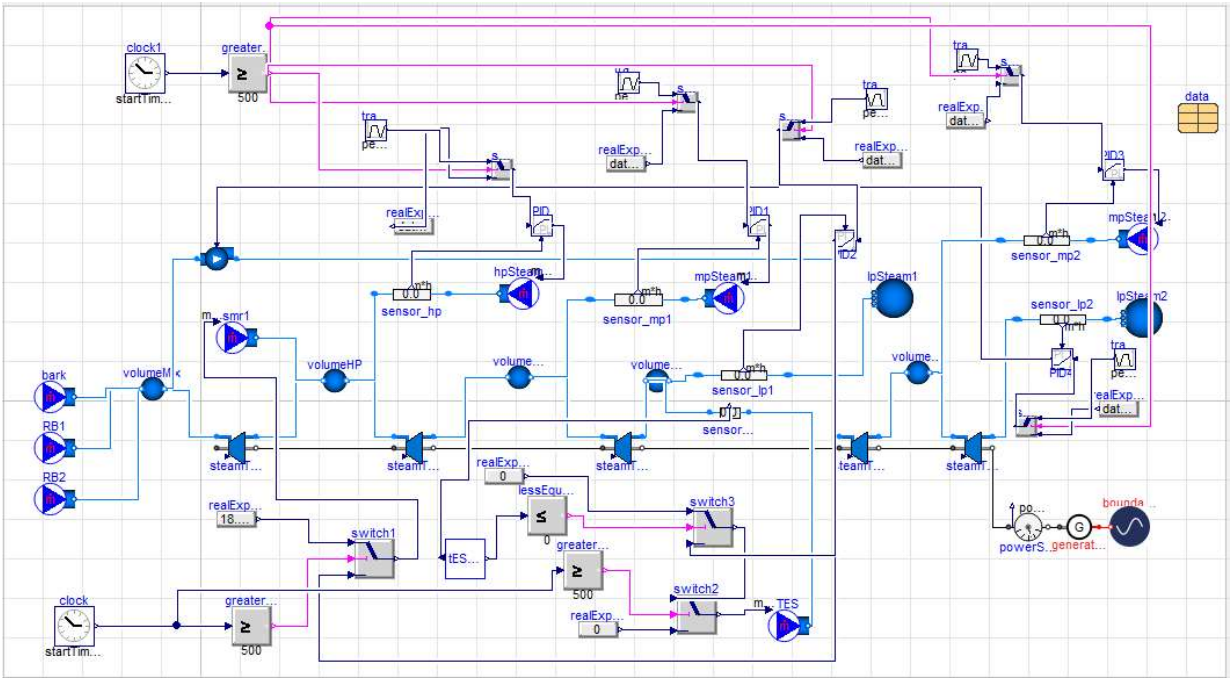

Figure 106. Case 5 Model for Plant A.

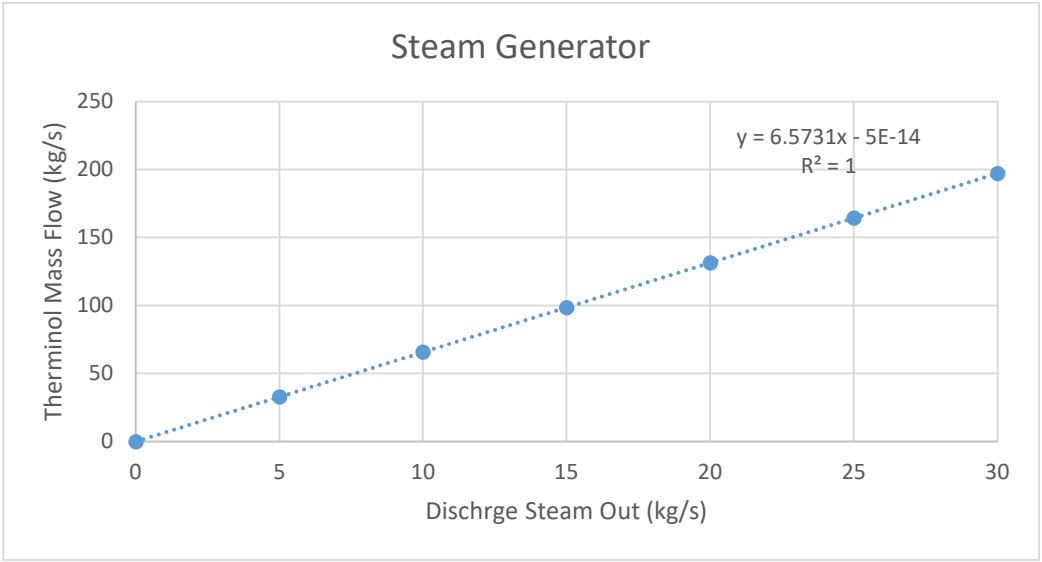

Figure 107. Therminol-Steam Relationship for Discharging.

The first step is verifying the function of the TESS block. According to the analysis in the previous section, if the TESS discharges with all demands at 110%, it will take 4 hours to fully discharge the system. In the model according to Figure 108, the system discharges in 14,400 seconds, or exactly 4 hours. The simplified model of the thermal storage system is a good representation of the actual design.

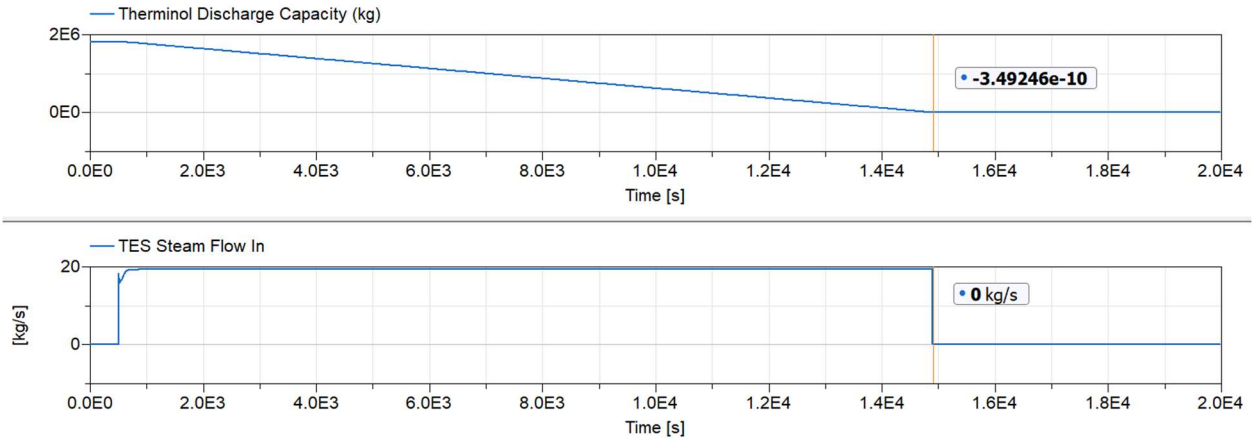

Figure 108. Discharge Verification for Case 5.

As expected in Figure 109, the system discharges 19.2 kg/s when all the demands are at maximum.

The demand curve used for Case 5 is in Table 38. The difference from the demand source curve from Cases 2 and 3 is that the demand only varies from the nominal point to the highest point.

Table 38. Trapezoidal Demand Source Curve for Case 5.

Parameter	HP Steam	MP1 Steam	LP1	MP2	LP2
Amplitude	[HP Steam Nominal Heat Demand]*1.1 – [HP Steam Nominal Heat Demand]	[MP1 Steam Nominal Heat Demand]*1.1 – [MP1 Steam Nominal Heat Demand]	[LP1 Steam Nominal Heat Demand]*1.1 – [LP1 Steam Nominal Heat Demand]	[MP2 Steam Nominal Heat Demand]*1.1 – [MP2 Steam Nominal Heat Demand]	[LP2 Steam Nominal Heat Demand]*1.1 – [LP2 Steam Nominal Heat Demand]
Rising (s)	500	350	500	800	400
Width (s)	750	700	700	750	600
Falling (s)	600	500	500	1200	250
Period (s)	3000	2500	2000	3000	1500
Nperiod	-1 (inf)	-1 (inf)	-1 (inf)	-1 (inf)	-1 (inf)
Offset	[HP Steam Nominal Heat Demand]	[MP1 Steam Nominal Heat Demand]	[LP1 Steam Nominal Heat Demand]	[MP2 Steam Nominal Heat Demand]	[LP2 Steam Nominal Heat Demand]
startTime (s)	500	500	500	500	500

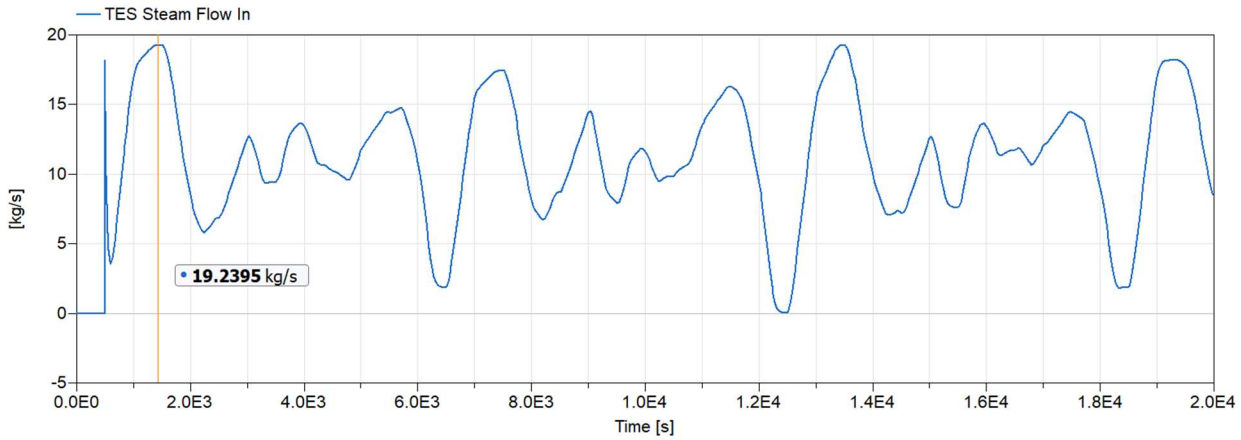

Figure 109. Discharge from TESS When All Demands are at Minimum.

In Figure 110 the discharge from the TESS is effectively 0 kg/s when all the demands are at the nominal. While this is good for the verification of the model, realistically there will have to be some steam flow going through the TESS at all times to maintain the heat exchanger.

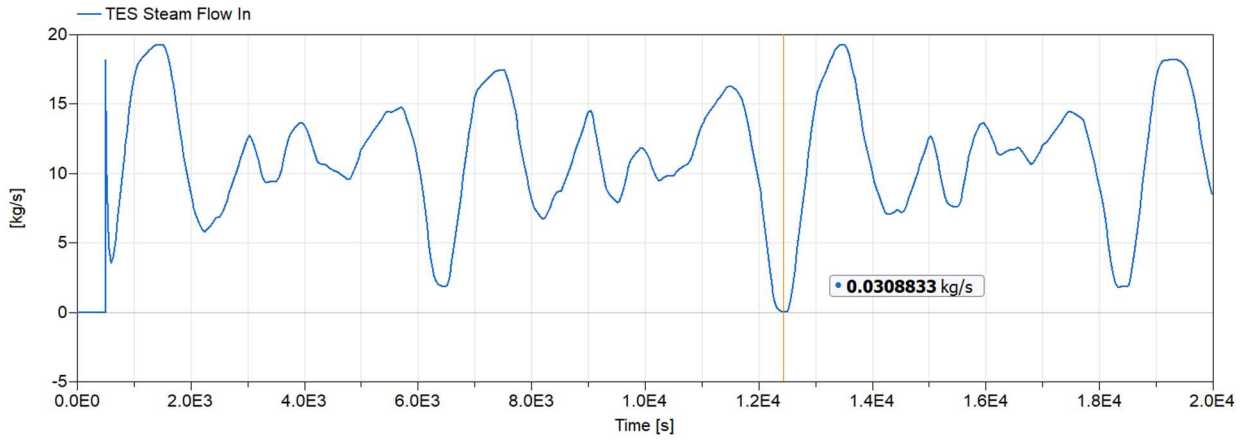

Figure 110. Discharge from TESS When All Demands are Maximum.

For this specific demand curve, the TESS discharges fully at 25,000 seconds (beginning discharge at 500 seconds), or 6.9 hours, shown in Figure 111. This is longer than the design discharge time of 4 hours, because the demands are not maximum the whole time.

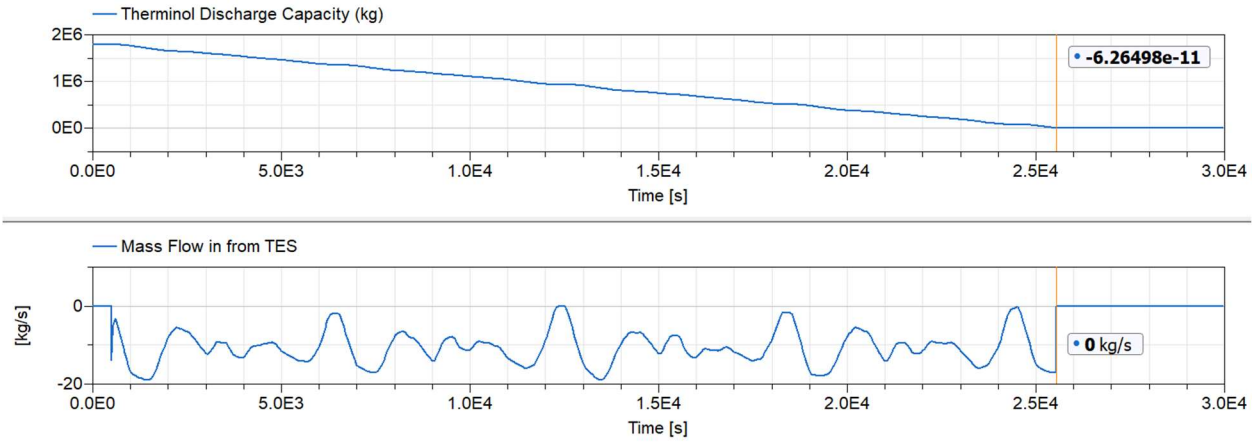

Figure 111. Actual Discharge Time and Mass Flow Based on Demand Curve for Case 5.

In Figure 112 and Figure 113, the power varies very little between demands because the steam is discharge directly into the LP1 stream rather than into a turbine. The minor changes in power are due to changes in steam flow that goes out through the HP and MP1 streams. Overall the range of power production is about 1 MW.

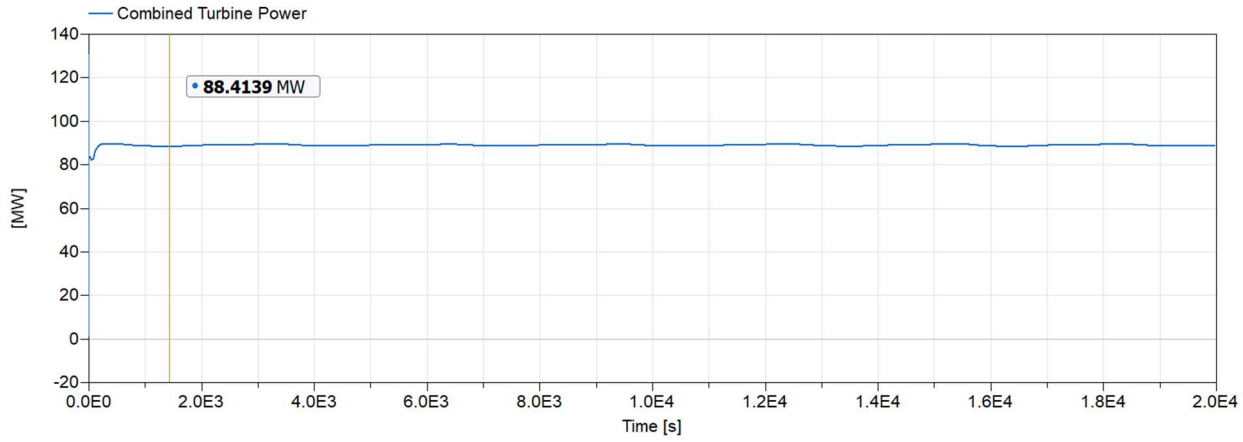

Figure 112. Combined Turbine Power when Demands are at Maximum.

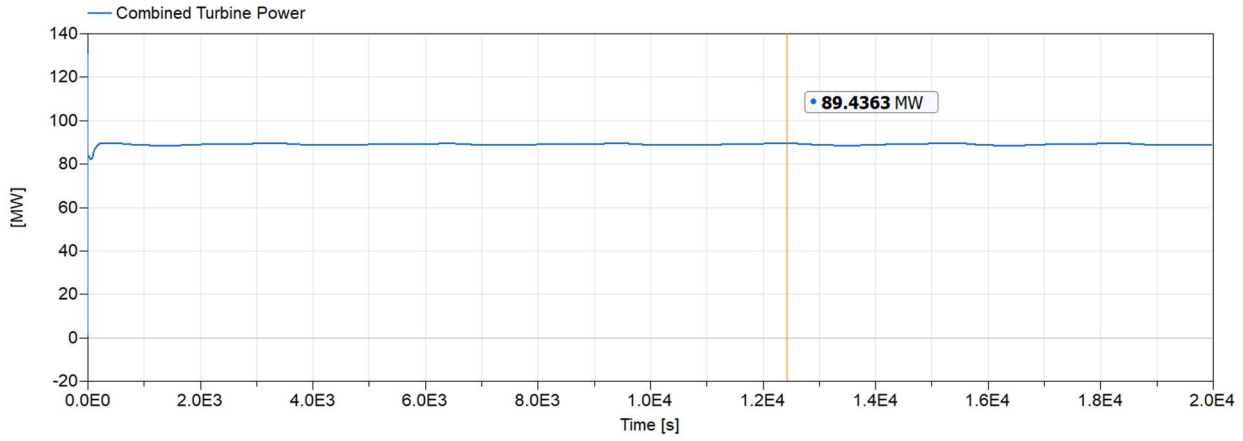

Figure 113. Combined Turbine Power when Demands are at Minimum.

6.4 Conclusion

6.4.1 Case 2: SMR steam flow varies based on demands

Case 2 is essentially the current operation of the plant. Steam generation is mostly constant from the boilers with variable NG steam generation, and any excess steam is vented from the system or sent to the condenser. Although this does not improve the efficiency of the plant, it does improve the steady-state function of the system.

For both plants, the control scheme presented in Case 2 is infeasible for several reasons. A control scheme which requires a near-constant change in SMR flow rate requires a lot of monitoring and eventually may cause concerns with the reactor function. The best control scheme will be one in which the SMR function is stable.

This scheme is especially infeasible for Plant A. The dynamic model showed a negative flow rate when demands were low, meaning that even if the steam supply from the SMR stopped completely, there would still be a surplus of heat in the system.

6.4.2 Case 3: SMR at constant nominal

The main problem with this control scheme is that by keeping the SMR as a constant nominal, it does not account for peaking loads. It is much more difficult to increase steam production from the SMR than it is to increase steam production from natural gas. One way to remedy this to increase the nominal SMR load to the peak load, depending on how much time the process typically spends at peak load. This would cause a greater heat surplus, but it would increase the power production of the plant.

Advantages to this scheme is that power production is less varied, and It requires less complicated controls. For Plant B, this may not be the best control scheme because it is already generating a surplus of electricity with the addition of the SMR. Alternatively, this may be a

desirable control scheme for Plant A. Generating more electricity would mean that less would have to be purchased or generated by another source. The original operation of Plant A included a condenser that condensed about 10% of the steam flow through the second turbine. The SMR operation eliminated the condenser in order to improve total plant efficiency. The condenser could be used to take in excess steam from the plant operation. The condenser may need to be increased in size in order to take in the higher nominal amount of steam.

6.4.3 Cases 4 and 5: Addition of Thermal Storage

The addition of thermal storage increases the efficiency of both plants by reducing excess steam production, and also assists the plant in times of peak load. However, the charging process causes significant variations in the power production of the plant, and once the storage system is fully charged, the plant will continue to release the surplus heat. The discharge process, however, keeps the electric production stable. A plant like Plant A may not be able to sustain the swing electricity loads, or they may be undesirable because of increased electricity costs. For Plant B, the swing loads may be sustainable. Another disadvantage is that the SMR nominal load may need to be increased because steam would need to be flowing through the heat exchangers at all times. Adding the thermal storage system will also increase equipment costs and complicate the controls needed to operate the plant.

The feasibility of the TESS will depend on ability of the plant to tolerate heat and electric load swings, the plant electric power needed, and cost limitations. Apart from the thermal storage systems suggested in this study, there are also other methods such as concrete storage that can be studied to find a configuration that works best for the plant.

Chapter 7: Future Work

With the introduction of renewable energy, the way we generate and receive our electricity is fundamentally changing. Renewables like wind and solar make up an ever-increasing percentage of the grid, driving down the price of electricity when they are online. However, when the sun isn't shining and the wind isn't blowing, electrical demands on traditional base load generators become variable. This oscillatory pricing structure is economically challenging for base-load power plants, as predictions of profits and losses are no longer straightforward. One solution to this is to use the steam generated by base-load plants during times of low load or price to produce other valuable products such as hydrogen or water, or simply store energy in a thermal reservoir. The Joint Use Modular Plant (JUMP) program at INL proposes to use a NuScale power module to support the research and demonstration of such systems. This program establishes INL in a key position to support the development of Small Modular Reactors (SMRs) while interfacing with potential future adopters of SMR technologies.

Manufacturing plants are a natural application for SMRs because many utilize both steam and electricity to deliver products. The US Department of Energy encourages industrial use of Combined Heat and Power (CHP), or cogeneration, to increase the amount of energy extracted from a given amount of fuel and to decrease carbon production. SMRs can function as CHP systems without the use of carbon-producing fuels. Intensive manufacturing processes like paper products, metals, chemicals and petroleum products dominate the energy market. Each of these industries would benefit from cogeneration and SMRs and are options for demonstration with the JUMP program. Each plant can be accommodated by the flexible sizing of NuScale SMRs.

Preliminary conclusions from this work suggest that feasibility is strongly dependent on the current operations of the plant because the steam offtake from the SMR for other processes is

limited to 50% of the total steam output. Factors that affect the sizing of the SMR system for a particular plant are fixed internal steam generation processes such as the chemical recovery process of the paper mill, a large steam demand but small electricity demand, or differences between SMR steam pressure and current boiler pressure. Exploring the integration of SMRs with various manufacturing sectors and different types of plant operations will frame the potential applications for SMRs while building awareness for the technology and relationships between researchers and industry leaders.

The best way to foster this relationship is to develop a research program that works between research teams and manufacturing plants to introduce them to SMR technology and find ways to incorporate them into industry. The first stage would deliver literature and low fidelity, generic models to these industries to familiarize them with SMR technology and allow for more effective conversations between private companies and research laboratories. This literature would include background information about SMR specs, and examples of simple steam processes implemented with SMRs. Examples built with Dymola will demonstrate cases for outage, sudden increase in steam demand, and operations with and without steam storage. This will educate companies on their options and give them the ability to determine if SMR technology is appropriate for their goals.

The next level would be signing an NDA and obtaining real data from manufacturing facilities. Low fidelity steady-state models will be developed use ASPEN HYSYS, which will allow for an initial estimated of the required cost and number of SMR modules for each plant. Further suggestions such as carbon sequestration or changes to other fuel sources will be included to support environmental goals, account for potential policy changes in the next 10 years and improve the economics of the SMR. Low fidelity dynamic models of manufacturing

plants can be created using Dymola, a software using the Modelica framework. Dymola models can be distributed to companies using the Functional Mockup Interface (FMI), an open source user interface for Modelica files. These models will include the integral components of the steam system built with real data from the facility. Using the procedures of this dissertation as a guideline, one could determine the best way to integrate the SMR into the steam system based on current demands and boiler conditions, simulating how the SMR integrated system responds to changes in demands throughout the plant. In addition to determining feasibility, these simulations can give an idea of optimal control schemes. If LWR technology does not appear to be a good fit, they could connect them with other groups at within the Integrated Energy Systems groups at INL, Oak Ridge and Argonne National Laboratories to explore advanced reactor technology.

This research has shown that integrating SMRs with manufacturing is not economically feasible unless plants partner with their local utilities to create PPA agreements. The number of modules required for a manufacturing plant varies greatly based on the differences in steam and electricity demand, resulting in an over or under generation of electricity. With a PPA, plants can sell their excess electricity to the utility to decrease the financial impact of purchasing and maintaining the SMR. Alternatively, the manufacturing plant could sell power via the SMR to the utility. With a relationship with NuScale and the utility, high fidelity models can be created to model the steam system with the NuScale module directly.

References

[1] J. Vujić, R. M. Bergmann, R. Škoda, and M. Miletić, "Small modular reactors: Simpler, safer, cheaper?," *Energy*, vol. 45, no. 1, pp. 288–295, 2012.

[2] Y. I. Chang, M. Konomura, and P. Lo Pinto, "A case for small modular fast reactor," *J. Nucl. Sci. Technol.*, vol. 44, no. 3, pp. 264–269, 2007.

[3] M.-A. Ochiai, "A very small LWR installed in the underground in the city," *Prog. Nucl. Energy*, vol. 37, no. 1–4, pp. 259–263, 2000.

[4] O. Sambuu and T. Obara, "Conceptual design for a small modular district heating reactor for Mongolia," *Ann. Nucl. Energy*, vol. 47, pp. 210–215, 2012.

[5] J. Doyle, B. Haley, C. Fachiol, B. Galyean, and D. T. Ingersoll, "Highly Reliable Nuclear Power for Mission-Critical Applications," 2016.

[6] D. Ingersoll, Z. Houghton, R. Bromm, C. Desportes, M. McKellar, and R. Boardman, "Extending Nuclear Energy to Non-Electrical Applications," *19th Pacific Basin Nucl. Conf. (PBNC 2014)*, no. Pbnc, p. 3, 2014.

[7] A. B. Lovins, I. Sheikh, and A. Markevich, "Forget Nuclear," *Cogeneration*, no. April, pp. 1–10, 2008.

[8] I. Khamis, T. Koshy, and K. C. Kavvadias, "Opportunity for Cogeneration in Nuclear Power Plants," in *Advances in Nano, Biomechanics, Robotics, and Energy Research*, 2013, pp. 455–462.

[9] M. D. Carelli *et al.*, "Economic features of integral, modular, small-to-medium size reactors," *Prog. Nucl. Energy*, vol. 52, no. 4, pp. 403–414, 2010.

[10] D. T. Ingersoll, "2 - A brief history of small nuclear power (1950–2000)," *Small Modul. React.*, pp. 21–38, 2016.

[11] MIT, *Future of nuclear power*. 2003.

[12] M. D. Carelli and B. Petrovic, “A flexible & economic small reactor,” *Nucl. Plant J.*, vol. 24, no. 5, 2006.

[13] M. Jaskólski, A. Reński, and T. Minkiewicz, “Thermodynamic and economic analysis of nuclear power unit operating in partial cogeneration mode to produce electricity and district heat,” *Energy*, vol. 141, pp. 2470–2483, 2017.

[14] M. R. Islam and H. A. Gabbar, “Study of small modular reactors in modern microgrids,” *Int. Trans. Electr. Energy Syst.*, vol. 25, no. 9, pp. 1943–1951, 2015.

[15] A. Lokhov, “Load-following with nuclear power plants,” *NEA News*, no. 29, pp. 18–20, 2011.

[16] J. Tian, “A nuclear-natural gas coupled-cycle for power generation,” *Ann. Nucl. Energy*, vol. 77, pp. 281–284, 2015.

[17] C. Cany, C. Mansilla, G. Mathonnière, and P. da Costa, “Nuclear power supply: Going against the misconceptions. Evidence of nuclear flexibility from the French experience,” *Energy*, vol. 151, pp. 289–296, 2018.

[18] A. F. Wibisono and E. Shwageraus, “Thermodynamic performance of Pressurized Water Reactor power conversion cycle combined with fossil-fuel superheater,” *Energy*, vol. 117, pp. 190–197, 2016.

[19] D. T. Ingersoll, C. Colbert, Z. Houghton, R. Snuggerud, J. W. Gaston, and M. Empey, “Can Nuclear Power and Renewables be Friends?,” in *Proceedings of ICAPP*, 2015, p. 9.

[20] O. P. Rakereng and C. J. Hah, “Simplified load follow schemes to simulate long-term daily load follow operation,” *Ann. Nucl. Energy*, vol. 110, pp. 896–902, 2017.

[21] Nuclear Energy Agency, “Technical and Economic Aspects of Load Following with

Nuclear Power Plants," *Development*, no. June, pp. 1–51, 2011.

[22] G. Fischer, F. Sontheimer, I. Ruyter, and J. Markgraf, "Experiments on the load following behaviour of PWR fuel rods," *Nucl. Eng. Des.*, vol. 108, no. 3, pp. 429–432, 1988.

[23] P. Hu, F. Zhao, and Y. Tai, "Coordination control and simulation for small nuclear power plant," *Prog. Nucl. Energy*, vol. 58, pp. 21–26, 2012.

[24] B. Gjorgiev and M. Čepin, "Nuclear Power Plant Load Following: Problem Definition and Application," in *International Conference Nuclear Energy for New Europe*, 2011.

[25] B. Frogner and H. Rao, "Control of nuclear power plants," *IEEE Trans. Automat. Contr.*, vol. 23, no. 3, 1978.

[26] G. Locatelli, A. Fiordaliso, S. Boarin, and M. E. Ricotti, "Cogeneration: An option to facilitate load following in Small Modular Reactors," *Progress in Nuclear Energy*, vol. 97. pp. 153–161, 2017.

[27] G. Locatelli, S. Boarin, A. Fiordaliso, and M. E. Ricotti, "Load following of Small Modular Reactors (SMR) by cogeneration of hydrogen: A techno-economic analysis," *Energy*, vol. 148, pp. 494–505, 2018.

[28] M. A. Rosen, "Energy, environmental, health and cost benefits of cogeneration from fossil fuels and nuclear energy using the electrical utility facilities of a province," *Energy Sustain. Dev.*, vol. 13, no. 1, pp. 43–51, 2009.

[29] D. T. Ingersoll, Z. J. Houghton, R. Bromm, and C. Desportes, "NuScale small modular reactor for Co-generation of electricity and water," *Desalination*, vol. 340, no. 1, pp. 84–93, 2014.

[30] V. Tulkki, E. Pursiheimo, T. J. Lindroos, and V. Sahlberg, "Small Modular Reactors as a part of a District Heating System," *Trans. Am. Nucl. Soc. , Vol . 118 , Philadelphia ,*

Pennsylvania , June 17 – 21 , 2018, vol. 118, pp. 685–687, 2018.

[31] E. D. Larson, S. Consonni, and R. E. Katofsky, "A Cost-Benefit Assessment of Biomass Gasification Power Generation in the Pulp and Paper Industry," 2003.

[32] H. Tran and E. K. Vakkilainnen, "The Kraft Chemical Recovery Process," *TAPPI Kraft Recover. Course*, pp. 1–8, 2012.

[33] S. Farahani, E. Worrell, and G. Bryntse, "CO2-free paper?," *Resour. Conserv. Recycl.*, vol. 42, no. 4, pp. 317–336, 2004.

[34] C. Merritt and F. T. Corp, "Steam Accumulators and Steam Boiler Response to Load Changes Boiler Response to Sudden Steam Demand," no. Figure 1, pp. 1–10.

[35] W. Sun, Y. Hong, and Y. Wang, "Operation optimization of steam accumulators as thermal energy storage and buffer units," *Energies*, vol. 10, no. 1, 2017.

[36] V. D. Stevanovic, B. Maslovaric, and S. Prica, "Dynamics of steam accumulation," *Appl. Therm. Eng.*, vol. 37, pp. 73–79, 2012.

[37] W. D. Steinmann and M. Eck, "Buffer storage for direct steam generation," *Sol. Energy*, vol. 80, no. 10, pp. 1277–1282, 2006.

[38] M. T. Daniels, "Integration of Large-Scale Steam Accumulators for Energy Storage in Nuclear Hybrid Energy Systems."

[39] M. Heidari Tari and M. Söderström, "Modelling of thermal energy storage in industrial energy systems the method development of MIND," *Appl. Therm. Eng.*, vol. 22, no. 11, pp. 1195–1205, 2002.

[40] P. Yang, X. Hu, and G. Liao, "Dynamic Characteristics of the Steam Accumulator Charging," vol. 3005, 2017.

[41] UNECE Group of Experts on Cleaner Electricity Production from Fossil Fuels, "Room

Document: Baseline Efficiency Analysis of Fossil Fuel Power Plants."

[42] University of Michigan Center for Sustainable Systems, "Nuclear Energy Fact Sheet," 2019.

[43] Department of Energy office of Nuclear Energy, "The Ultimate Fast Facts Guide to Nuclear Energy."

[44] Engineers Edge, "Parallel and Counter Flow Designs," 2019. [Online]. Available: https://www.engineersedge.com/heat_transfer/parallel_counter_flow_designs.htm. [Accessed: 08-Dec-2019].

[45] R. Ravi, "Why are heat exchangers generally horizontal?"

[46] F. A. S. Mota, E. P. Carvalho, and M. A. S. S. Ravagnani, "Modeling and Design of Plate Heat Exchanger," *IntechOpen*, 2015.

[47] A. D. Thomas, "Modeling Multiple Effect Evaporation in Conjuncture with Small Modular Nuclear Reactors to Generate Power, Fresh Water, and Chilled Water," *NCSU Thesis*, 2019.

[48] C. Roos, "Clean Heat and Power Using Biomass Gasification for Industrial and Agricultural Clean Heat and Power Using Biomass Gasification for Industrial and Agricultural Projects," no. March 2010, 2016.

[49] H. Spliethoff, "Power generation from solid fuels," *Power Syst.*, vol. 21, 2010.

[50] ALL Power Labs, "How Gasification Works," 2018. .

[51] B. Jones-Albertus, "Confronting The Duck Curve: How to Address Over-Generation of Solar Energy," 2017. [Online]. Available: https://www.energy.gov/eere/articles/confronting-duck-curve-how-address-over-generation-solar-energy. [Accessed: 08-Dec-2019].

[52] U. S. E. P. Agency, “CHP Benefits.” [Online]. Available: https://www.epa.gov/chp/chp-benefits.

[53] C. McMillan, R. Boardman, M. McKellar, P. Sabharwall, M. Ruth, and S. Bragg-Sitton, “Generation and Use of Thermal Energy in the US Industrial Sector and Opportunities to Reduce its Carbon Emissions,” *Contract*, 2016.

[54] X. Zhang, R. C. O. Brien, and G. Tao, “High Temperature Steam Electrolysis : Demonstration of Improved Long-Term Performance 2011 Fuel Cell Seminar & Exposition,” 2011.

[55] I. Shiklomanov, “World fresh water resources,” *Water in crisis a guide to the world’s fresh water resources*. 1993.

[56] B. Peterson, “Desalination and Energy Consumption,” *The Energy Collective Group*, 2017. [Online]. Available: https://www.energycentral.com/c/ec/desalination-and-energy-consumption. [Accessed: 08-Dec-2019].

[57] D. T. Ingersoll, “Integration of Nuscale Smr With Desalination Technologies,” pp. 1–8, 2016.

[58] K. Frick, J. M. Doster, and S. Bragg-Sitton, “Design and Operation of a Sensible Heat Peaking Unit for Small Modular Reactors,” *Nucl. Technol.*, vol. 205, no. 3, pp. 415–441, 2018.

[59] Spirax Sarco, “Desuperheating,” 2019. [Online]. Available: https://beta.spiraxsarco.com/learn-about-steam/desuperheating/basic-desuperheater-types. [Accessed: 08-Dec-2019].

[60] NPTEL, “Lecture 11: Pinch Point Technology,” *Module 1: Classical Thermodynamics*. [Online]. Available: https://nptel.ac.in/courses/112103016/module1/lec11/3.html.

[61] F. L. Rubin and F. L. Rubin, “Multizone Condensers : Desuperheating , Multizone Condensers : Desuperheating , Condensing , Subcooling,” vol. 7632, 2007.

[62] I. S. Hussaini, S. M. Zubair, and M. A. Antar, “Area allocation in multi-zone feedwater heaters,” *Energy Convers. Manag.*, vol. 48, no. 2, pp. 568–575, Feb. 2007.

[63] Engineers Edge, “Overall Heat Transfer Coefficient Table Charts and Equation.” [Online]. Available: https://www.engineersedge.com/thermodynamics/overall_heat_transfer-table.htm. [Accessed: 07-Jan-2019].

[64] R. Swaminathan and S. Nadhipite, “Design of Solar Lime Kiln,” 2017. [Online]. Available: https://www.omicsonline.org/open-access/design-of-solar-lime-kiln.php?aid=95264.

[65] M. Blanco and L. Ramirez Santigosa, *Advances in Concentrating Solar Thermal Research and Technology*. Woodhead Publishing, 2017.

[66] Solar Energy Industries Association, “Concentrating Solar Power.” [Online]. Available: https://www.seia.org/initiatives/concentrating-solar-power.

[67] S. Ebrahim Ghasemi and A. Akbar Ranjbar, “Thermal performance analysis of solar parabolic trough collector using nanofluid as working fluid: A CFD modelling study,” *J. Mol. Liq.*, vol. 222, pp. 159–166, 2016.

[68] Office of Energy Efficiency and Renewable Energy, “Power Tower System Concentrating Solar Power Basics,” 2013. [Online]. Available: https://www.energy.gov/eere/solar/articles/power-tower-system-concentrating-solar-power-basics. [Accessed: 11-Feb-2019].

[69] M. Sengupta, Y. Xie, A. Lopez, A. Habte, G. Maclaurin, and J. Shelby, “The National Solar Radiation Data Base (NSRDB),” *Renew. Sustain. Energy Rev.*, vol. 89, no. June, pp.

51–60, 2018.

[70] K. Kuparinen and E. K. Vakkilainnen, “Green pulp mill: Renewable alternatives to fossil fuels in lime kiln operations,” *BioRes*, vol. 12, no. 2, pp. 4031–4048, 2017.

[71] U.S. Energy Information Administration, “North Carolina Natural Gas Industrial Price,” 2019. [Online]. Available: https://www.eia.gov/dnav/ng/hist/n3035nc3m.htm.

[72] Electricity Local, “Raleigh Electricity Rates.” [Online]. Available: https://www.electricitylocal.com/states/north-carolina/raleigh/.

[73] S. Patel, “NuScale Boosts SMR Capacity, Making it Cost Competitive with Other Technologies,” *Power*, 2018. [Online]. Available: https://www.powermag.com/nuscale-boosts-smr-capacity-making-it-cost-competitive-with-other-technologies/.

[74] U.S. Energy Information Administration, “Natural Gas Summary.” [Online]. Available: https://www.eia.gov/dnav/ng/NG_SUM_LSUM_A_EPG0_PIN_DMCF_A.htm.

[75] U.S. Energy Information Administration, “Annual Energy Outlook 2020,” 2020.

[76] B. Plumer and N. Popovich, “These Countries Have Prices on Carbon. Are they Working?,” *The New York Times*, 02-Apr-2019.

[77] Spirax Sarco, “Steam Accumulators.” [Online]. Available: https://www.spiraxsarco.com/learn-about-steam/the-boiler-house/steam-accumulators. [Accessed: 02-Jan-2020].